



Detectors & Co

Detectors & detection methods

Toni Baroncelli



Content (and Disclaimer)

This lecture will give an overview of how to assemble detectors into experiments at Colliders.

- Experiments of the recent past and
- present experiments

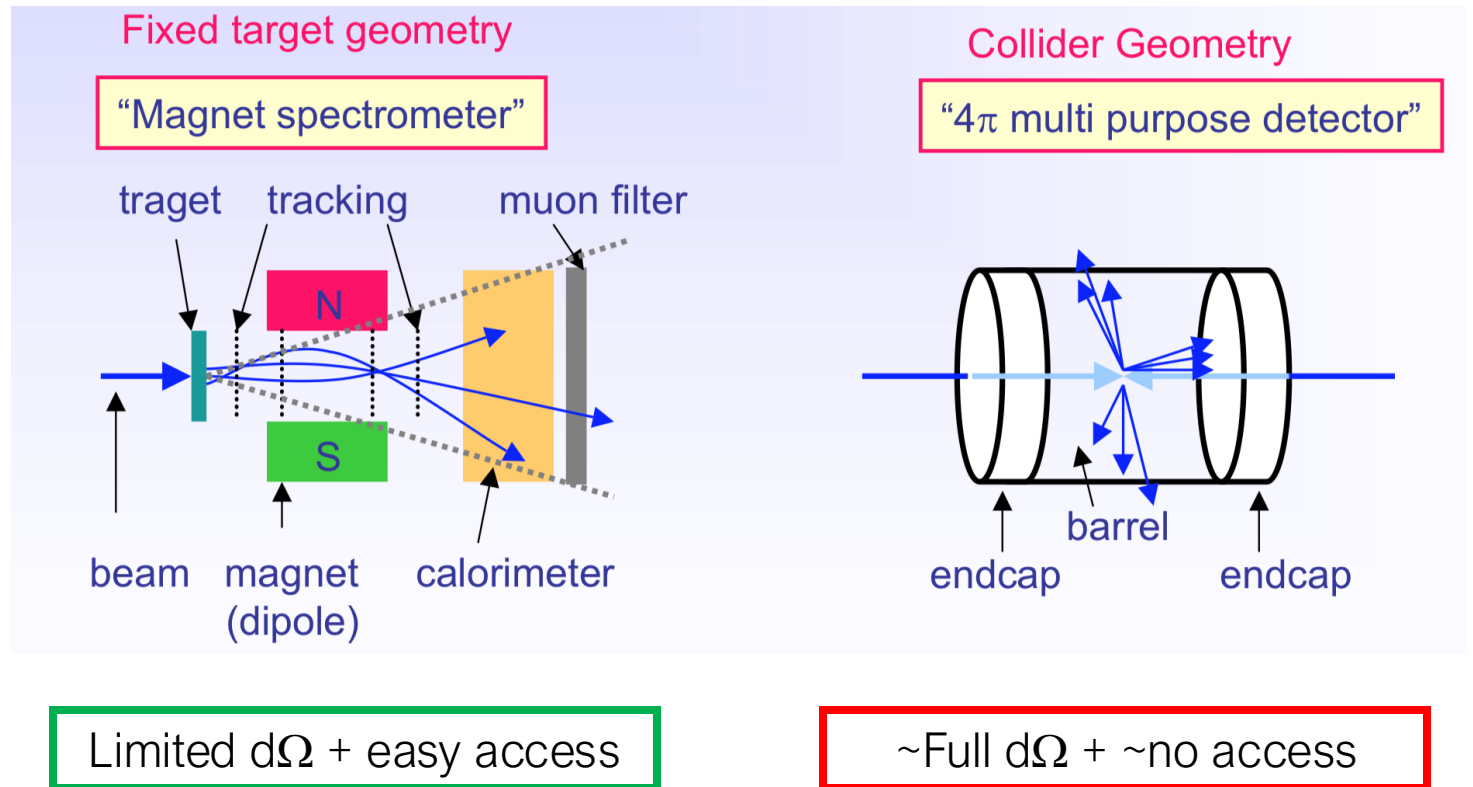
Experiment: assembly of detectors

Goal of Ideal experiments: measure

- Characteristics of **ALL** charged and neutral particles
- Characteristics of a full Event (topology & much more)

This cannot be done by a single detector

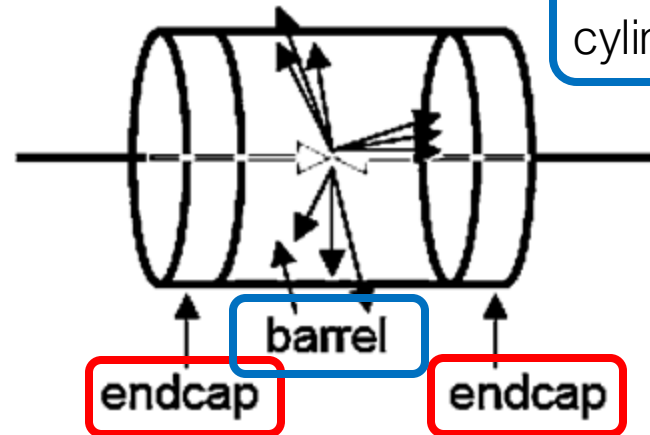
- integrate several detectors
- experiments





Designing a 4π Collider Experiment

the end-cap (forward / backward part), it consists of disks that are perpendicular to the beam line.



the barrel (large angle / large p_T / large η) cylindrical and co-axial with the beam axis

The experiment (== assembly of many detectors) 'should':

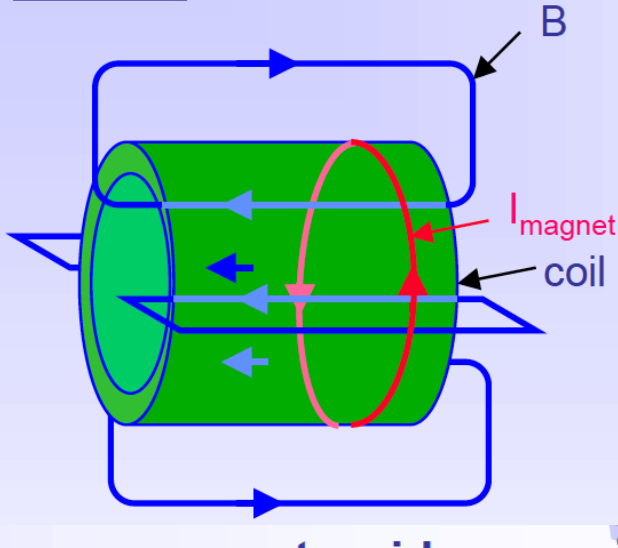
- *Be capable of measuring known physics processes but also unexpected new physics;*
- Be as hermetic as possible;
- Measure momentum of all charged particles \rightarrow B field
- Measure energy of all hadrons and electrons;
- Filter muons using a large amount of material and measure its momentum;
- Be capable of identifying particles (mass and charge)
- Reconstruct primary and secondary vertices
- Have excellent triggering performance and sustain the rate of interactions;
- The position of all the different detectors should be known with high accuracy.

Is this possible at all? Yes but with caveats and limitations.

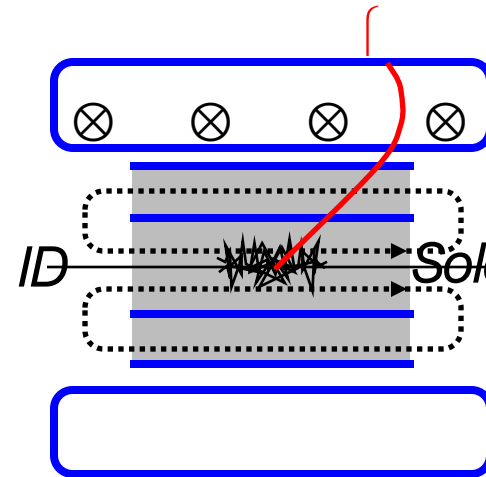
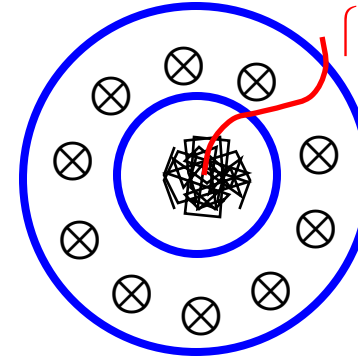
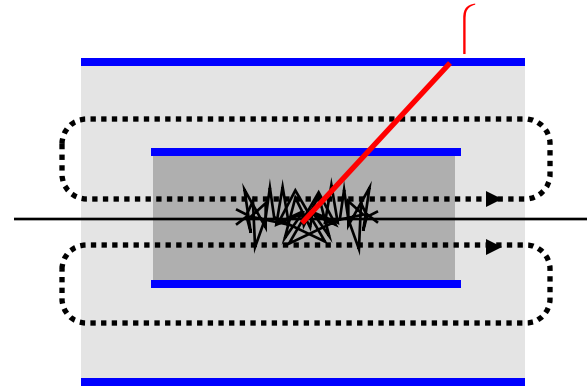
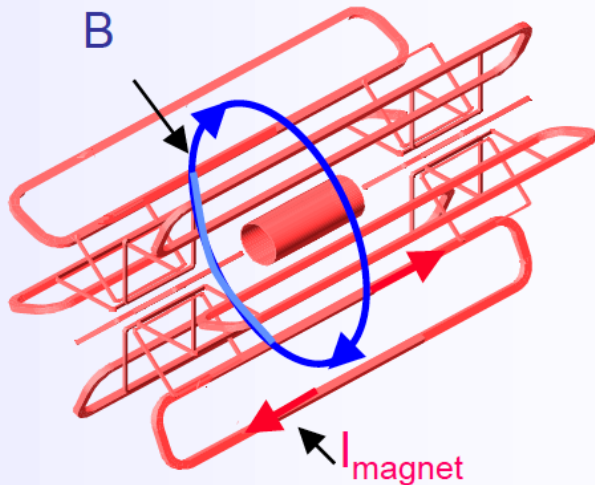


Choosing a B-Field Configuration

solenoid

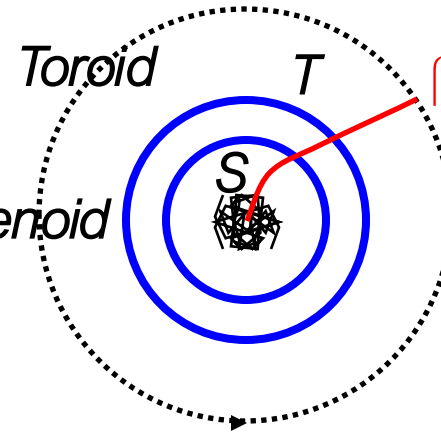


toroid



Toroid

Solenoid



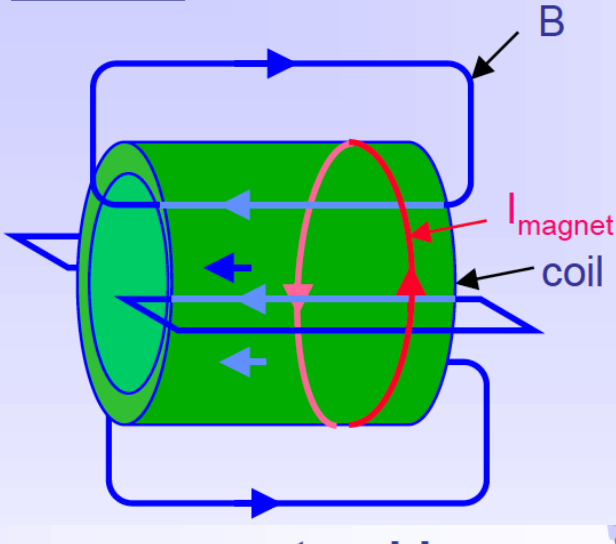
- *Bending in the transverse plane*
- Large homogenous field inside coil
- weak opposite field in return yoke
- Size limited (cost)
- rel. high material budget

- *Bending in the longitudinal plane*
- Rel. large fields over large volume
- Rel. low material budget (air toroid)
- non-uniform field → measure!
- complex structure

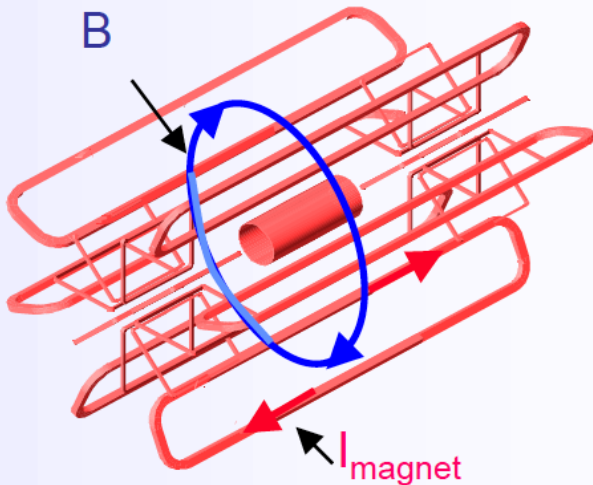


Solenoids Vs Toroids

solenoid



toroid



- Large homogenous field inside coil
- weak opposite field in return yoke
- Size limited (cost)
- rel. high material budget

| Type | Experiment | B-Field (T) | Cold/Warm | Diameter (m) | Length (m) |
|------|--------------------------|-------------|-----------|--------------|------------|
| S | DELPHI | 1.2 | C | 5.2 | 7.4 |
| S | L3 | 0.5 | W | 11.9 | 11.9 |
| S | CMS | 4.0 | C | 5.9 | 12.5 |
| S | ATLAS (ID) | 2.0 | C | 2.5 | 5.8 |
| T | ATLAS (μ , barrel) | 0.5 | C | 9.4/20 | 24.3 |
| T | ATLAS (μ , end-cap) | 1.0 | C | 1.7/10.7 | 5 |

- Rel. large fields over large volume
- Rel. low material budget
- non-uniform field
- complex structure



Time Laps of Physics

A modern experiment should be “capable of ... unexpected new physics (generally indicated with NP)”

The *Higgs case* @ LHC experiments.

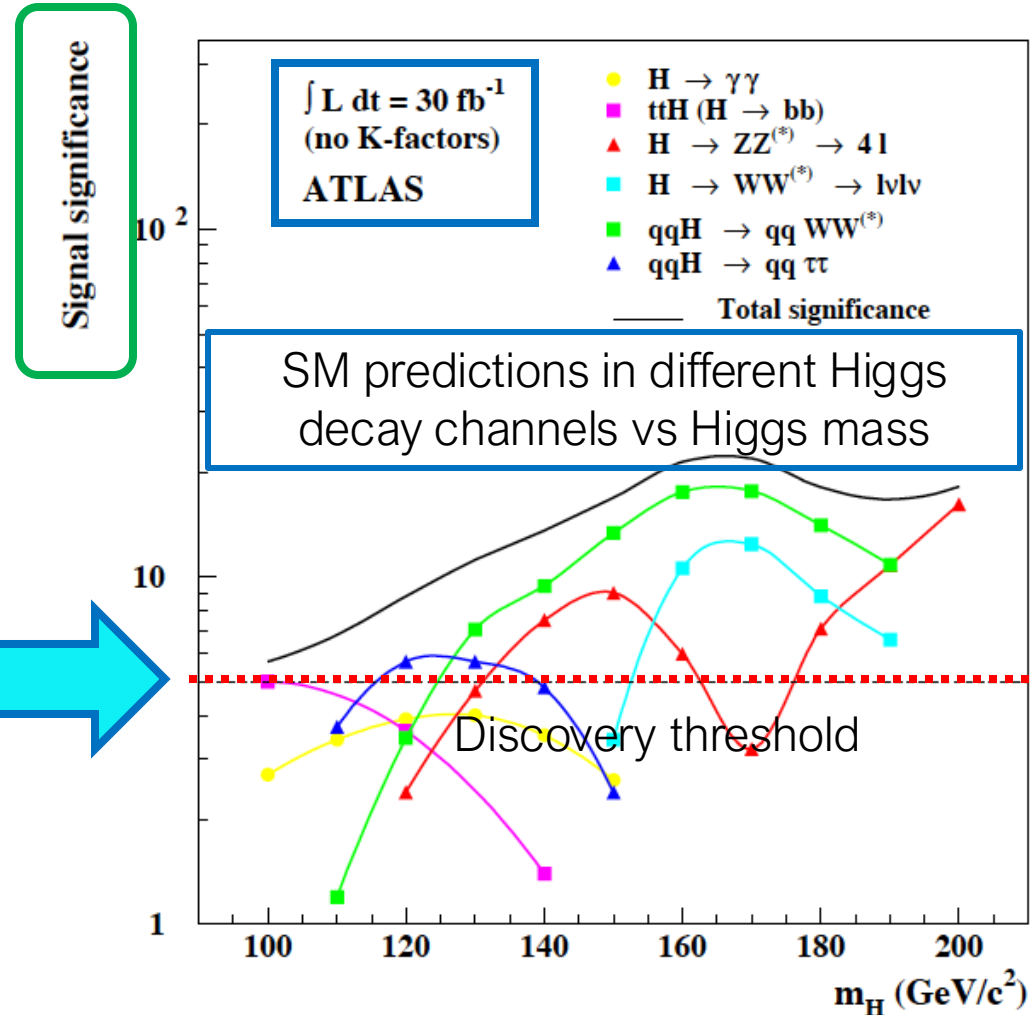
Higgs = “New Physics < 2012”

- SM: couplings versus (unknown) mass known → cross section and decay rates known
- Higgs events for different mass **simulated**
- LHC Experiments designed to detect Higgs decays ‘all masses’



A good / excellent discovery potential for some models beyond SM (SUSY).

Where is the problem?





Time Laps of Physics - continued

A modern experiment at a collider should be “capable of measuring known physics processes but also unexpected new physics (generally indicated with NP)”.

~20 years between the conception / design and operation
(~10 years of project ~10 years of construction) *(Find the money!)*

What if after the ‘no-return point’ some new discovery or theory development changes the landscape?

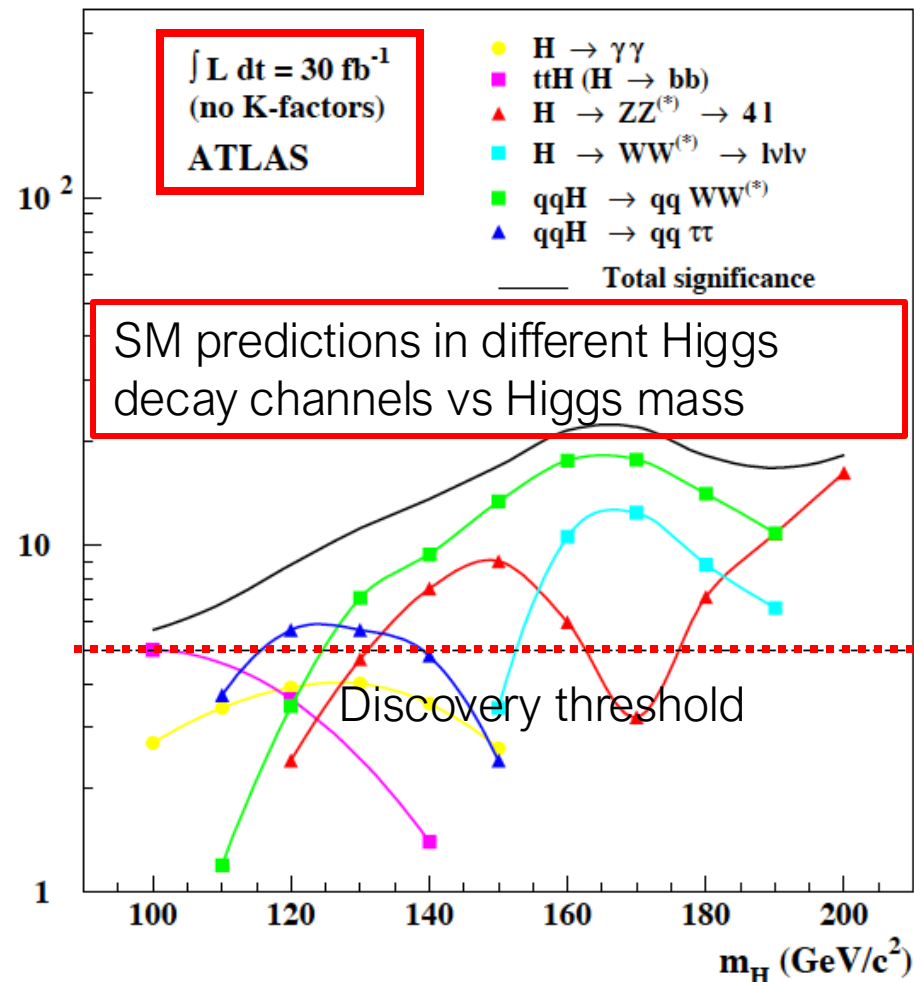
The design cannot change much
→ risk of a ‘poor’ experiment.

However:

- Modern experiments extremely versatile + very large detection potential
- past indicates that New Physics ~means ‘large masses’
- Look for high energy leptons, jets, missing energies

Signal significance

Pre-LHC situation : simulation





Time Laps of Technology (1990 – 2000)

Table 1. Typical detector characteristics.

| Detector Type | Accuracy (rms) | Resolution Time | Dead Time |
|----------------------|------------------------------|-------------------|--------------------|
| Bubble chamber | 10 to 150 μm | 1 ms | 50 ms ^a |
| Streamer chamber | 300 μm | 2 μs | 100 ms |
| Proportional chamber | $\geq 300 \mu\text{m}^{b,c}$ | 50 ns | 200 ns |
| Drift chamber | 50 to 300 μm | 2 ns ^d | 100 ns |
| Scintillator | .. | 150 ps | 10 ns |
| Emulsion | 1 μm | | |
| Silicon strip | 2.5 μm | <i>e</i> | <i>e</i> |

PDG. 1990 edition

Table 28.1: Typical resolutions and deadtimes of common detectors. Revised September 2009.

| Detector Type | Accuracy (rms) | Resolution Time | Dead Time |
|---------------------------------|------------------------------------|-------------------------------|----------------------|
| Bubble chamber | 10–150 μm | 1 ms | 50 ms ^a |
| Streamer chamber | 300 μm | 2 μs | 100 ms |
| Proportional chamber | 50–100 $\mu\text{m}^{b,c}$ | 2 ns | 200 ns |
| Drift chamber | 50–100 μm | 2 ns ^d | 100 ns |
| Scintillator | — | 100 ps/ <i>n</i> ^e | 10 ns |
| Emulsion | 1 μm | — | — |
| Liquid argon drift [7] | $\sim 175\text{--}450 \mu\text{m}$ | $\sim 200 \text{ ns}$ | $\sim 2 \mu\text{s}$ |
| Micro-pattern gas detectors [8] | 30–40 μm | $< 10 \text{ ns}$ | 20 ns |
| Resistive plate chamber [9] | $\lesssim 10 \mu\text{m}$ | 1–2 ns | — |
| Silicon strip | pitch/(3 to 7) ^f | <i>g</i> | <i>g</i> |
| Silicon pixel | 2 μm^h | <i>g</i> | <i>g</i> |

PDG. ~2010 edition

Comparison between typical detectors characteristics in 1990 and 2010

| | | Accuracy (μm) | | Time Resolution | | | | |
|-----------|------|----------------------------|----------------------|-----------------|------------------|-----------------------------|-------|-------|
| ~20 years | Year | Streamer chamber | Proportional chamber | Drift chamber | RPC | Micro-pattern gas detectors | | |
| | 1990 | 300 | >300 | 50 ns | 50-300 | - | - | |
| 2010 | 300 | 50-100 | 2 ns | 50-100 | 10 μm | <10ns | 30-40 | 10 ns |

Detectors designed ~ 10y < data taking

- Detectors at the frontier of technology or (more often) detectors in R&D phase → optimise while constructing
- Expected duration of future experiments > 30 years!
- Long term planning for **upgrade** and / or replacement of technologies (increase of luminosity, radiation damage)



And of SC Magnets used in Experiments

Table 34.10: Progress of superconducting magnets for particle physics detectors.

| Experiment | Laboratory | B [T] | Radius [m] | Length [m] | Energy [MJ] | X/X_0 | E/M [kJ/kg] | |
|------------|---------------|------------|---------------|---------------|----------------|-----------|------------------|-------------|
| TOPAZ* | KEK | 1.2 | 1.45 | 5.4 | 20 | 0.70 | 4.3 | 1987 - 2011 |
| CDF* | Tsukuba/Fermi | 1.5 | 1.5 | 5.07 | 30 | 0.84 | 5.4 | |
| VENUS* | KEK | 0.75 | 1.75 | 5.64 | 12 | 0.52 | 2.8 | |
| AMY* | KEK | 3 | 1.29 | 3 | 40 | † | | |
| CLEO-II* | Cornell | 1.5 | 1.55 | 3.8 | 25 | 2.5 | 3.7 | |
| ALEPH* | Saclay/CERN | 1.5 | 2.75 | 7.0 | 130 | 2.0 | 5.5 | 1989 - 2000 |
| DELPHI* | RAL/CERN | 1.2 | 2.8 | 7.4 | 109 | 1.7 | 4.2 | |
| ZEUS* | INFN/DESY | 1.8 | 1.5 | 2.85 | 11 | 0.9 | 5.5 | 1992 - 2007 |
| H1* | RAL/DESY | 1.2 | 2.8 | 5.75 | 120 | 1.8 | 4.8 | |
| BaBar* | INFN/SLAC | 1.5 | 1.5 | 3.46 | 27 | † | 3.6 | |
| D0* | Fermi | 2.0 | 0.6 | 2.73 | 5.6 | 0.9 | 3.7 | |
| BELLE* | KEK | 1.5 | 1.8 | 4 | 42 | † | 5.3 | |
| BES-III | IHEP | 1.0 | 1.475 | 3.5 | 9.5 | † | 2.6 | |
| ATLAS-CS | ATLAS/CERN | 2.0 | 1.25 | 5.3 | 38 | 0.66 | 7.0 | |
| ATLAS-BT | ATLAS/CERN | 1 | 4.7-9.75 | 26 | 1080 | (Toroid)† | | |
| ATLAS-ET | ATLAS/CERN | 1 | 0.825-5.35 | 5 | 2 × 250 | (Toroid)† | | |
| CMS | CMS/CERN | 4 | 6 | 12.5 | 2600 | † | 12 | |
| SiD** | ILC | 5 | 2.9 | 5.6 | 1560 | † | 12 | > 2035 |
| ILD** | ILC | 4 | 3.8 | 7.5 | 2300 | † | 13 | |
| SiD** | CLIC | 5 | 2.8 | 6.2 | 2300 | † | 14 | |
| ILD** | CLIC | 4 | 3.8 | 7.9 | 2300 | † | | |
| FCC** | | 6 | 6 | 23 | 54000 | † | 12 | |

* No longer in service

** Conceptual design in future

† EM calorimeter is inside solenoid, so small X/X_0 is not a goal

Radius of curvature of a charged particle in a B field $\rightarrow p$

Super-conducting magnets are used for the momentum measurement of charged tracks (curvature):

$$\frac{\sigma(p_T)}{p_T} \propto \frac{1}{B}$$

- 4 x B \rightarrow 4 x resolution in p_T
- Magnets are the largest structure of an experiment



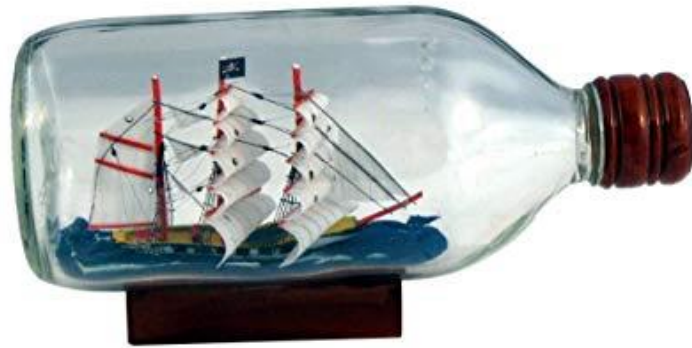
- You may replace (part of the) detectors
- Magnets in experiments have to last for ~30 to 40 y



A 4π Collider Experiment: the Real Life

A 4π hermetic experiment is inaccessible, like a ship in a bottle.

Interventions at the LHC are planned since the construction and **opening / intervening / closing back takes ~ 2 y** and the coordinated work of a large number of engineers and technicians. The periods of stop are called 'LS', Long Shutdowns.



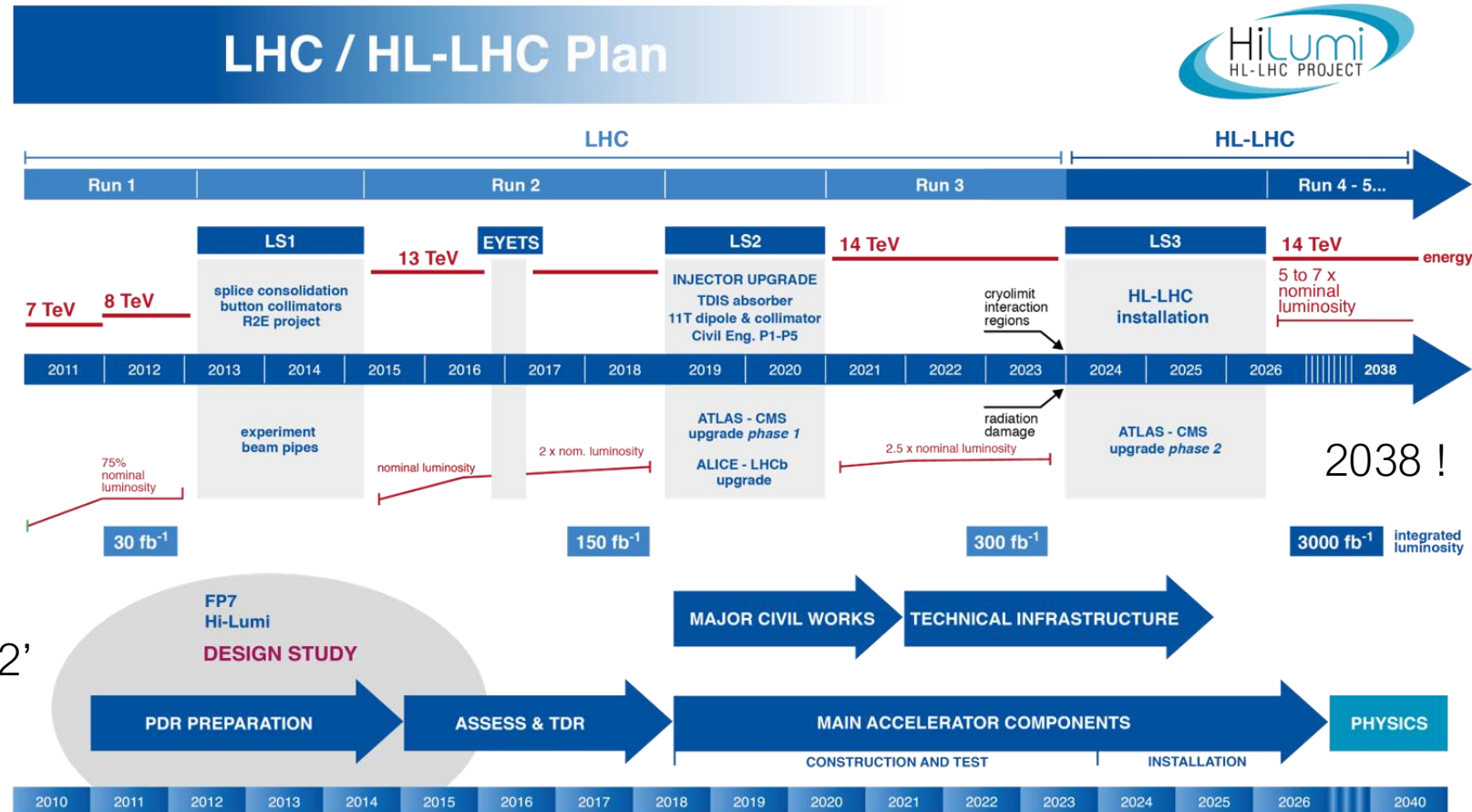
LS Long Shutdowns :

LS2 2019+2020 'Upgrade Phase 1'

LS3 2024 → ½ 2026 'Upgrade Phase 2'

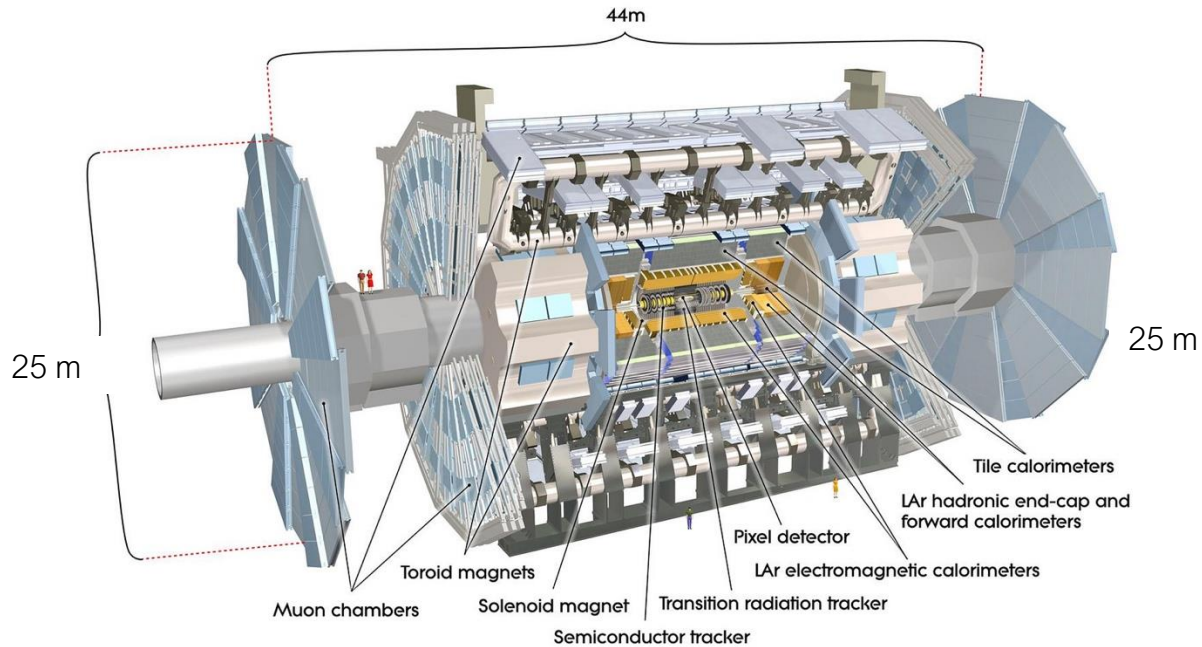
..... COVID delays!!

Expected data taking end ~ 2040

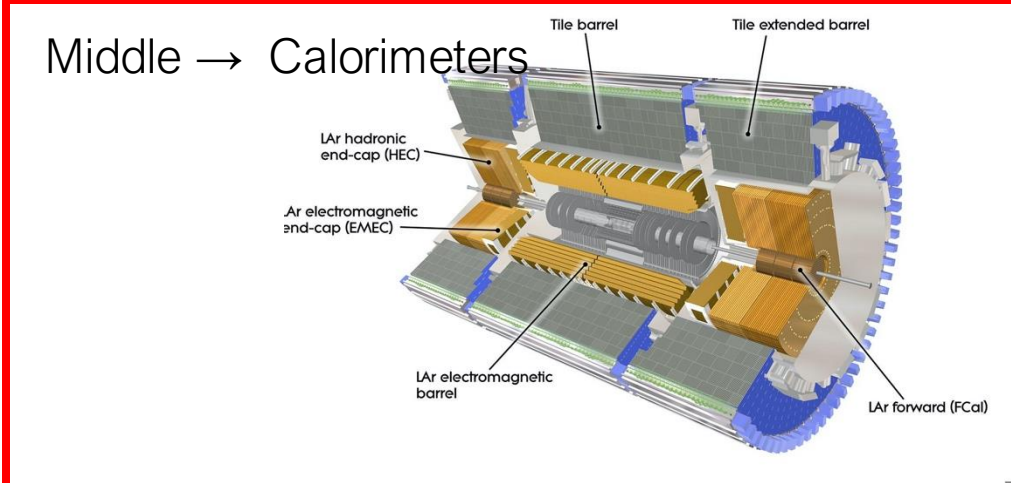
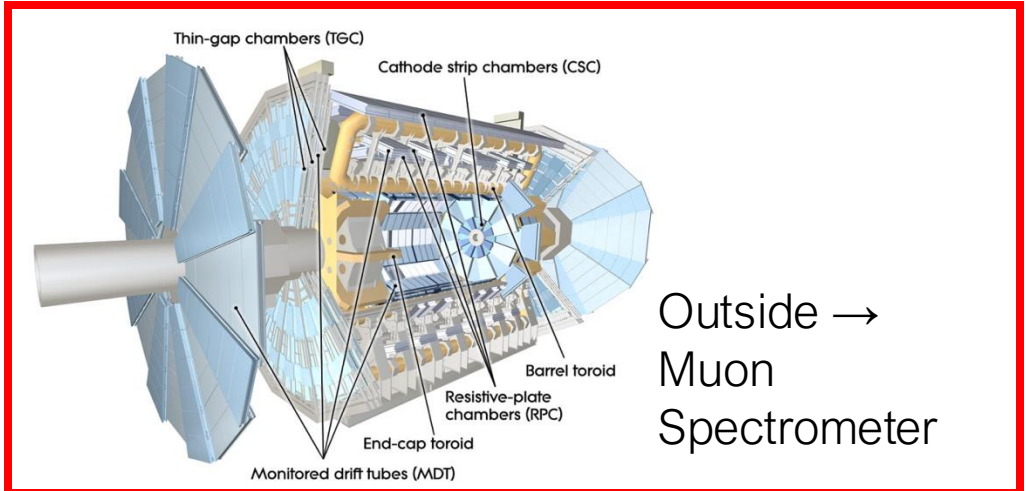
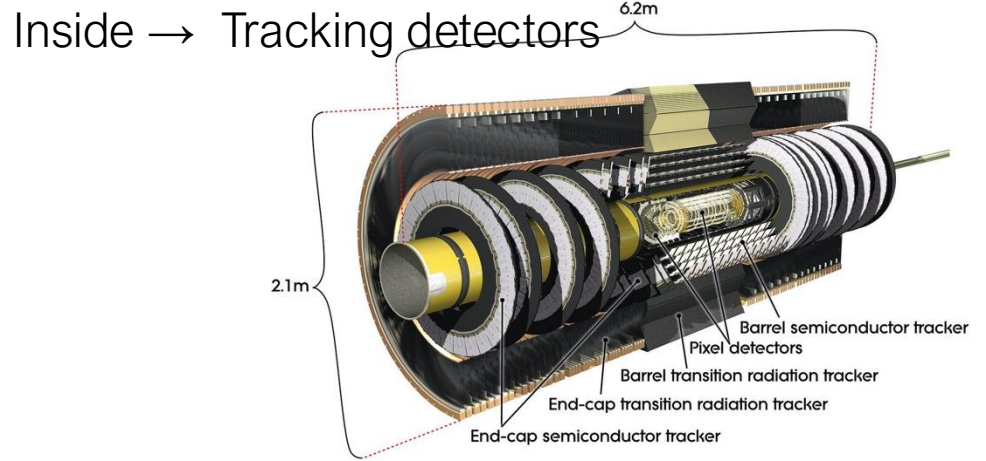




General Overview

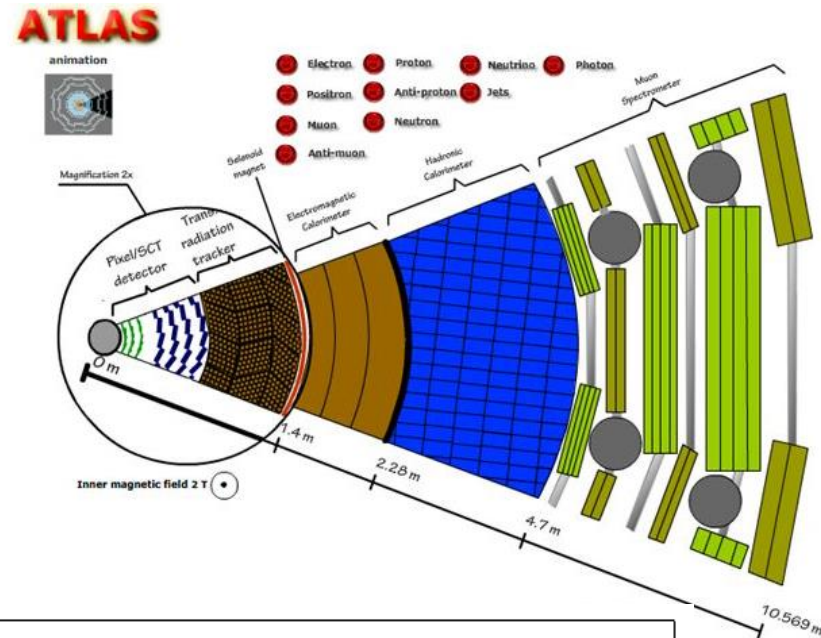
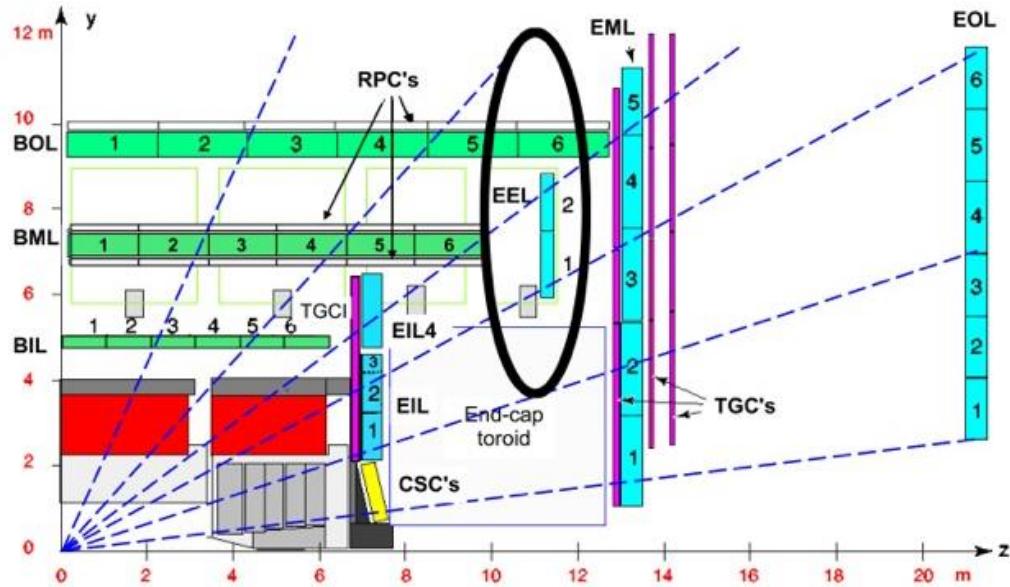


From Inside → Out



Toni Barancelli: Detectors

General Overview



| Detector component | Required resolution | η coverage | |
|-----------------------------|--|----------------------|----------------------|
| | | Measurement | Trigger |
| Tracking | $\sigma_{p_T}/p_T = 0.05\% p_T \oplus 1\%$ | ± 2.5 | |
| EM calorimetry | $\sigma_E/E = 10\%/\sqrt{E} \oplus 0.7\%$ | ± 3.2 | ± 2.5 |
| Hadronic calorimetry (jets) | | | |
| barrel and end-cap | $\sigma_E/E = 50\%/\sqrt{E} \oplus 3\%$ | ± 3.2 | ± 3.2 |
| forward | $\sigma_E/E = 100\%/\sqrt{E} \oplus 10\%$ | $3.1 < \eta < 4.9$ | $3.1 < \eta < 4.9$ |
| Muon spectrometer | $\sigma_{p_T}/p_T = 10\%$ at $p_T = 1$ TeV | ± 2.7 | ± 2.4 |

Non destructive measurements

Destructive measurements

~ mixed measurements



General Overview

| <i>Position</i> | <i>Name</i> | <i>Purpose</i> |
|-----------------|---------------------|--|
| Innermost | Vertex Detector | charged tracks close to beam pipe; primary (+ secondary <i>vertices</i> of decaying particles) (small Δ Radius \rightarrow no momentum!) |
| Inner | Tracking Detectors | <i>charged tracks</i> with a large Δ Radius |
| Middle | EM Calorimeters | Measure the energy of <i>electrons and photons</i> |
| Middle | Hadron Calorimeters | Measure the energy of <i>hadronic particles</i> |
| Outer | Muon Spectrometer | Measure the momentum of penetrating particles \rightarrow <i>muons</i> |

| <i>Position</i> | <i>Name</i> | <i>Hadrons[±]</i> | <i>Hadrons⁰</i> | <i>Photons</i> | <i>e[±]</i> | <i>μ[±]</i> |
|-----------------|---------------------|----------------------------|----------------------------|--|----------------------|----------------------|
| Innermost | Vertex Detector | ✓ | | | ✓ | ✓ |
| Inner | Tracking Detectors | ✓ | | | ✓ | ✓ |
| Middle | EM Calorimeters | ✓ | ✓ | ✓ | ✓ | ✓ |
| Middle | Hadron Calorimeters | ✓ | ✓ | | | ✓ |
| Outer | Muon Spectrometer | | | Penetration limit ————— | | ✓ |



Basic Measurements: Summary

| Type of Measurement | Quantity measured | Detector | Position in Experiment |
|---|---|--|--|
| Non destructive (~light detectors in ~vacuum or in gas) | Trajectory of charged particles close to interaction point | Vertex detectors, Si detectors (excellent spatial resolution & rad-hard) | Cylinders with radii ~ 10/20 cm |
| | Radius of curvature of charged particles in magnetic field | Inner Detectors, typically Si or gaseous detectors | Cylinders in barrel, disks in end-caps. Radially out of Vertex Detectors |
| Destructive (detectors made of heavy materials) | Energy of em particles (electrons & photons) | EM calorimeters ~ Lead sandwiched with energy detectors | Cylinders in barrel, disks in end-caps. Radially out of Inner Detectors |
| | Energy of hadronic particles (charged & neutral) | Hadron Calorimeters: Fe/Cu sandwiched with energy detectors | Cylinders in barrel, disks in end-caps. Radially out of Inner Detectors |
| Mixed | Radius of curvature of charged particles emerging from EM & HCAL calorimeters | Muon detectors: tracking detectors, typically gaseous detectors | Cylinders in barrel, disks in end-caps. At the outmost position |



Glossary

| | Definition | Measurement | Comment |
|--------------------|---|--|---|
| Efficiency | probability that a detector gives a signal when a particle traverses it | measured using a beam of known particles or using simulation | |
| Response time | time that the detector takes to form an electronic signal after the arrival of the particle | Test beams | during this time, a second event may not be recorded |
| Dead time | time between the passage of a particle and the moment at which the detector is ready to record the passage of the next particle | Test beams | The length of the signal, the electronics used, and the recovery time of the detector influence the dead time |
| Spatial resolution | precision with which the passage of a particle is located in space | Test beams | |
| Energy resolution | possibility of a detector to distinguish two close energies | “test beam” with particles of known energy | The energy resolution is the half-width of the energy distribution |



Charged Particles Detectors

Particle Data Group: https://pdg.lbl.gov/2024/reviews/contents_sports.html

Table 35.1: Typical resolutions and deadtimes of common charged particle detectors. Revised September 2023.

| Detector Type | Intrinsic Spatial Resolution (rms) | Time Resolution | Dead Time |
|--|---|------------------------------------|--------------------------------|
| Resistive plate chamber | 50 μm | 50–1000 ps* | 10 ns [†] |
| Liquid argon TPC | 0.5–1 mm [‡] | 0.01–1 μs [§] | — [¶] |
| Scintillation tracker | ~100 μm | 100 ps/n | 10 ns |
| Bubble chamber | 10–150 μm | 1 ms | 50 ms ^{**} |
| Wire chambers (proportional and drift chambers) | 50–100 μm | 5–10 ns ^{††} | 20–200 ns ^{‡‡} |
| Micro-pattern gas detector | 30–40 μm | 5–10 ns ^{††} | 20–200 ns ^{‡‡} |
| Silicon strips/pixels | \lesssim 10 μm ^{§§} | few ns ^{¶¶} ^{‡‡} | \lesssim 50 ns ^{‡‡} |

← Typical detectors in modern colliders

*LHC: ~2 mm gap, ~1 ns. HL-LHC: ~1 mm gap, ~350 ps. Timing RPC: ~50 ps

[†]Limited by amplifier and discriminator bandwidth, usually around 100 MHz

[‡]Detector geometry dependent

[§]Using the scintillation signal

[¶]No deadtime for medium

^{||} n = index of refraction.

^{**}Multiple pulsing time.

^{††}For fast particles

^{‡‡}Depending/limited by the amplifying electronics [8]

^{§§}Depending on electrode pitch, best values around 2–4 μm have been achieved

^{¶¶}Resolutions < 100 ps are reached in dedicated pixel developments



Combined Measurements

Complex observables need the combination of different detectors

- E_{tot} , = Total event energy, p_{tot} = event momentum balance;
 - $(E_{CM} - E_{tot})$ = energy carried by invisible particles
 - $(\vec{0} - \vec{p}_{tot})$ gives the direction of invisible particles
 - Total momentum only in the transverse plane (E_{CM} is not known in hadronic colliders)
- Muons (Inner Detector + Muon Spectrometer)
- EM and Hadron calorimeters to distinguish hadrons from electrons and photons
- Associate showers with charged tracks extrapolated to the entrance of calorimeters
- showers not associated to any charged particle (\rightarrow neutral EM or hadronic particle)
- Reconstruct jets

| | <i>p of charged tracks</i> | <i>Energy of all particles</i> | <i>Identify photons electrons</i> | <i>Identify muons</i> | <i>Associate tracks & showers</i> | <i>Jets</i> | <i>E_{tot} & p_{tot}</i> |
|-------------|----------------------------|--------------------------------|-----------------------------------|-----------------------|---------------------------------------|-------------|--|
| ID | ✓ | | ✓ | ✓ | ✓ | ✓ | ✓ |
| EM-calo | | ✓ | ✓ | ✓ | ✓ | ✓ | ✓ |
| H-Calo | | ✓ | | ✓ | ✓ | ✓ | ✓ |
| μ -spec | ✓ | | | ✓ | | | ✓ |



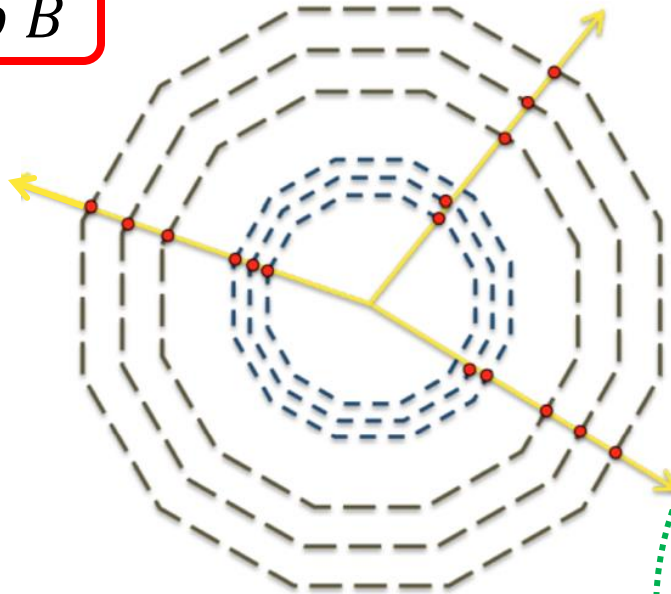
Tracking Detectors

Tracking Detectors

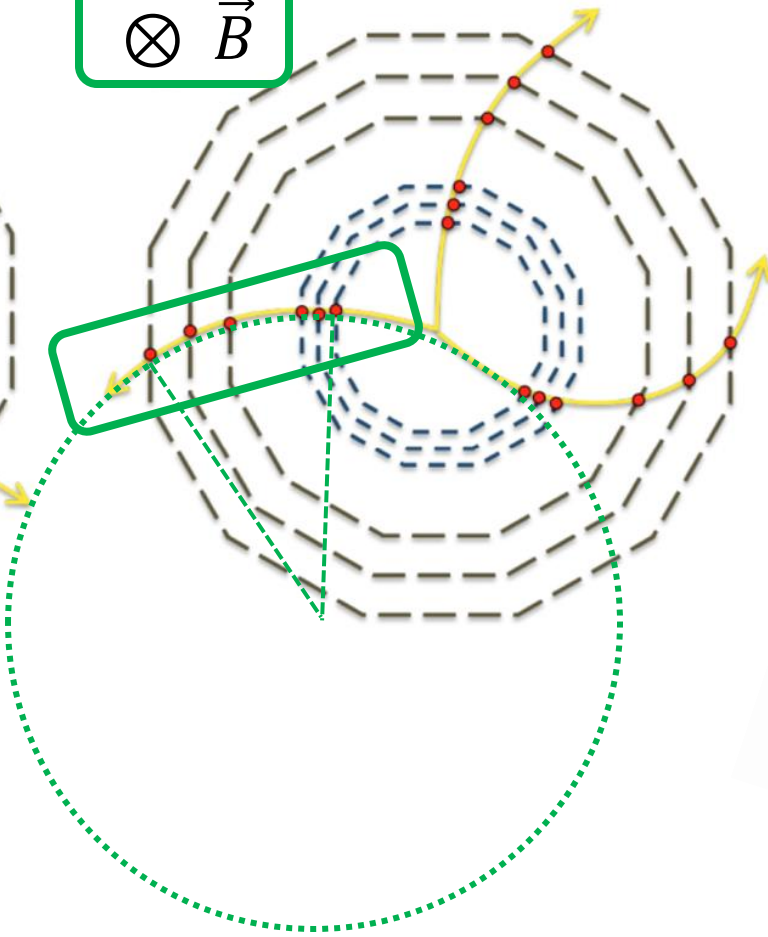


Measurement of Momentum p in a B Field

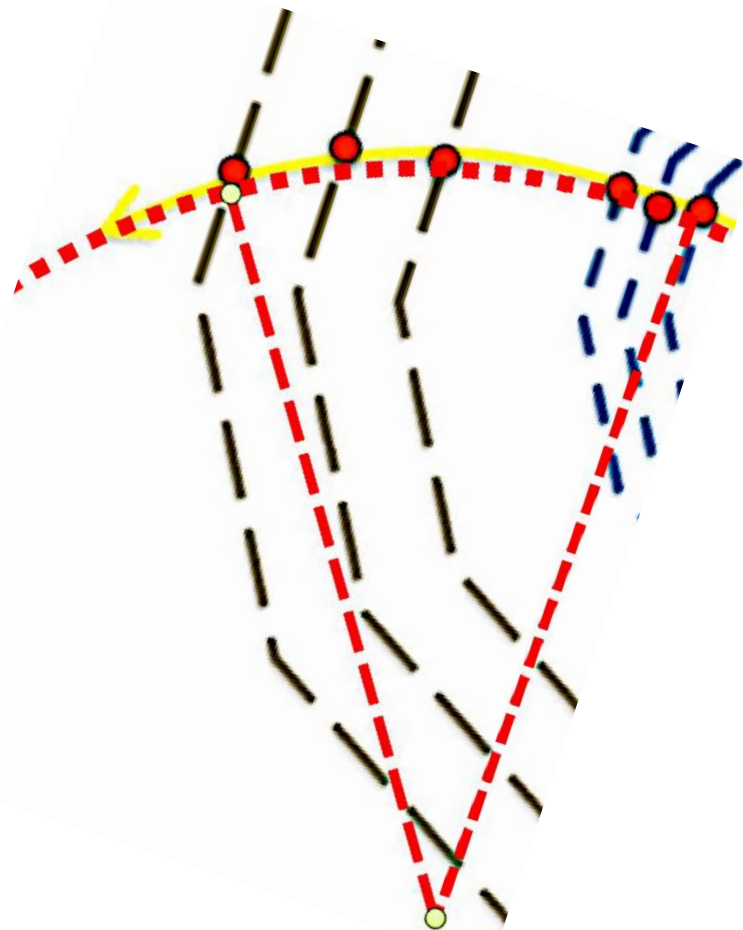
No \vec{B}



$\otimes \vec{B}$



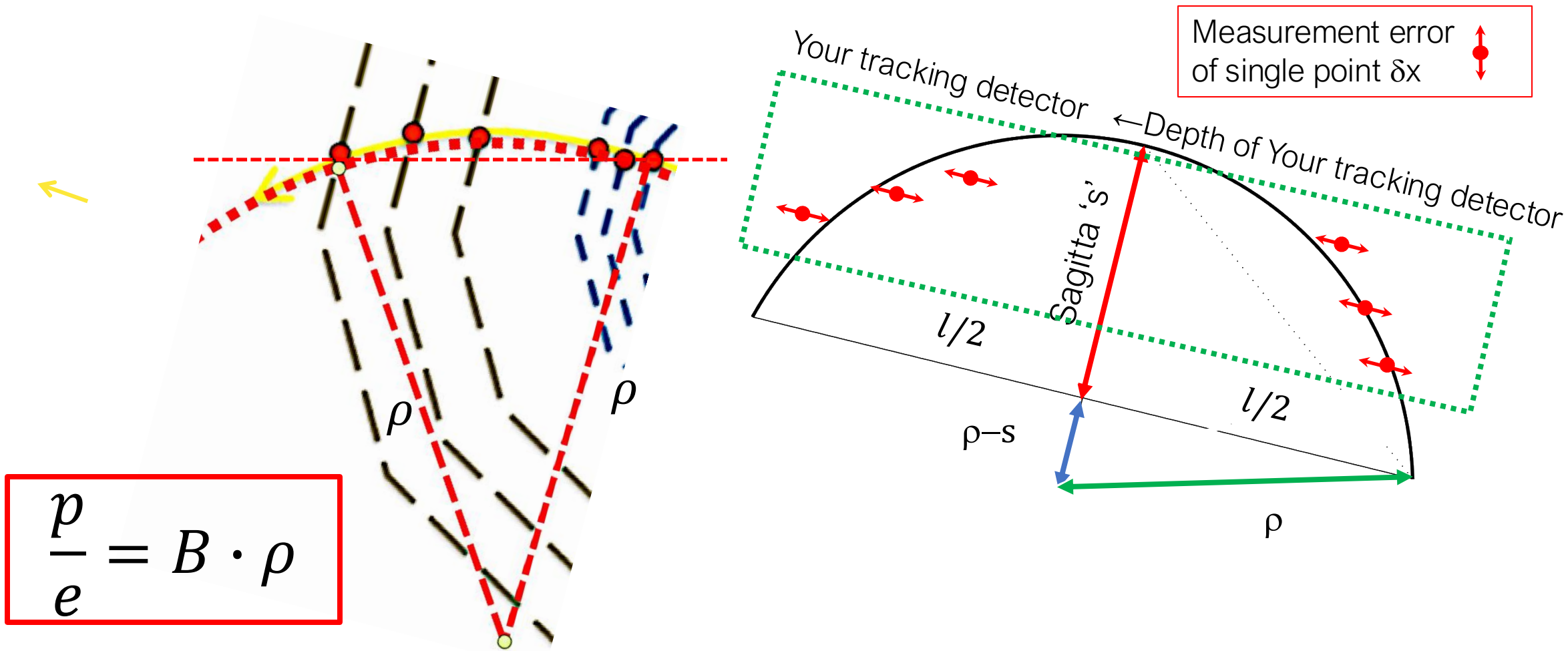
$$\frac{p}{e} = B \cdot \rho$$



- Curvature of a trajectory in B field
- Non-destructive measurement \rightarrow ionization energy losses (det. elements) are $\ll p$
- Tracking detectors are \sim perpendicular to the trajectory of the charged track
- Multiple position measurement along the trajectory \rightarrow the curvature \rightarrow momentum



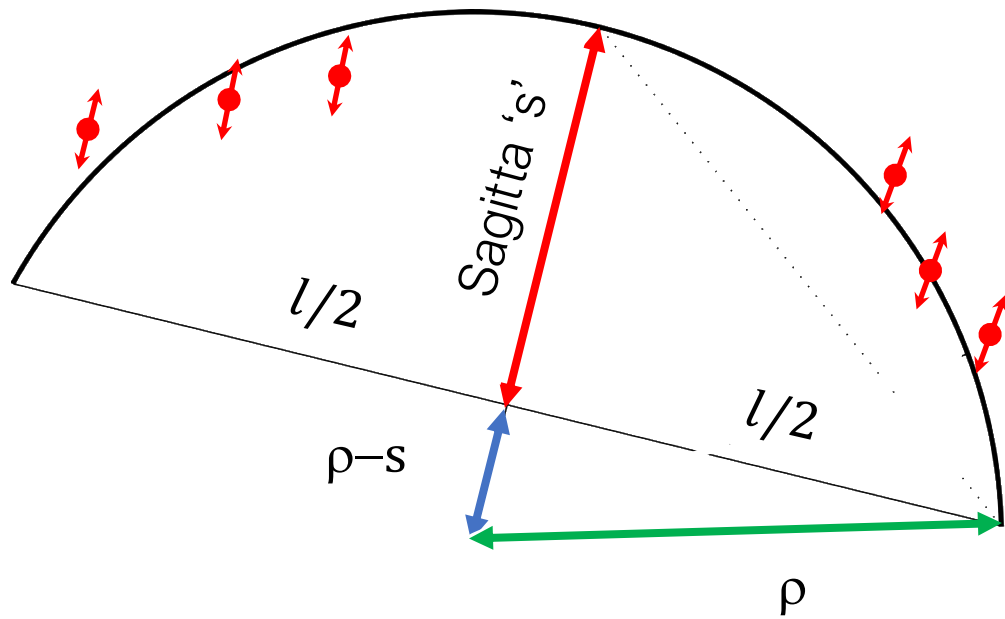
Measurement of Momentum p



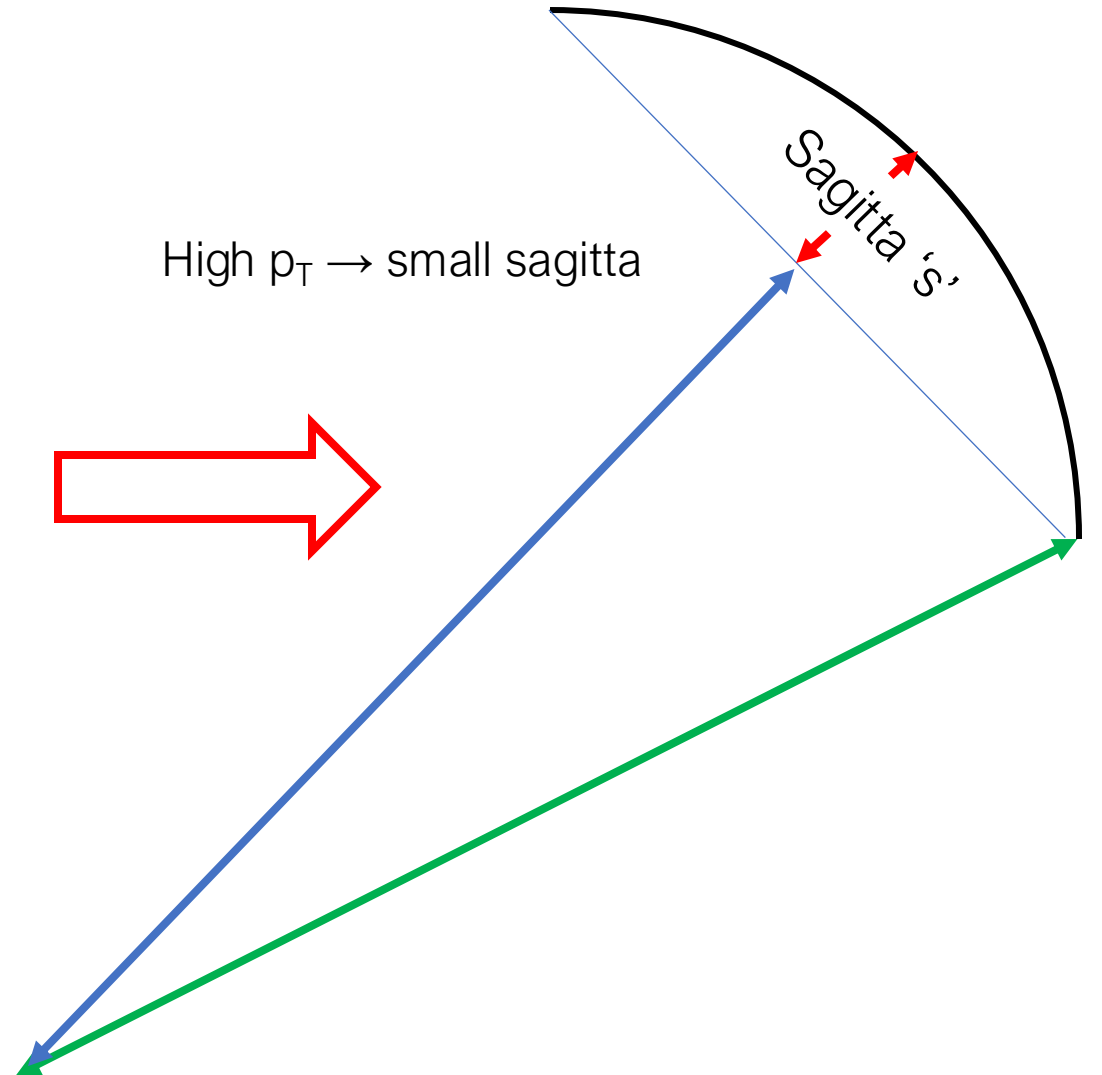
Momentum is determined by measuring the radius of curvature in magnetic field $p \propto \rho$.
Measuring the sagitta 's' is a possible & simple method



High p_T



High $p_T \rightarrow$ small sagitta



$$\frac{p}{e} = B \cdot \rho$$



Measuring Physical Quantities

The component p_T perpendicular to the direction of B is given by

$$\sin\left(180 - 90 - \frac{\theta}{2}\right) = \cos\left(\frac{\theta}{2}\right)$$

$$\frac{p}{e} = B \cdot \rho \rightarrow$$

$$p_T(\text{GeV}/c) = 0.3 \cdot B(l) \cdot \rho(\text{Tesla} \cdot m)$$

$$\frac{1}{p_T} = \frac{1}{\rho \cdot B(l) \cdot 0.3}$$

with units GeV, Tesla, meters. ρ is the radius of curvature and l is the position along the trajectory.

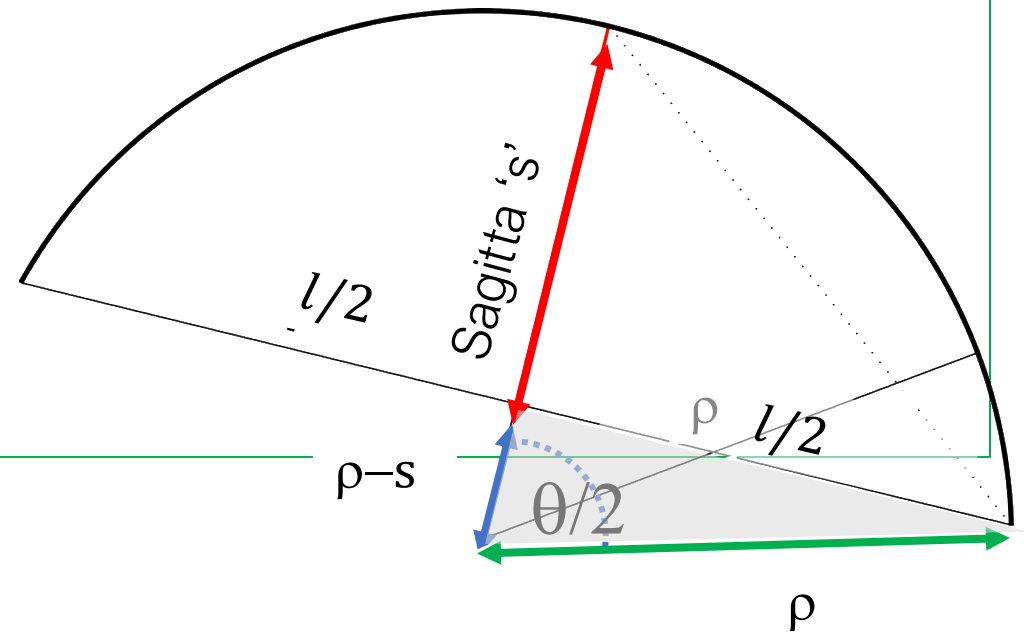
If we consider the triangle enclosed by ' $l/2$ ', $\rho-s$ and ρ we can write the relation

$$(\rho - s)^2 + (l/2)^2 = \rho^2$$

$$\rho \cdot \cos\left(\frac{\theta}{2}\right) = \rho - s \rightarrow s = \rho \cdot \left(1 - \cos\left(\frac{\theta}{2}\right)\right)$$

for small $\frac{\theta}{2}$ we expand $\cos\left(\frac{\theta}{2}\right) \approx 1 - \theta^2/8$

$$s = \rho \cdot \left(1 - \cos\left(\frac{\theta}{2}\right)\right) \approx \rho \cdot \theta^2/8$$





Measurement of Momentum in B Field

$$s = \rho \cdot (1 - \cos(\frac{\theta}{2})) \approx \rho \cdot \theta^2 / 8$$

$$\theta \approx \frac{l}{\rho} \rightarrow s = \rho \cdot \frac{l^2}{\rho^2 \cdot 8} = \frac{l^2}{\rho \cdot 8}$$

The example shown on this figure refers to a VERY low momentum charged track, in practice the sagitta is always much smaller than the radius of curvature

From the slide before

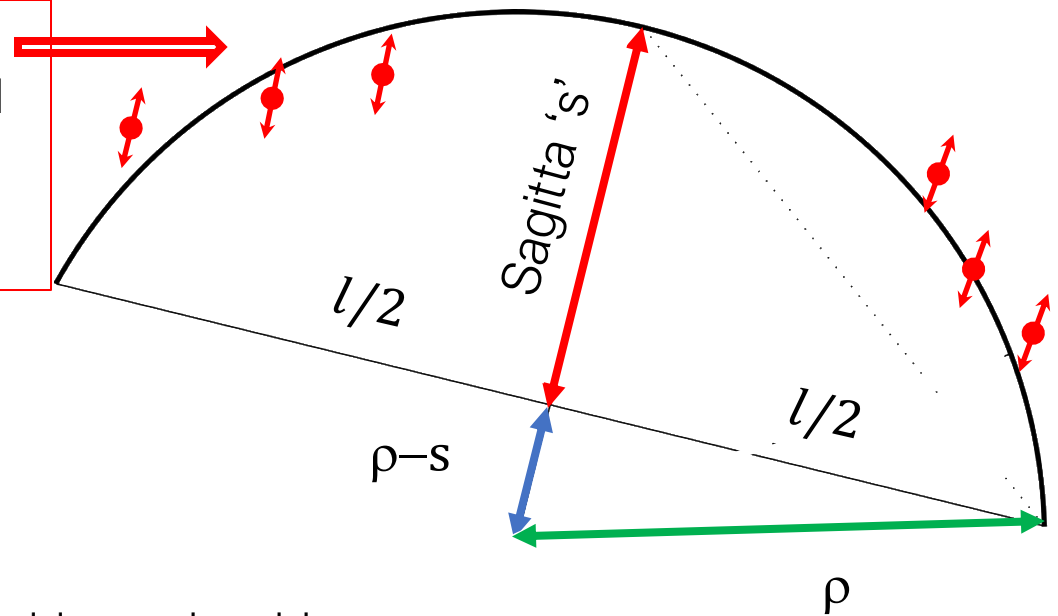
$$\frac{1}{p_T} = \frac{1}{\rho \cdot B(s) \cdot 0.3}$$

→

$$s = \rho \cdot \frac{l^2 \cdot 0.3 \cdot B(l)}{p_T \cdot 8}$$

Two ways to measure the sagitta:

Measurement inside the B field → points with error σ_x



- Using measurements **inside the B field**: Inner Detectors inside a solenoid → circle that **best** passes through the measurement → fit
- Using measurements done **outside the magnetic field**, in this case the direction of the track before and after the B field region



Relative Error on p_T

Simplified example measurement with 3 points $x_{1,2,3}$:

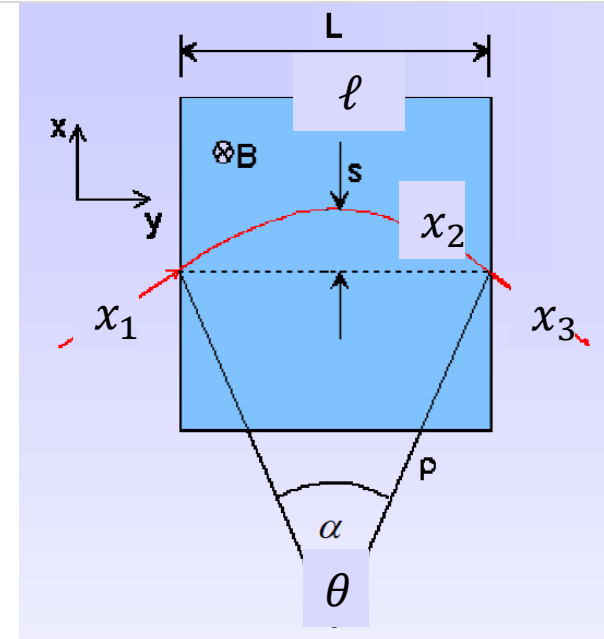
$$s = x_2 - \frac{x_1 + x_3}{2} \rightarrow \frac{\sigma(p_T)}{p_T} = \frac{\sigma(s)}{s} = \frac{\sqrt{3/2} \cdot \sigma_x}{s} = \frac{\sqrt{3/2} \cdot \sigma_x \cdot 8p_T}{0.3 \cdot B(l) \cdot l^2}$$

A more general formula has been derived for N equidistant measurements (R.L. Gluckstern, NIM 24 (1963) 381):

$$\text{Relative Error on } p_T = \frac{\sigma_x p_T}{0.3 \cdot B(l) \cdot l^2} \cdot \frac{\sqrt{720}}{\sqrt{N+4}} \text{ for } N \geq \sim 10$$

- on the precision of the single measurement and
- linearly on p_T : it worsen with increasing momentum. This is qualitatively intuitive if one considers that the curvature becomes larger (and the sagitta smaller) when p_T increases.
- On the inverse of square root of the number N of measurements
- On the dimension of the measurement area l

$$\sqrt{3/2} = \sqrt{1^2 + 1/2^2 + 1/2^2}$$



Important effect: the multiple scattering.
Charged particles undergo a large number of small deflections when passing through matter



Multiple Scattering Impact on p_T

The deflection of a charged particle, θ_{plane} , after ℓ of a material with $X_0 \sim$

$$\theta_{plane} = (14 \frac{MeV}{p\beta c}) \sqrt{\ell/X_0}$$

$$Rad.Length(cm) = Rad.Length(g/cm^2) * density$$

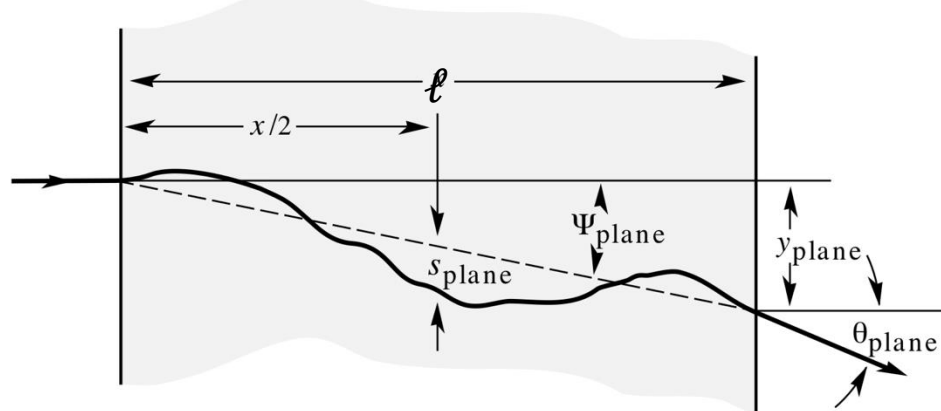


Figure 27.8: Quantities used to describe multiple Coulomb scattering. The particle is incident in the plane of the figure.

$$B(T)\rho(m) = p(GeV/c) \cdot 3.33$$

→ Material of Inner Detectors (walls, cables and services) has an impact on p_T .

The relative effect is ~

$$\frac{\delta p_n}{p_n} = \frac{\delta \theta}{\theta} = \frac{14 MeV}{\beta c \cdot 0.3 \int B(\ell) d\ell} \left[\frac{\ell}{X_0} \right]^{1/2} \rightarrow \text{no } p_T \text{ dependence}$$

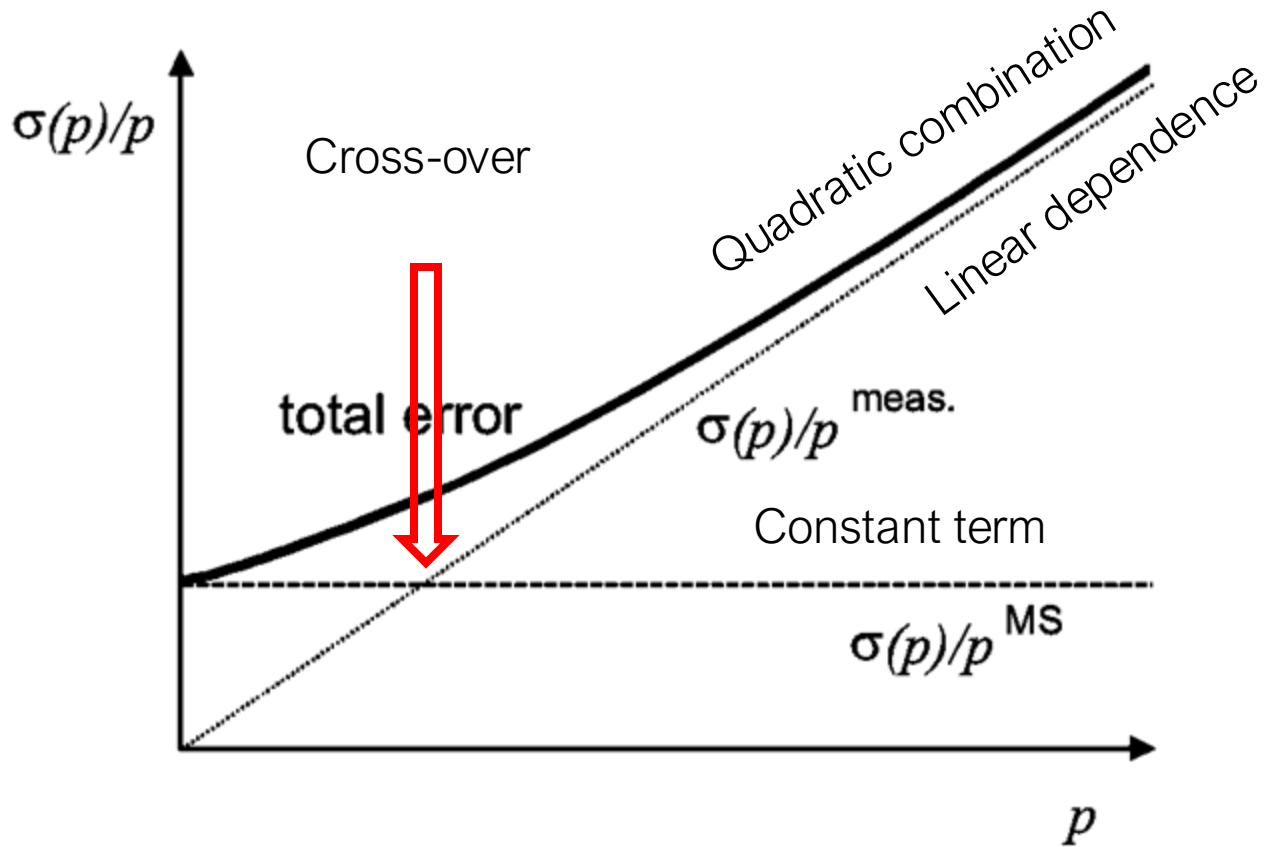
The two effects (detector resolution and effect of multiple scattering have to be combined quadratically):

$$\frac{\delta p_T}{p_T} = \sqrt{A_{det-res}^2 \cdot p_T^2 + A_{mult-scatt.}^2}$$

| Element | Z | Rad. Length (expt.) [g.cm ⁻²] |
|---------|----|---|
| H | 1 | 63.04 |
| He | 2 | 94.32 |
| C | 6 | 42.7 |
| N | 7 | 37.99 |
| O | 8 | 34.24 |
| F | 9 | 32.93 |
| Ne | 10 | 28.93 |
| Na | 11 | 27.74 |
| Mg | 12 | 25.03 |
| Al | 13 | 24.01 |
| Si | 14 | 21.82 |
| P | 15 | 21.21 |
| S | 16 | 19.5 |
| Cl | 17 | 19.28 |
| Ar | 18 | 19.55 |
| K | 19 | 17.32 |
| Ca | 20 | 16.14 |
| Ti | 22 | 16.16 |
| Cr | 24 | 14.94 |
| Fe | 26 | 13.84 |
| Ni | 28 | 12.68 |
| Cu | 29 | 12.86 |
| Zn | 30 | 12.43 |
| Ag | 47 | 8.97 |
| Pt | 78 | 6.54 |
| Au | 79 | 6.46 |
| Pb | 82 | 6.37 |



Ideal Situation



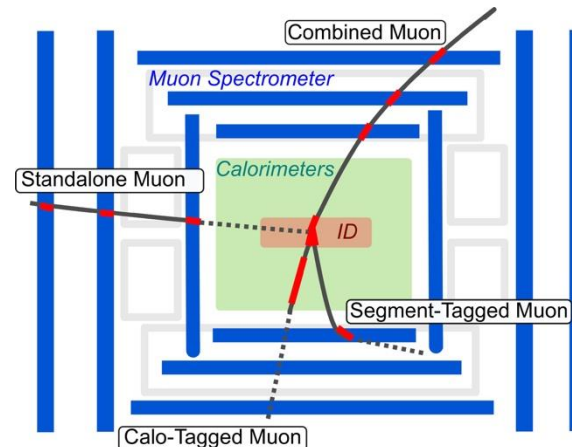
Example:

$$p_T = 1 \text{ GeV}, \ell = 1 \text{ m}, B = 1 \text{ T}, N = 10, \sigma_x = .2 \text{ mm}$$

$$\frac{\delta p_T}{p_T} \Big|_{det-res} = 0.5\%$$

Assume the detector to be filled with atmospheric pressure Argon (gas), $X_0 = 110 \text{ m}$

$$\frac{\delta p_T}{p_T} \Big|_{mult-scat} = 0.5\%$$



Note: calorimeters filter ALL particles but Muons !



(Muon) p_T Resolution in ATLAS

More effects (in the Muon system after traversing calorimeters!):

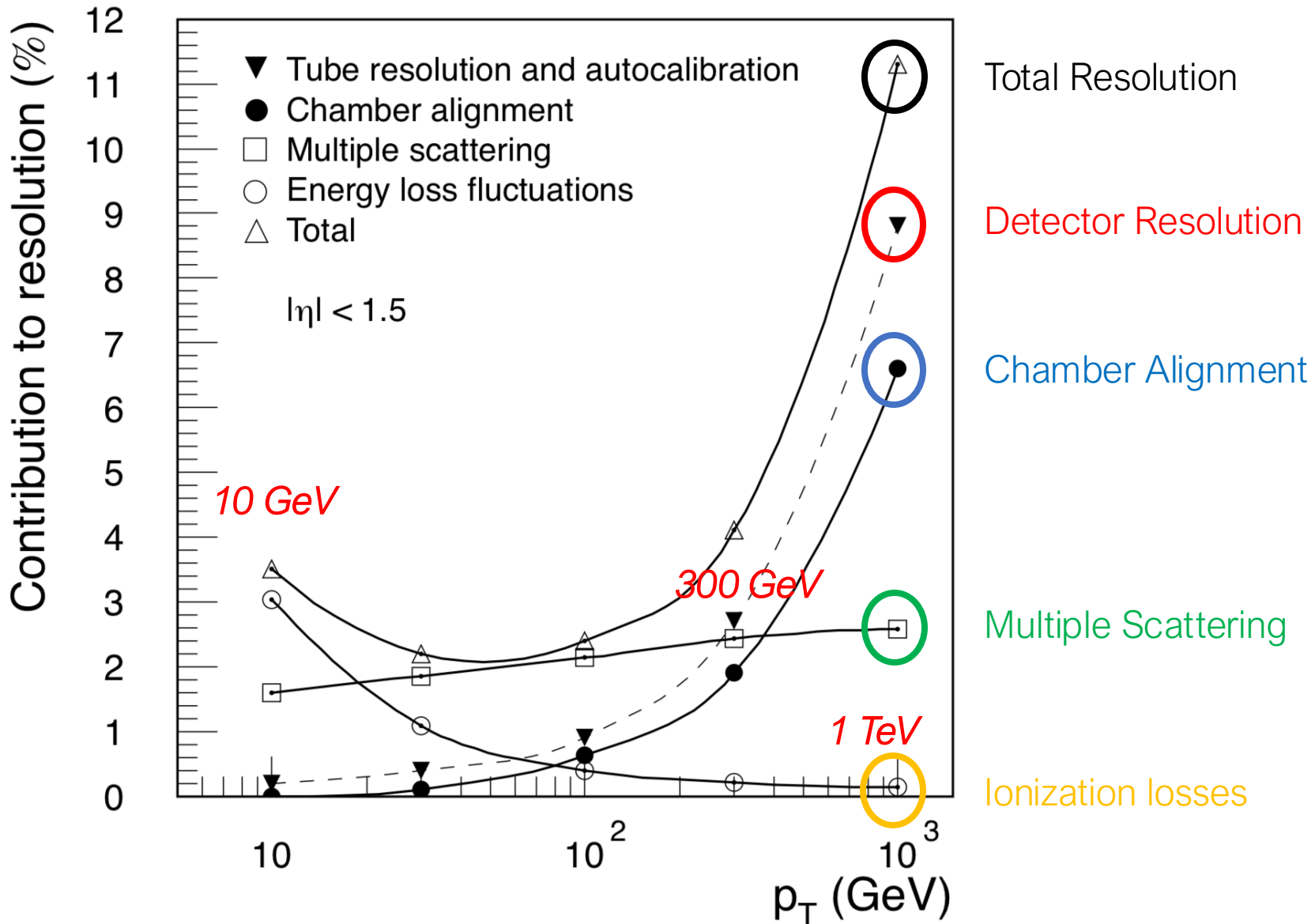
- Alignment of detector elements
- Energy losses when a charged particle (muon) traverses material.

At a p_T of ~ 10 GeV the dominant contribution is **ionization loss** and **multiple scattering**

For muons!

At a p_T of ~ 300 GeV **multiple scattering** and **detector resolution** are equally important

At a p_T of ~ 1 TeV **detector resolution** is most important effect





Calorimetry

Calorimetry



Energy Measurement in Calorimeters

- A destructive measurement: a large number of nuclear and/or EM processes in a dense medium.
- Showers; Shape depends on material and on particle → identify!

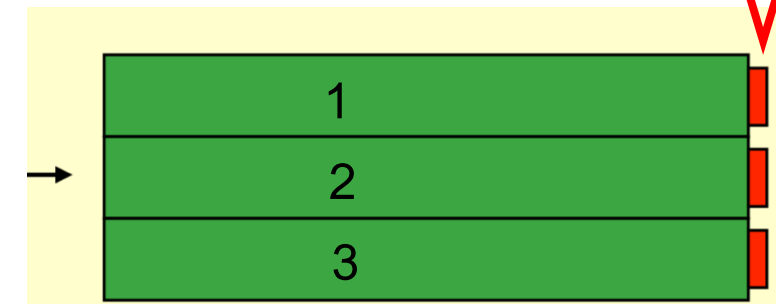
There are two types of calorimeters:

Convert signal into energy of primary particle → calibration

Detector to collect signal of segment

• Homogeneous calorimeters:

- A transparent material (scintillating crystals or high density glasses emitting Cerenkov light) absorbs the energy and measure it.
- **All charged particles in a shower seen → best energy resolution.**
- Uniform response in all points.
- Costly, can be hardly segmented (→ total energy, not shape).
- Used for electro-magnetic calorimeters → electrons and photons



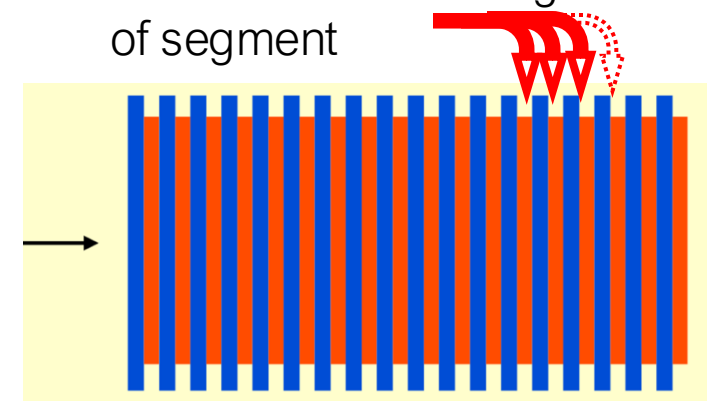
Detector to collect signal of segment

• Sampling:

- Sampling between dense material and detectors.
- Often sandwich type structure (absorber / detector) but also fibres.
- Limited cost, segmentation.

• **However only a fraction of energy is detected → lower resolution.**

$f_{sampling} = E_{detected} / E_{total}$ Generally used for both electrons & hadrons





Dimensions of Calorimeters

A characteristic parameter (\rightarrow used material) determines the development of showers

- electrons/photons: Radiation Length X_0 (EM interactions)
- hadrons showers the Interaction Length λ_{int} (Hadronic interactions)

| | Typical Length | Longitudinal Size (95% containment) | Transverse Size (95% containment) |
|----------------|---|-------------------------------------|-----------------------------------|
| EM Showers | Radiation Length $X_0 \sim \frac{A}{Z^2}$ if $A \approx Z \rightarrow$ $X_0 \sim 1/A$ | 15 to 20 X_0 | $\sim 2 X_0$ |
| Hadron Showers | interaction length $\lambda_{int} \sim A^{1/3}$ | 6 to 9 λ_{int} | 1 λ_{int} |

$$\lambda_{int}/X_0 \approx A^{4/3} \rightarrow \lambda_{int} \gg X_0$$

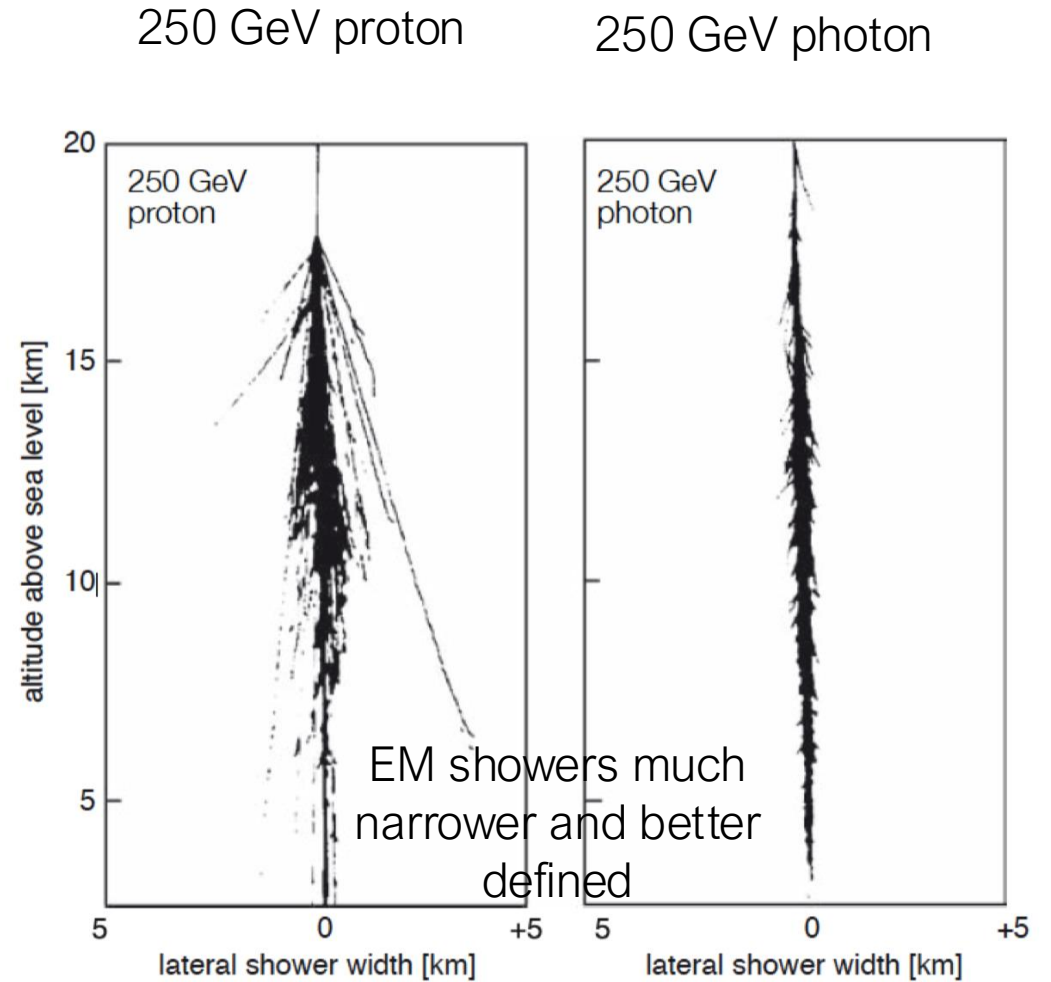
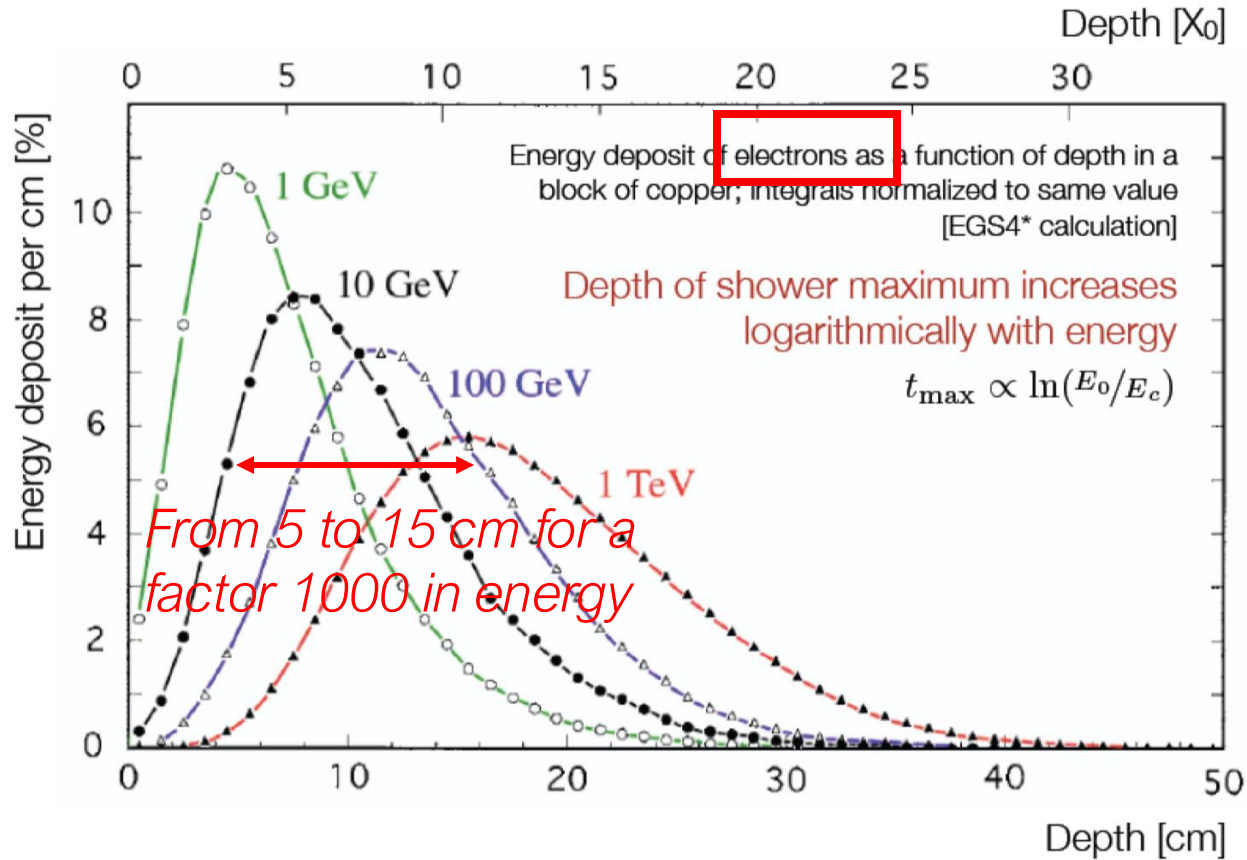
\rightarrow Hadron calorimeters much longer than EM calorimeters.

- The length of showers $\sim \log(\text{primary energy})$
- \rightarrow Calorimeters contain showers in large range of energies

| | λ_{int} [cm] | X_0 [cm] |
|-------|----------------------|------------|
| Scint | 79.4 | 42.2 |
| LAr | 83.7 | 14.0 |
| Fe | 16.8 | 1.76 |
| Pb | 17.1 | 0.56 |
| U | 10.5 | 0.32 |
| C | 38.1 | 18.8 |



The Shower Development



In the end all type of showers (Had & EM) degrade most of the initial energy by ionization losses

Simulated lateral development of showers in air



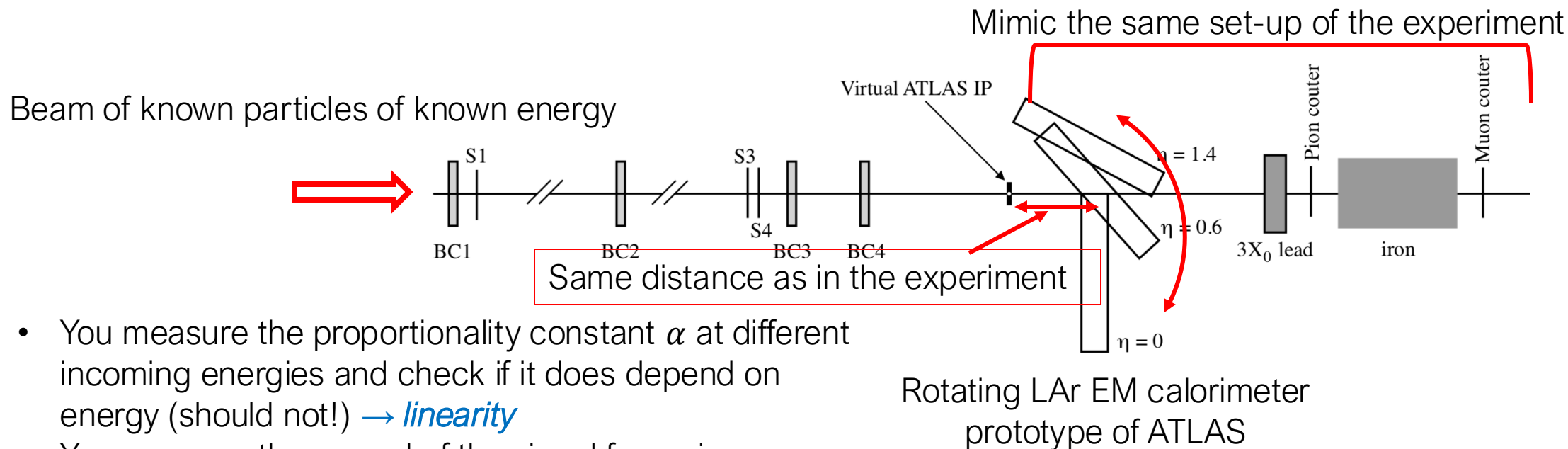
Calorimeters & Test Beams

A calorimeter signal S measured \propto number N of nuclear interactions \propto energy E .

$$S = \sum \text{nuclear interactions} = \alpha \cdot E$$

α converts the calorimeter signal into energy. α has to be determined.

One method is based on test beam(s).



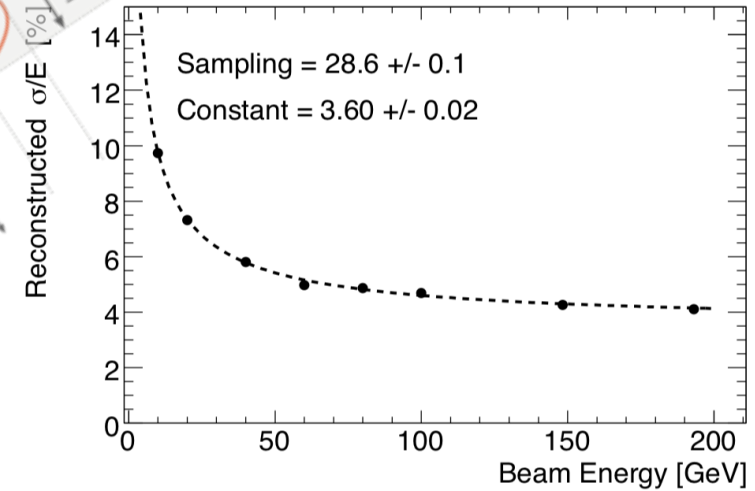
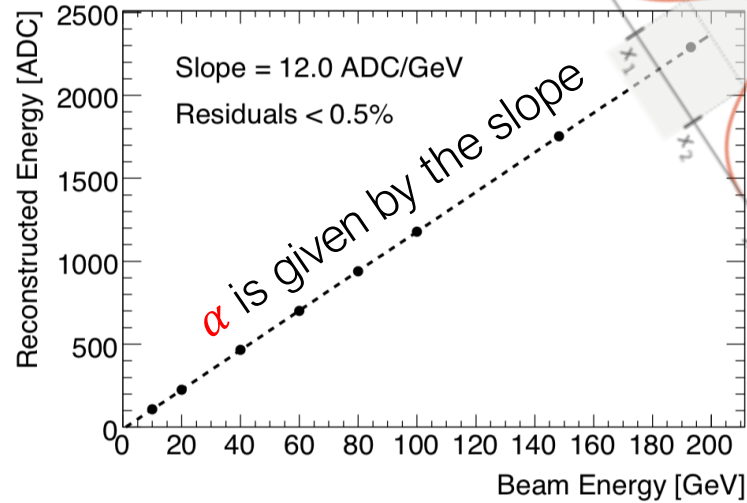
- You measure the proportionality constant α at different incoming energies and check if it does depend on energy (should not!) \rightarrow *linearity*
- You measure the spread of the signal for a given energy \rightarrow *resolution*



Energy Response

$$\frac{\sigma(p_T)}{p_T} = \frac{\sigma_x \cdot p_T}{0.3 \cdot B(l) \cdot l^2 \dots}$$

- The figure → the response of a calorimeter to beam particles of different energies is linear
- The distribution of the signal at a given energy gives the 'resolution'.



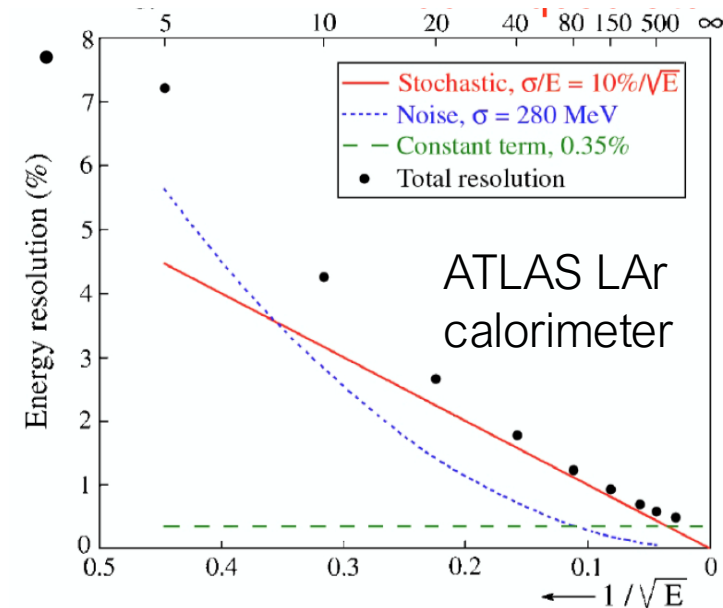
The signal of a shower is linear with energy, the resolution decreases with energy

$$\frac{\delta E}{E} \approx \frac{dN}{N} \approx \frac{\sqrt{N}}{N} = \frac{const}{\sqrt{E}} \quad \text{Decreases with energy}$$

In real life the resolution is subject to several effects, and they have to be combined quadratically → a more complex parametrisation is normally used:

$$\sigma_{tot}^2 = \sigma_{stat}^2 + \sigma_{leakage}^2 + \sigma_{electronic\ noise}^2 + \sigma_{non\ uniformities}^2$$

$$\frac{\sigma_{stat}}{E} = \frac{a}{\sqrt{E}} \quad \frac{\sigma_{leakage}}{E} = \frac{b}{\sqrt[4]{E}} \quad \frac{\sigma_{electronic\ noise}}{E} = \frac{c}{E} \quad \frac{\sigma_{non\ uniformities}}{E} = d$$



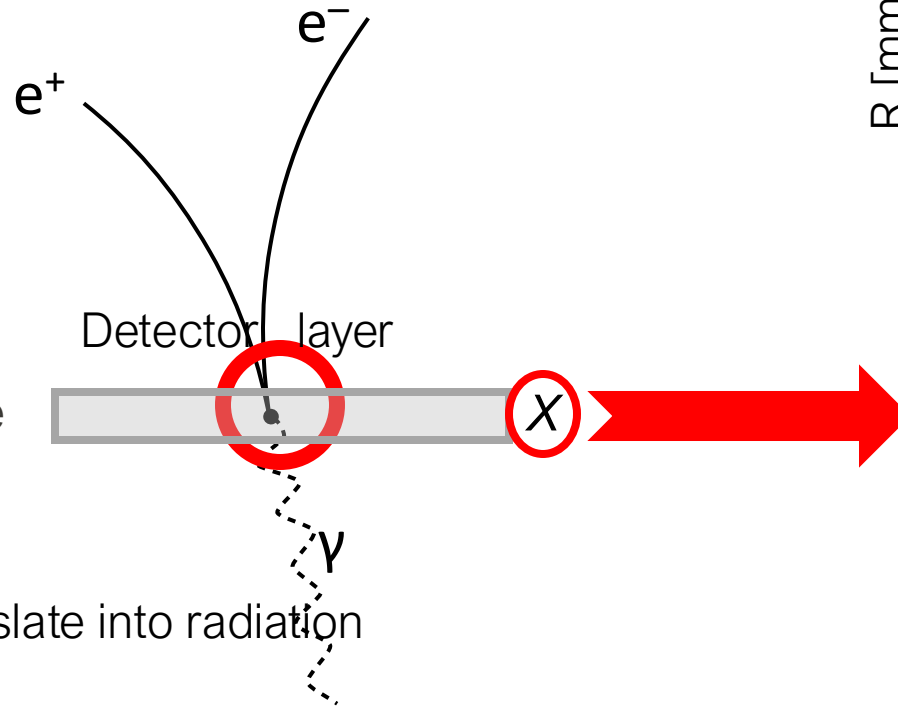


Dead Material: how to Measure it?

... via photon conversion

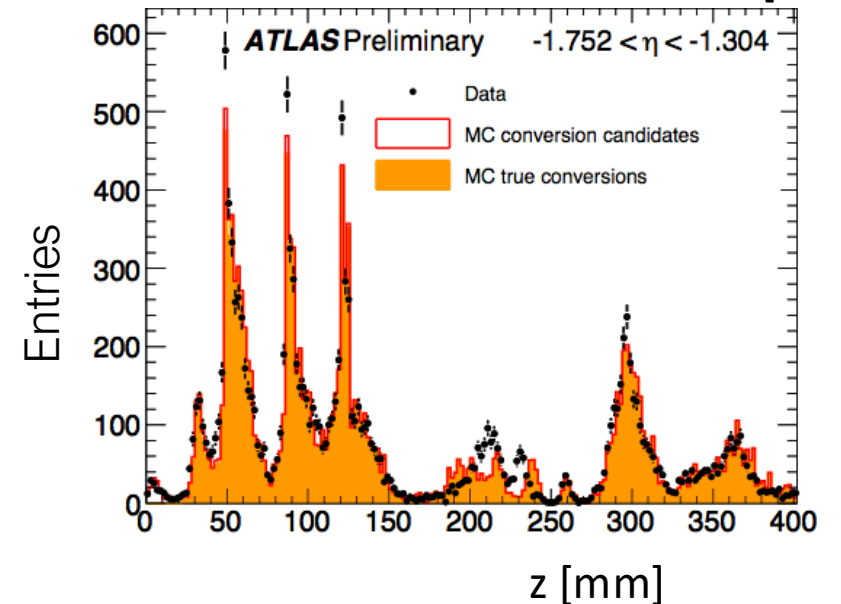
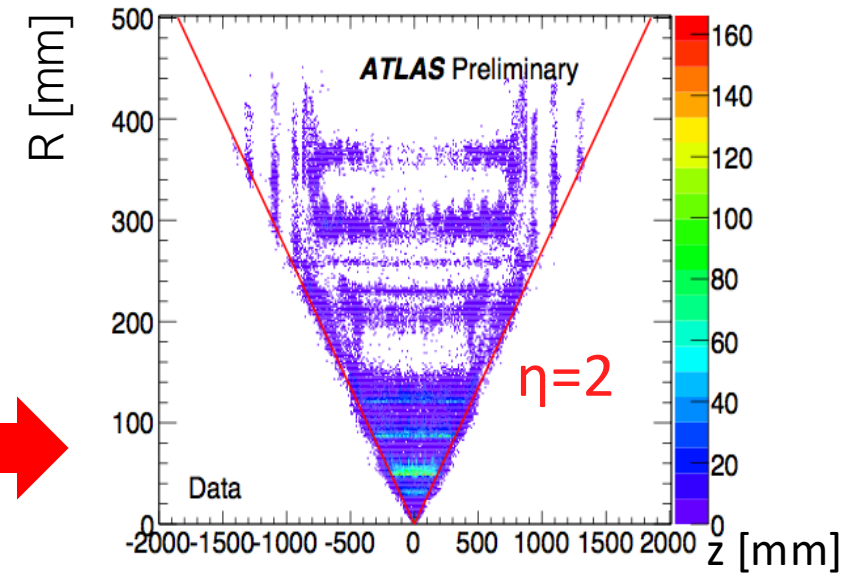
Selection:

- Two oppositely charged tracks with $p_T > 0.5$ GeV
- Small distance between tracks
- Good vertex; zero opening angle
- Well reconstructed tracks



Fraction of converted photons translate into radiation length

$$\frac{X}{X_0} = -\frac{9}{7} \ln(1 - F_{\text{conv}})$$



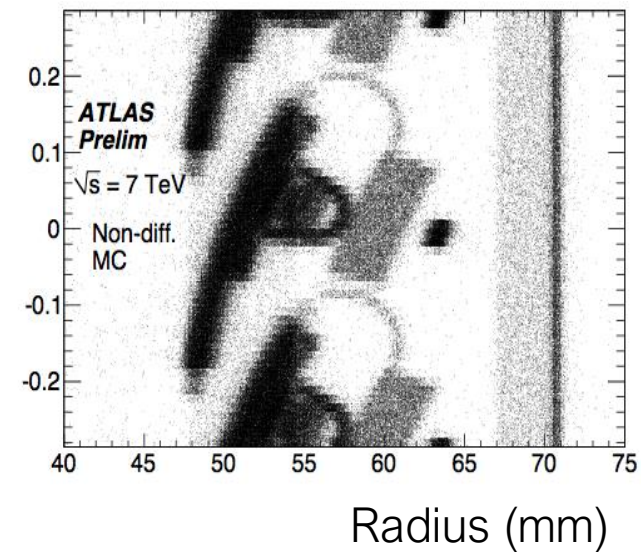
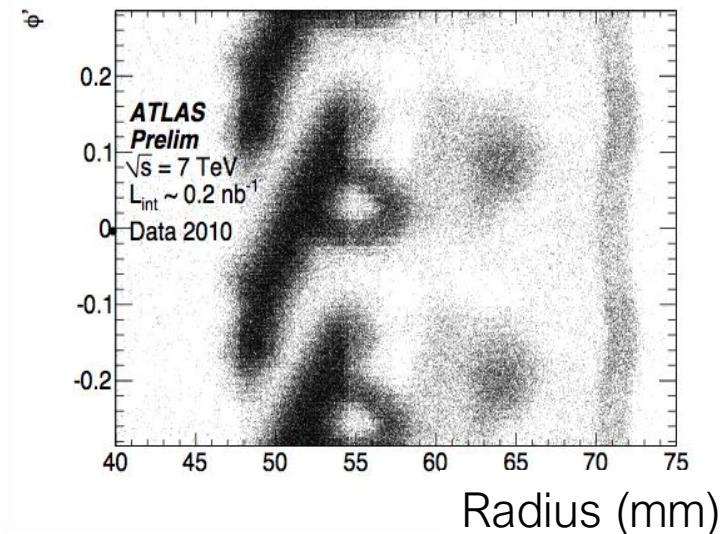
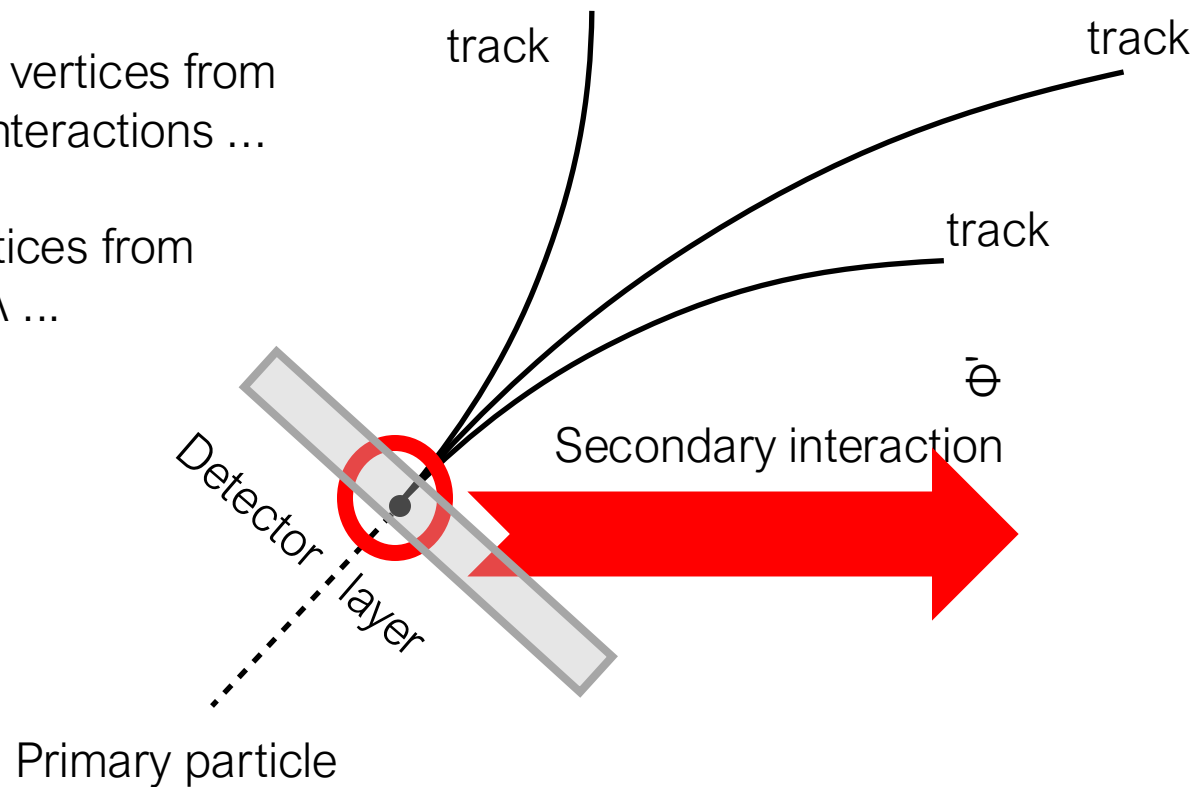


Hadronic Secondary Interactions

... via secondary vertices

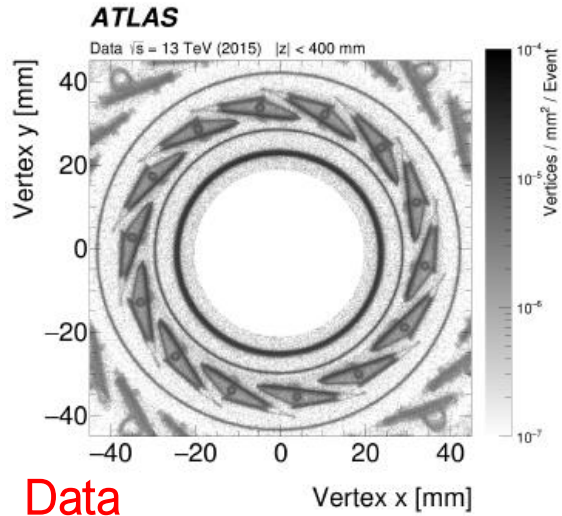
Reconstruct vertices from secondary interactions ...

Remove vertices from Kaons and Λ ...



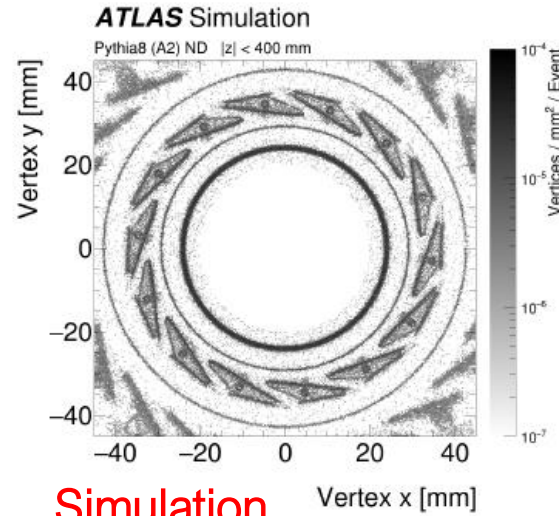


Radiography of the Detector



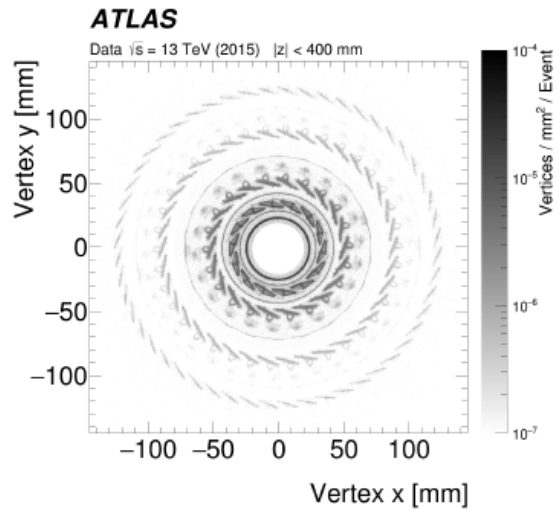
Data

(a)



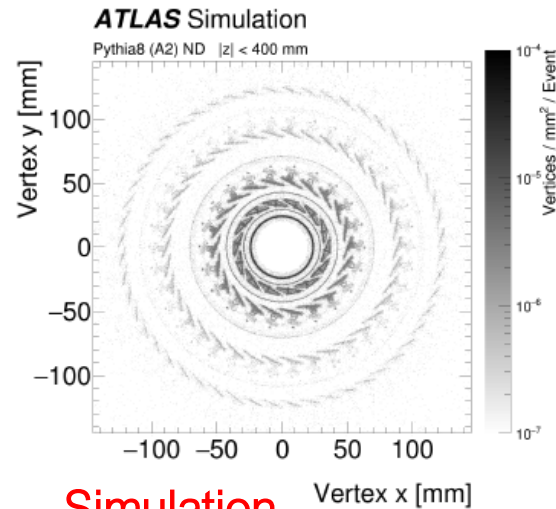
Simulation

(b)



Data

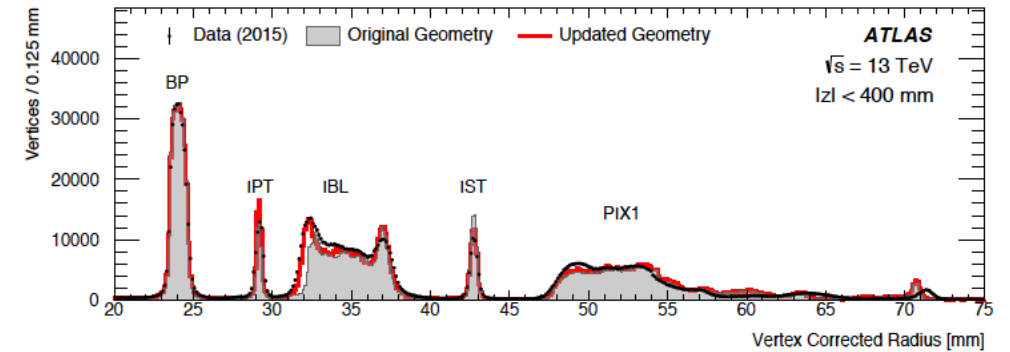
(c)



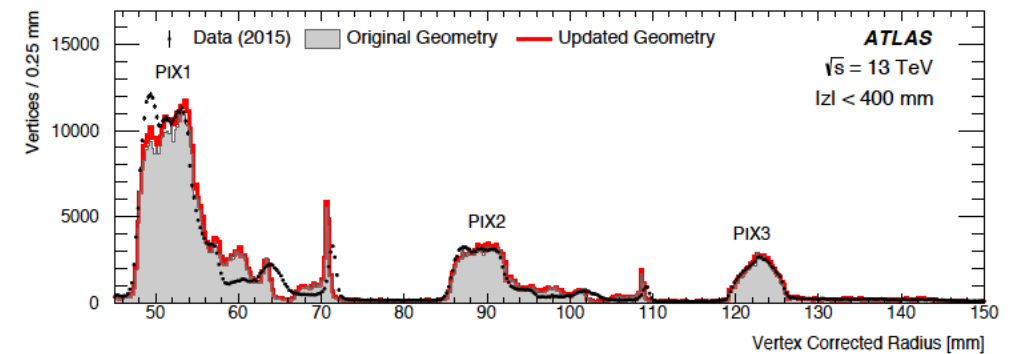
Simulation

(d)

(a), (b) The x-y view zooming-in to the beam pipe, IPT, IBL staves
(c), (d) of the pixel detector.



(a) 20 mm < r < 75 mm.



(b) 45 mm < r < 150 mm.



Time Evolution of Material Budget

TABLE 5 Evolution of the amount of material expected in the ATLAS and CMS trackers from 1994 to 2006

| Date | ATLAS | | CMS | |
|---------------------------------|------------------|--------------------|------------------|--------------------|
| | $\eta \approx 0$ | $\eta \approx 1.7$ | $\eta \approx 0$ | $\eta \approx 1.7$ |
| 1994 (Technical Proposals) | 0.20 | 0.70 | 0.15 | 0.60 |
| 1997 (Technical Design Reports) | 0.25 | 1.50 | 0.25 | 0.85 |
| 2006 (End of construction) | 0.35 | 1.35 | 0.35 | 1.50 |

The numbers are given in fractions of radiation lengths (X/X_0). Note that for ATLAS, the reduction in material from 1997 to 2006 at $\eta \approx 1.7$ is due to the rerouting of pixel services from an integrated barrel tracker layout with pixel services along the barrel LAr cryostat, to an independent pixel layout with pixel services routed at much lower radius and entering a patch panel outside the acceptance of the tracker (this material appears now at $\eta \approx 3$). Note also that the numbers for CMS represent almost all the material seen by particles before entering the active part of the crystal calorimeter, whereas they do not for ATLAS, in which particles see in addition the barrel LAr cryostat and the solenoid coil (amounting to approximately $2 X_0$ at $\eta = 0$), or the end-cap LAr cryostat at the larger rapidities.



Reconstruction

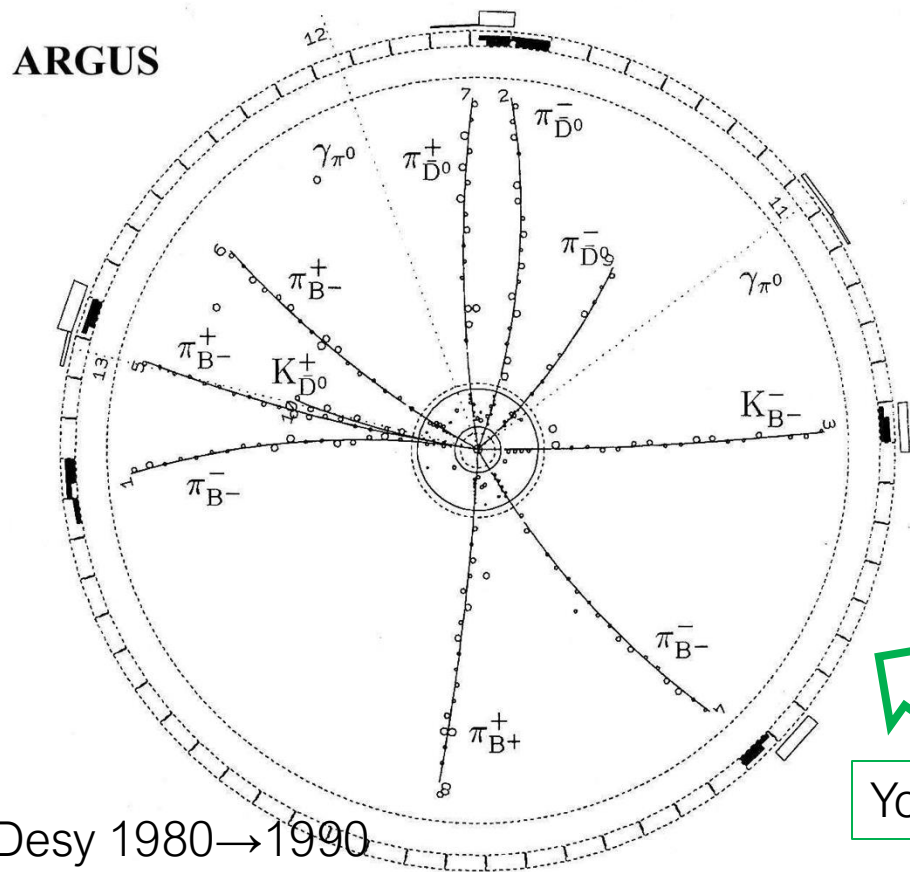
Reconstruction



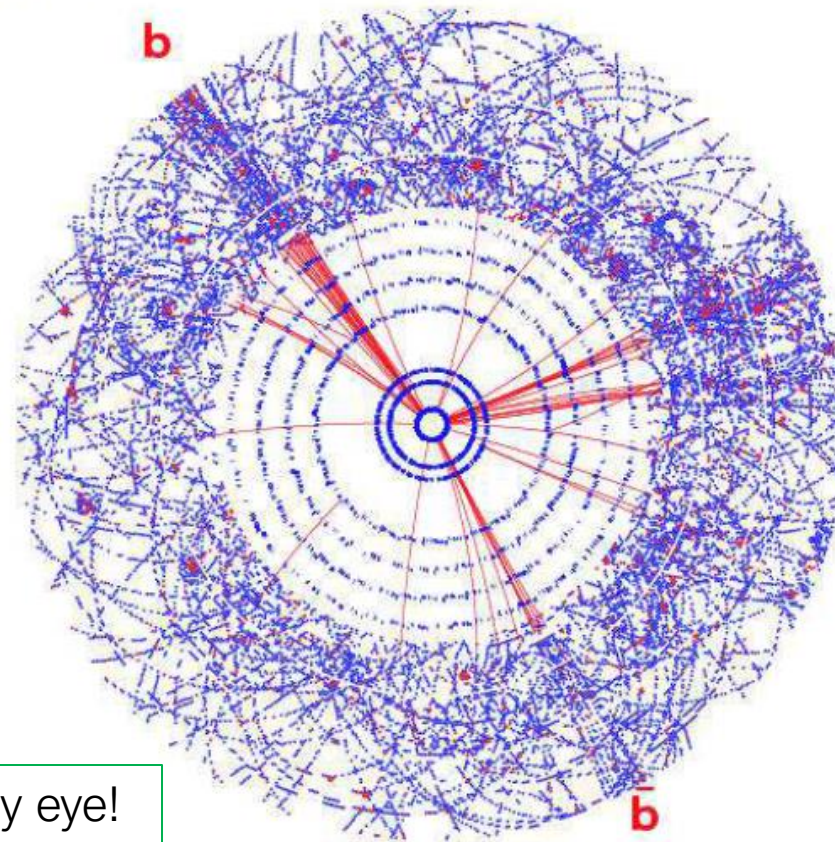
Pattern Recognition

How to find which measurements (*) (hits) make a track and have to be fitted to compute a trajectory?

ATLAS



You see by eye!



Invisible by eye!

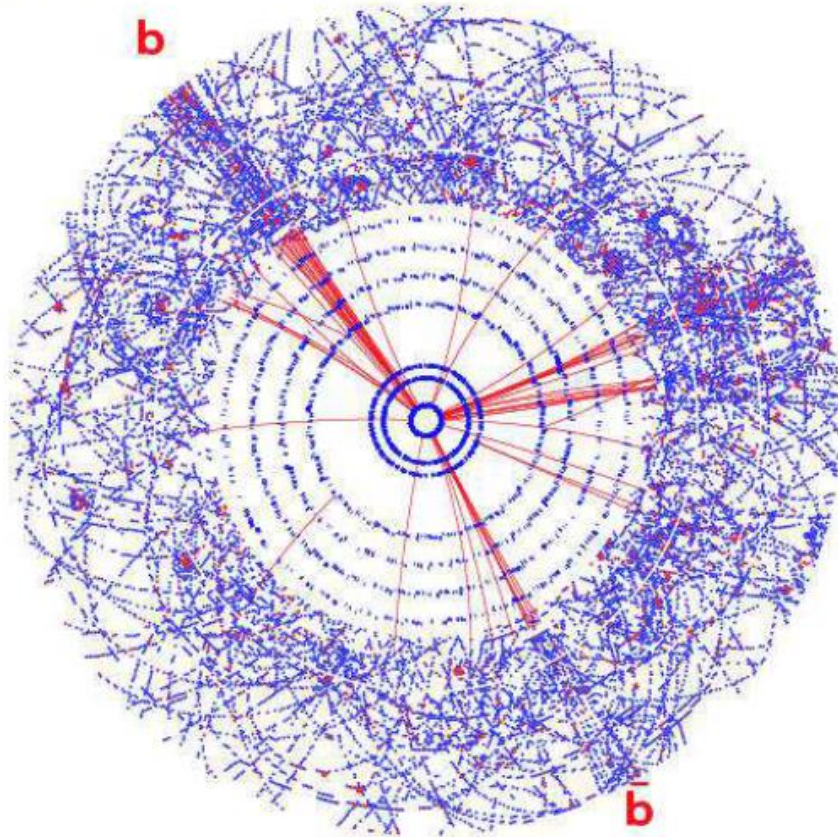
Simulated event:
 $H_0 \rightarrow b\bar{b}$

(*) One possible set of track parameters:

$$d_0, z_0, \phi_0, \vartheta_0, q/p \text{ (or tangent of the angles)}$$

Complexity of Collider Experiments

ATLAS



Invisible by eye!

Simulated event:
 $H_0 \rightarrow b\bar{b}$

In modern Experiments, already at the time the experiment is designed, you need to consider/know

- How different detectors contribute to the analysis of one single *feature* (=characteristic)
- How your analysis programs will solve the problem of very crowded and complex topologies
- → it is more and more difficult to think in terms of single/isolated detectors
- → it is more and more difficult to separate hardware and analysis programs

One Experiment = undistinguishable ensemble of many detectors and of analysis programs

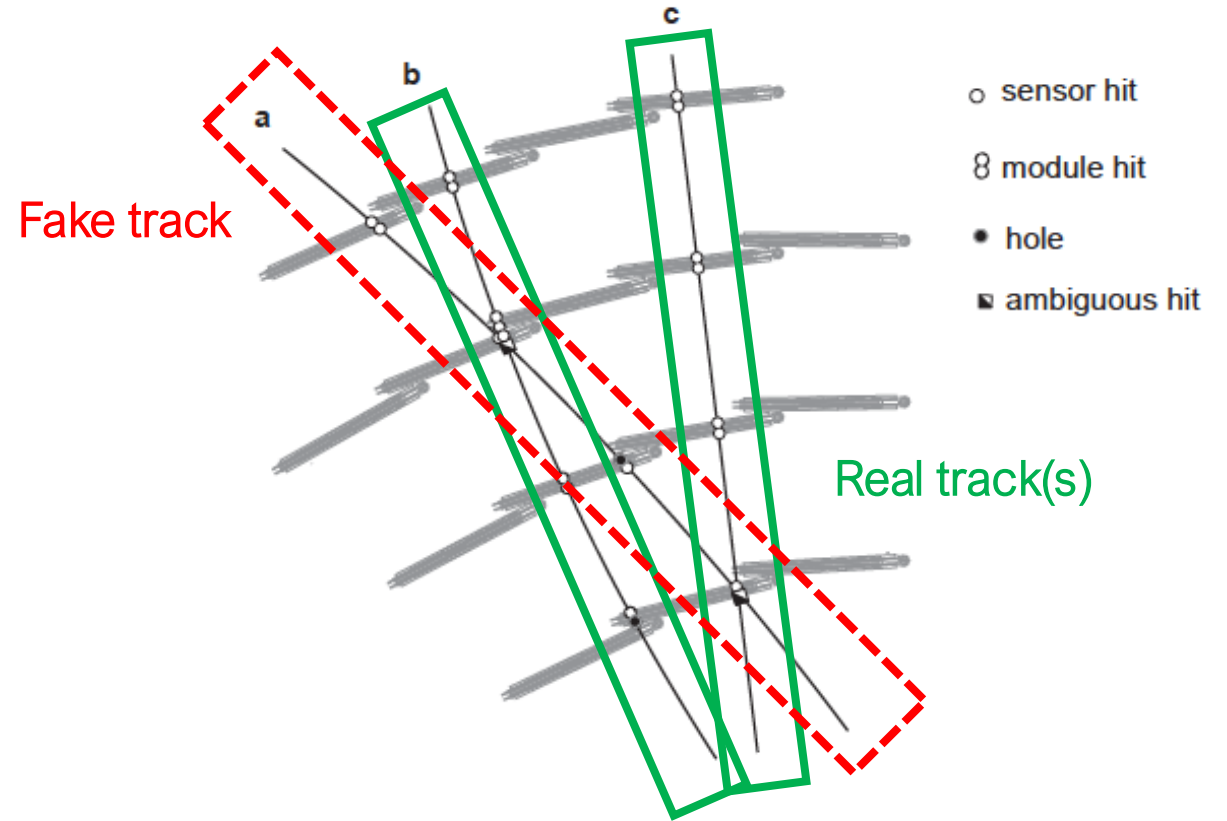
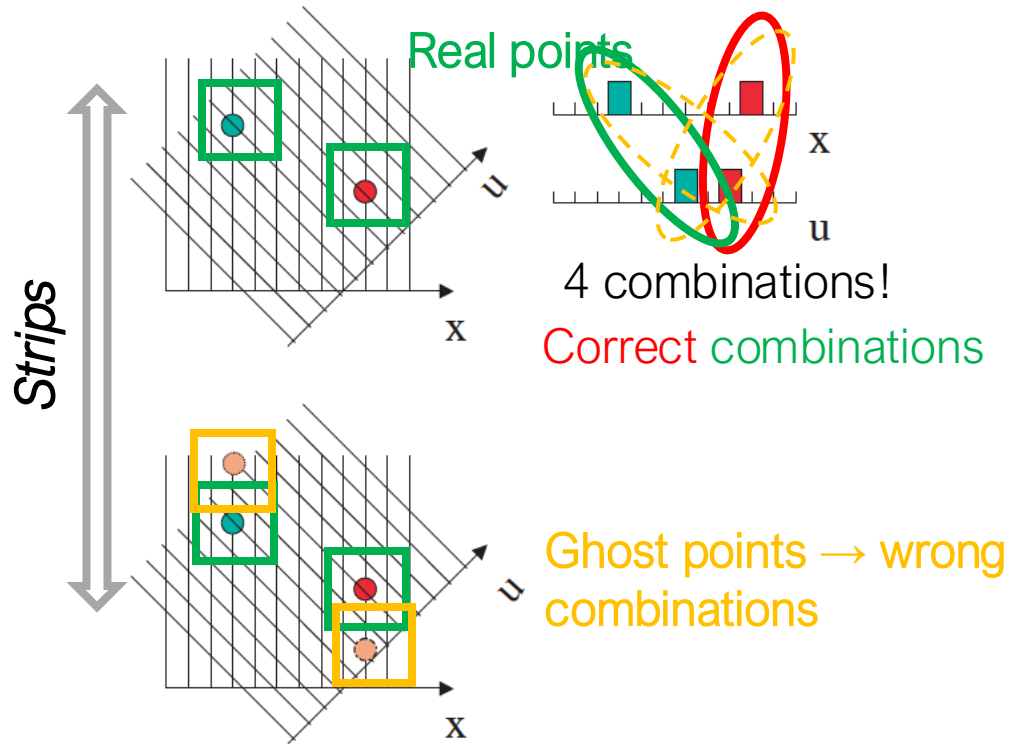


Ambiguities in Pattern Recognition (~History)

How to find **which measurements (*) (hits) make a track** and **have to be fitted to compute a trajectory?**

In some cases you may arrange your detector to give you an indication \rightarrow u,v geometry

In some other cases you may have to 'score' your points

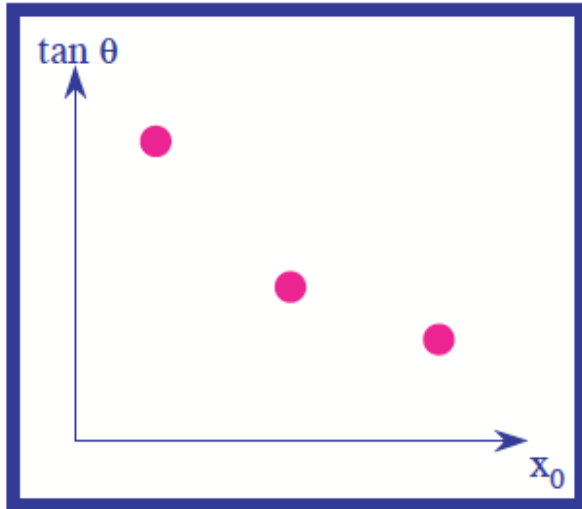


(*) One possible measurement: (impact parameter, direction and momentum) $d_0, z_0, \phi_0, \vartheta_0, q/p$



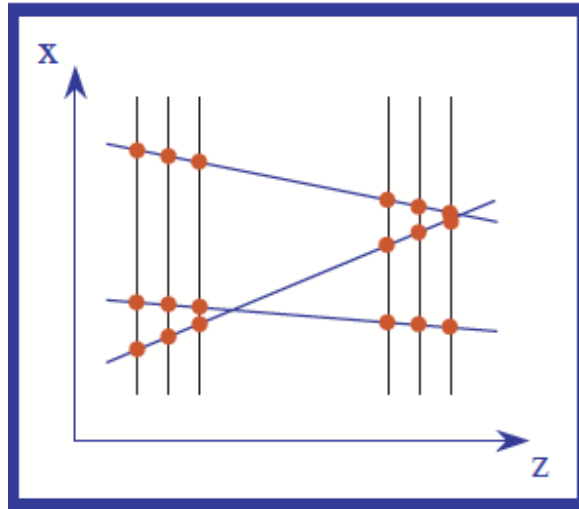
Basic Ideas in Pattern Recognition

Feature Space



Three tracks are defined by $\tan(\theta)$ and x_0

Pattern Space



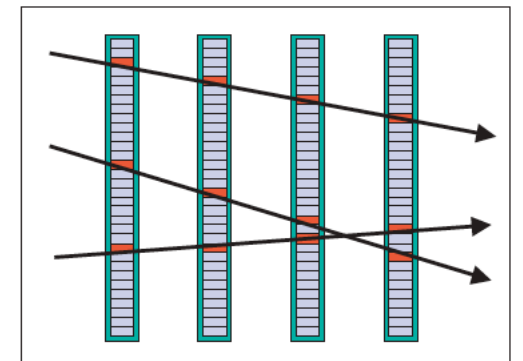
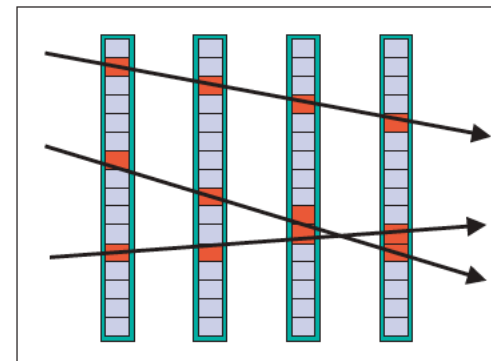
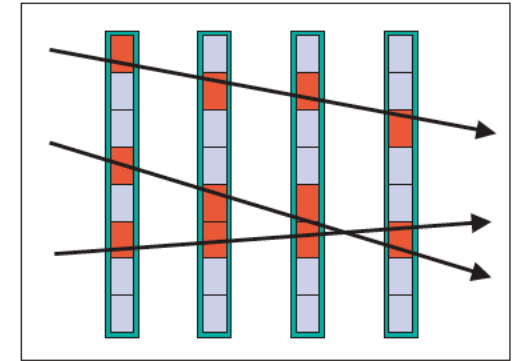
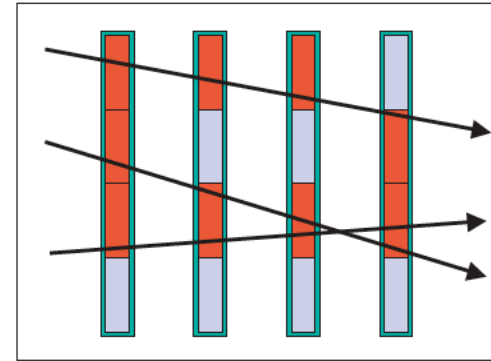
They appear like this in your detector



The goal of Pattern recognition is going from Pattern Space to Feature Space

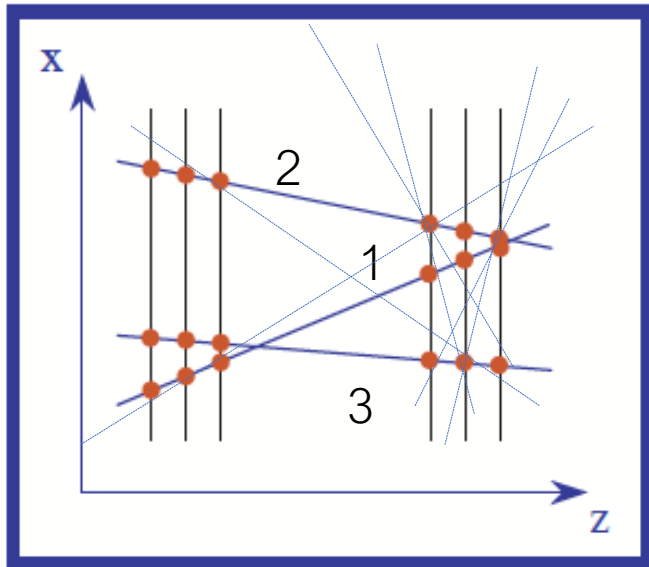
Templates are checked with increasing granularity

1. templates: if a limited set of topologies \rightarrow create a 'road' and compare it with your measurements. A correct 'road' will include a large number of points. Works for simple and few topologies

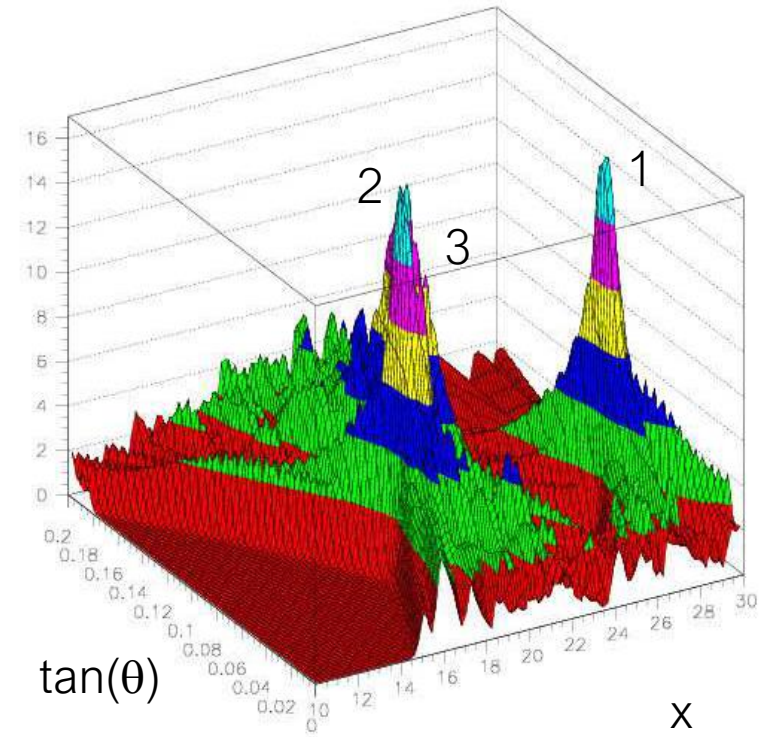
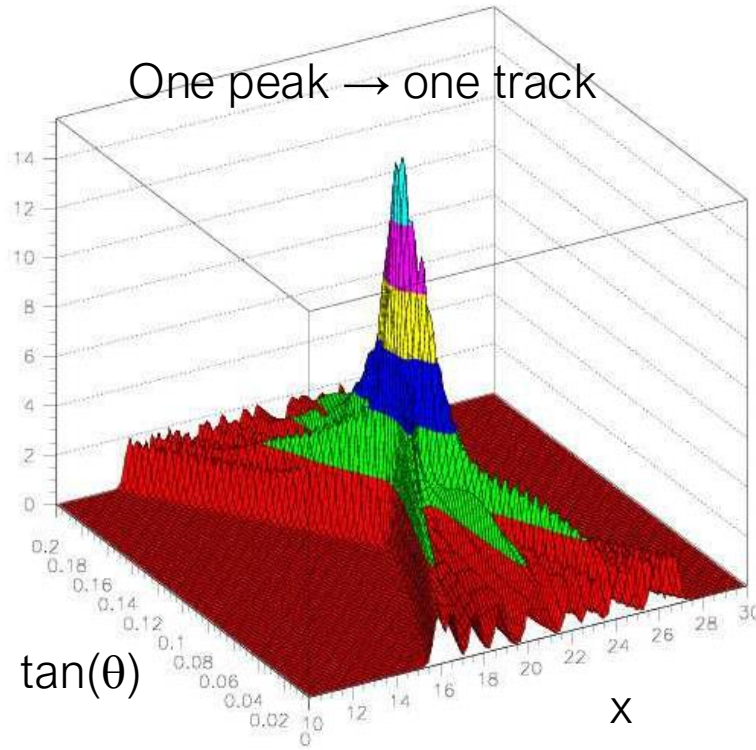


Hough Transform

Pattern Space



(only a few shown...)



2. Hough transform.

- Join all possible pairs of points with a line characterised by $\tan(\theta)$ and x_0 .
- each pair of hits in two dimensions becomes a line;
- real track, \rightarrow many aligned points \rightarrow same $\tan(\theta)$ and $x_0 \rightarrow$ peak in the 'Feature Space'.
- Wrong associations \sim flat distribution.

\rightarrow one peak indicates one track \rightarrow look for peaks

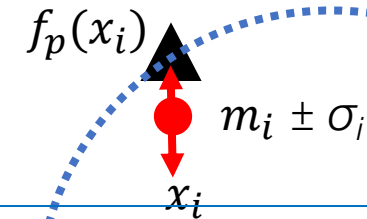


After Pattern Recognition: Track Fitting (~Old Way)

Use the least squares principle to estimate the kinematical parameters of a particle = track fitting.

Definition of "Chi Squared":

$$\chi^2 = \sum_i \frac{(m_i - f_p(x_i))^2}{\sigma_i^2}$$



Physical meaning: distance between fit function and hit normalised to measurement error

- measured points $m_i \pm \sigma_i$ (at position x_i) of a track have been correctly identified in the *pattern recognition step*.
- trajectory of a particle is described by an analytic expression f_p
 - p is the set of parameters → the momentum in B field is one parameter
 - $f_p(x_i)$ is the coordinate predicted by the function (f might be a circle in a solenoid or a straight line)

Find the set of parameters p that minimises the χ^2

Meaning: you find which is the trajectory which minimises the difference² between all measurements and trajectory

Better approach: include also multiple scattering and energy losses

$$\chi^2 = \sum_{meas} \frac{r_{meas}^2}{\sigma_{meas}^2} + \sum_{scat} \left(\frac{\theta_{scat}^2}{\sigma_{scat}^2} + \frac{(\sin \theta_{loc})^2 \phi_{scat}^2}{\sigma_{scat}^2} \right) + \sum_{Eloss} \frac{(\Delta E - \overline{\Delta E})^2}{\sigma_{Eloss}^2}$$

$$r_{meas}^2 = residual^2 = (difference\ measurement - function)^2$$



(~Modern) Pattern Recognition

In past experiments the track reconstruction consisted of two steps (possible in 'old' experiments):

- Pattern recognition
- Track fit

In modern track reconstruction, finding + fitting a track at the same time
no clear distinction between pattern finding and track fitting.

As a consequence, the full chain of pattern recognition and track fitting will be a single unit.

The ATLAS / CMS track finding / fitting currently consists of three sequences



1. the *main inside-out track reconstruction* (start with a seed defined by the beam spot and the innermost hits of the vertex detector)
2. Followed by a consecutive outside-in tracking (recover ~unused / unassigned hits)
3. As a third sequence, the pattern recognition for the finding of V_0 vertices, kink objects due to bremsstrahlung and their associated tracks follows



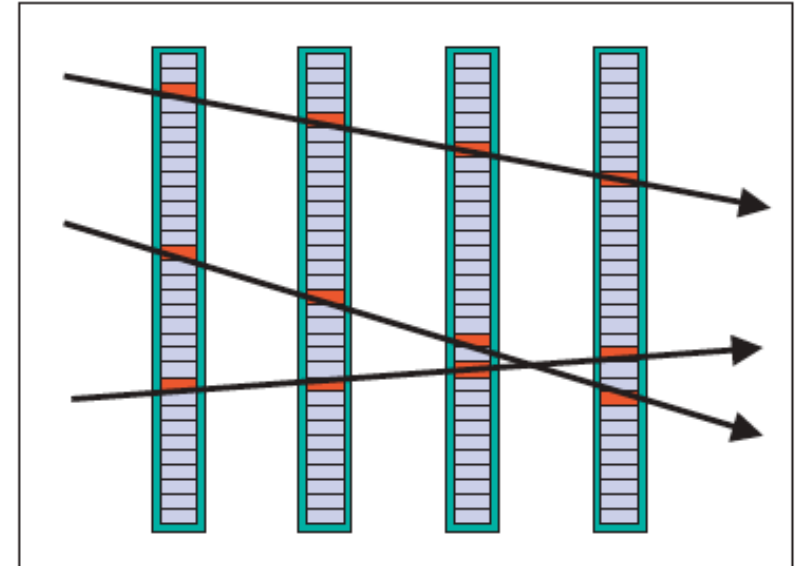
Track Fitting and Kalman Filter (~ Modern Way)

The X^2 method is not always convenient:

1. You need to have all points attributed to one track **before** the fit
2. It is expensive in terms of computing-time: **a large number of points have to be handled in the X^2 fit: # measurements x # parameters of each measurement**
3. to be repeated for many tracks!

$$N_{tracks} \cdot N_{hits} \cdot N_{parameters}$$

→ use pattern recognition methods which are based on **track following**, where it is not clear a-priori the right hit combination



track following == the path is not clear a-priori → the direction becomes clearer as you follow the trajectory
→ Kalman filter technique

The Kalman filter proceeds progressively from one measurement to the next, improving the knowledge about the trajectory with each new measurement.

With a traditional global fit, this would require a time consuming complete refit of the trajectory with each added measurement.



Kalman Filter in a Cartoon

Goal: compute X , observable using a sequence of measurements ($k=1,2,\dots$ indicates successive measurements/states)

Kalman filter is an iterative procedure

- Starts from a seed (2 hits)
- Extrapolates and includes next hit; accounts for material, multiple scattering, energy loss
- Recalculates track parameters, refines extrapolation

Hits left?

Yes

No

$$x_k = F_k \cdot x_{k-1}$$

x_{k-1} : 'state' at 'time k-1'

F_k : 'Transfer matrix'

x_k : 'new state' at 'time k'

1 (2 hits)

3 (4 hits)

4 (5 hits)

2 (3 hits)

- → does not require handling of all $k+1$ hits, only one measurement (~ 1 hit) + parameters of state before → very fast algorithm.
- → *Random trajectory perturbations, (multiple scattering or energy loss) can be accounted for efficiently.*



Kalman Filters

Kalman Filter approach consists of two steps:

- **The prediction step**: extrapolate current trajectory (state vector) to next measurement from the \rightarrow discard noise signals and hits from other tracks.
- **The transfer step**, which updates the state vector

System state vector at the time k includes $k-1$ measurements and contains the parameters of the fitted track, given at the position of the k^{th} hit (including hits before!)

The corresponding measurement errors **covariance matrix** (contains measurement errors) by C_k .

The **matrix F_k** describes the propagation of the track parameters from the $(k - 1)^{\text{th}}$ to the k^{th} hit.

Example: planar geometry with one dimensional measurements and straight-line tracks

$t_x = \tan \theta_x$ the track slope in the xz plane,

$F_k =$ transfer matrix

$$\mathbf{x}_k = F_k \cdot \mathbf{x}_{k-1}$$

State vector
@ measurement k

$$\begin{pmatrix} x \\ t_x \end{pmatrix}_k = \begin{pmatrix} 1 & z_k - z_{k-1} \\ 0 & 1 \end{pmatrix} \begin{pmatrix} x \\ t_x \end{pmatrix}_{k-1}$$

State vector
@ measurement $k-1$

$$\rightarrow x_k = x_{k-1} + t_x \cdot (z_k - z_{k-1})$$

$$\rightarrow t_x = t_x @ (k - 1)$$



Propagation of States

The extrapolation from one state to another (in page before) is valid in general:

$$x_k = F_k \cdot x_{k-1}$$

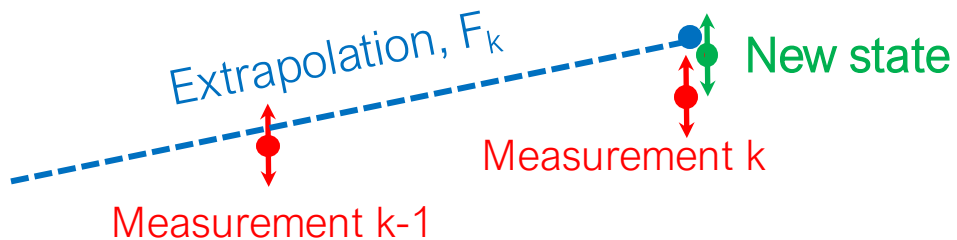
The transfer matrix F_k transports the state x_{k-1} (at the measurement point 'k-1') to the next state x_k at measurement point k

Error on track parameters

$$C_k = F_k C_{k-1} F_k^T + Q_k$$

- C_k is the error matrix extrapolated from the state x_{k-1} (generally called Covariance Matrix). It contains errors on measurements (diagonal terms) but also the correlation among different terms.

A new term appears: Q_k is due to 'random' perturbations to the particle trajectory (mostly) multiple scattering
→ ~ exact knowledge of material distribution



- We extrapolated the state x_{k-1} from measurement k-1 to state x_k at measurement point k
- We have to include new measurement k. The formalism is a bit complicated and can be found in reference (*)

A Kalman-Filter approach is used in modern collider experiments

(*) [Pattern Recognition and Event Reconstruction in Particle Physics Experiments: R. Mankel1](#)



Vertices in Events Produced at LHC

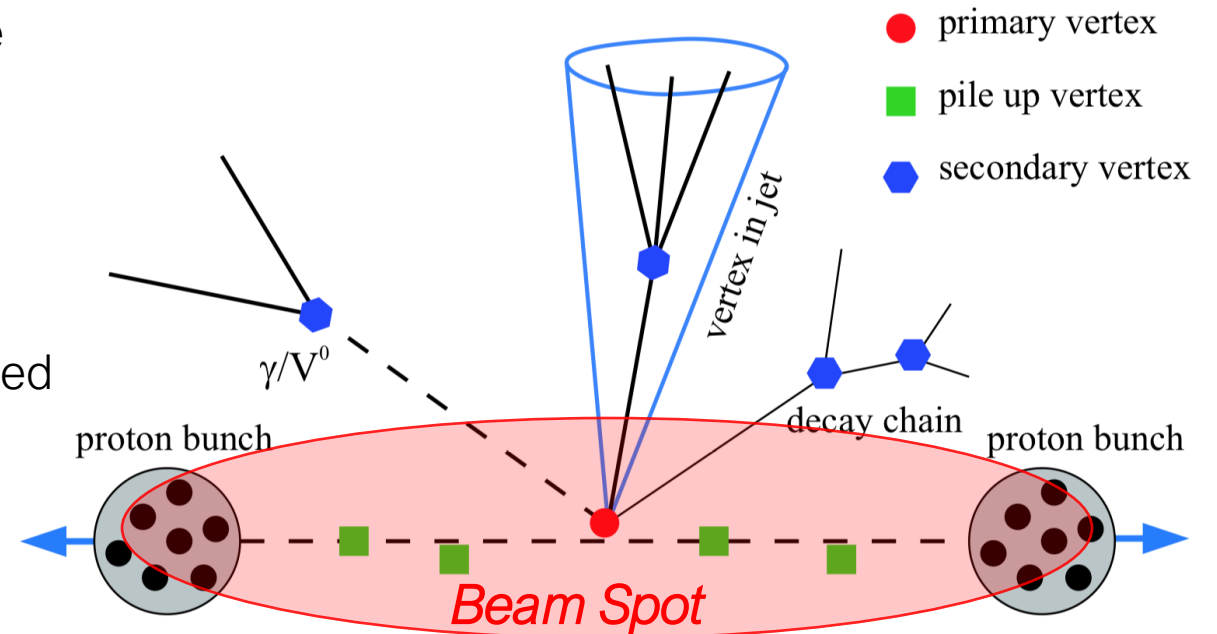
The recording of one event is started by the 'trigger system' that detects 'interesting characteristics'

→ primary vertex

→ during the time window of the trigger more than one interaction takes place → Pile-up vertices (*next slide*)

Collision event:

- One primary vertex from the hard inelastic collision
- Several pile-up vertices (pp interactions, superimposed to the *triggered* primary vertex)
- Secondary vertices are produced due to
 - ✓ Decay-chain: decays of long-lived b-particles decaying into c-particles (tertiary vertex)
 - ✓ (V^0) Decays of neutral particles (like photon conversions into electron pairs $\gamma \rightarrow e^+e^-$)



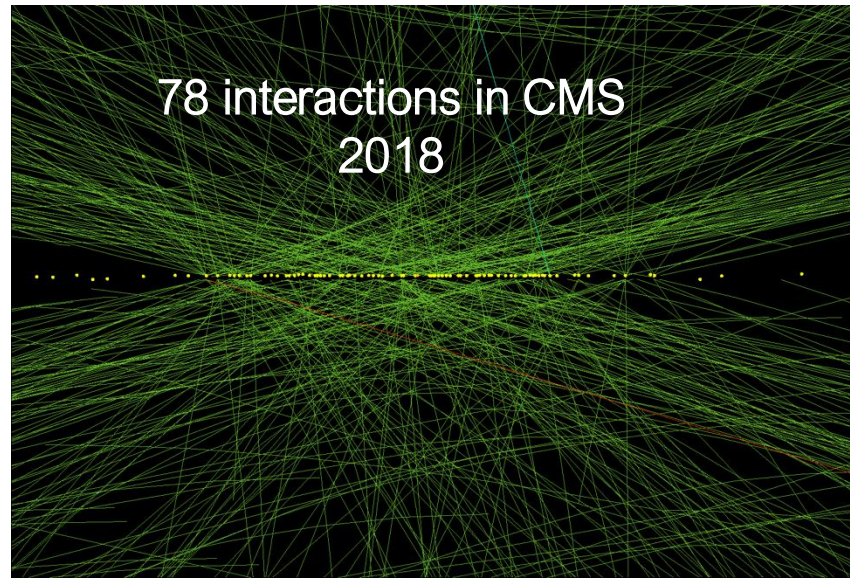
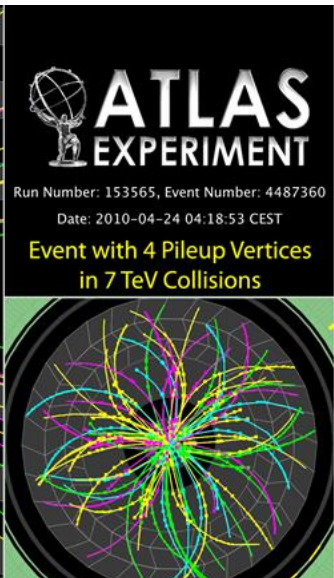
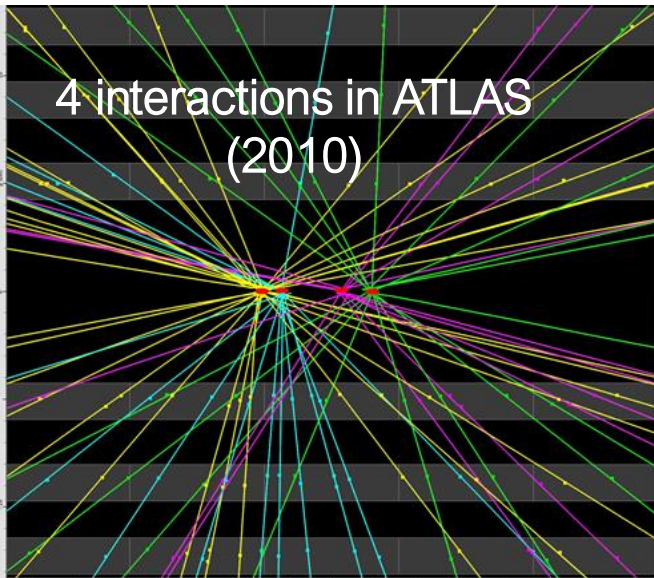
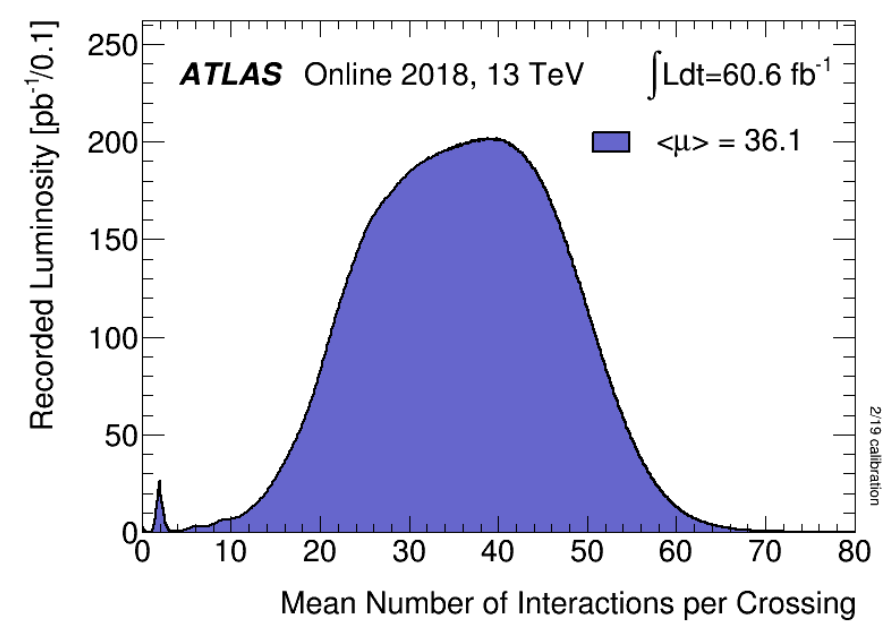
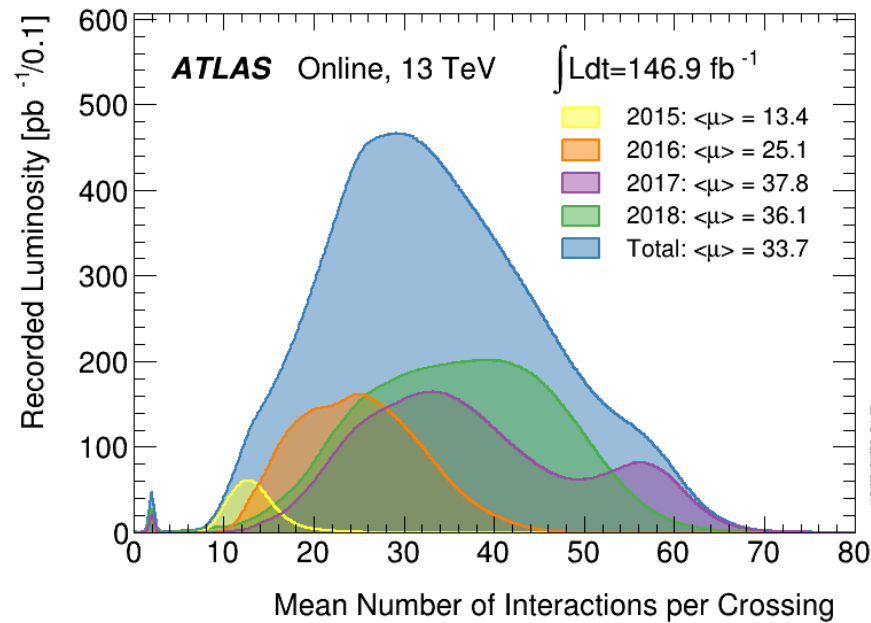


$$\langle \mu \rangle = \langle \text{Num. of interactions in 1 bunch} \rangle$$

Pile-up

The luminosity (\rightarrow intensity of the beams at LHC) is so high than MANY interactions occur during the same bunch crossing. \sim Only one (at most) is interesting \rightarrow **hard inelastic collision**

FILTER EVENTS!



- 2015: $\langle \mu \rangle = 13.4$
- 2016: $\langle \mu \rangle = 25.1$
- 2017: $\langle \mu \rangle = 37.8$
- 2018: $\langle \mu \rangle = 36.1$
- Total: $\langle \mu \rangle = 33.7$

Time \uparrow Pile-up \uparrow



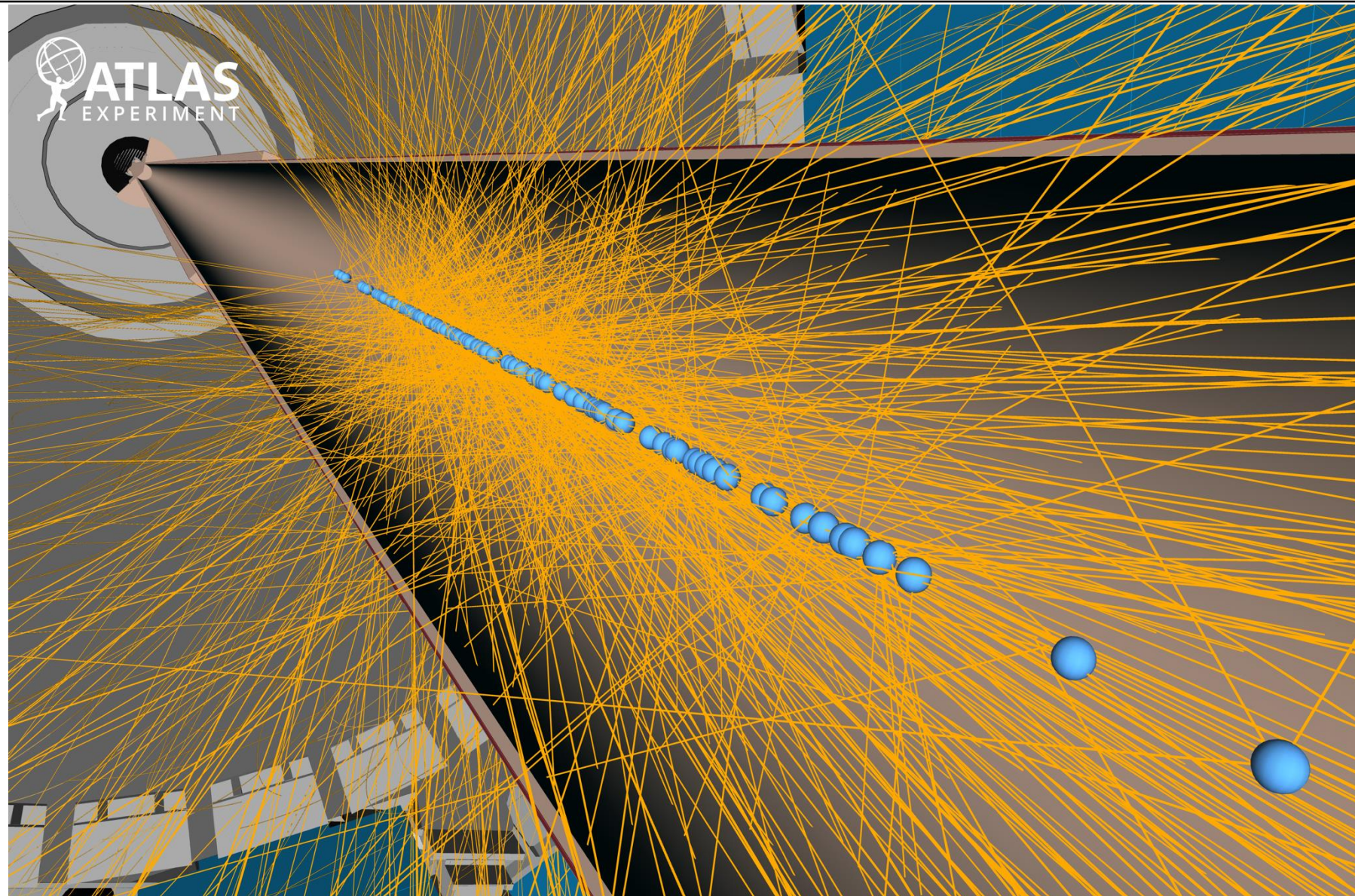
One simulated event with 88 reconstructed vertices

A visualisation of simulated $t\bar{t}$ quark pair production in a pp collision at

14 TeV HL-LHC

The simulated event includes approximately

- 200 pileup interactions in the same bunch crossing
- 88 primary vertices (blue balls) reconstructed along the beam line.

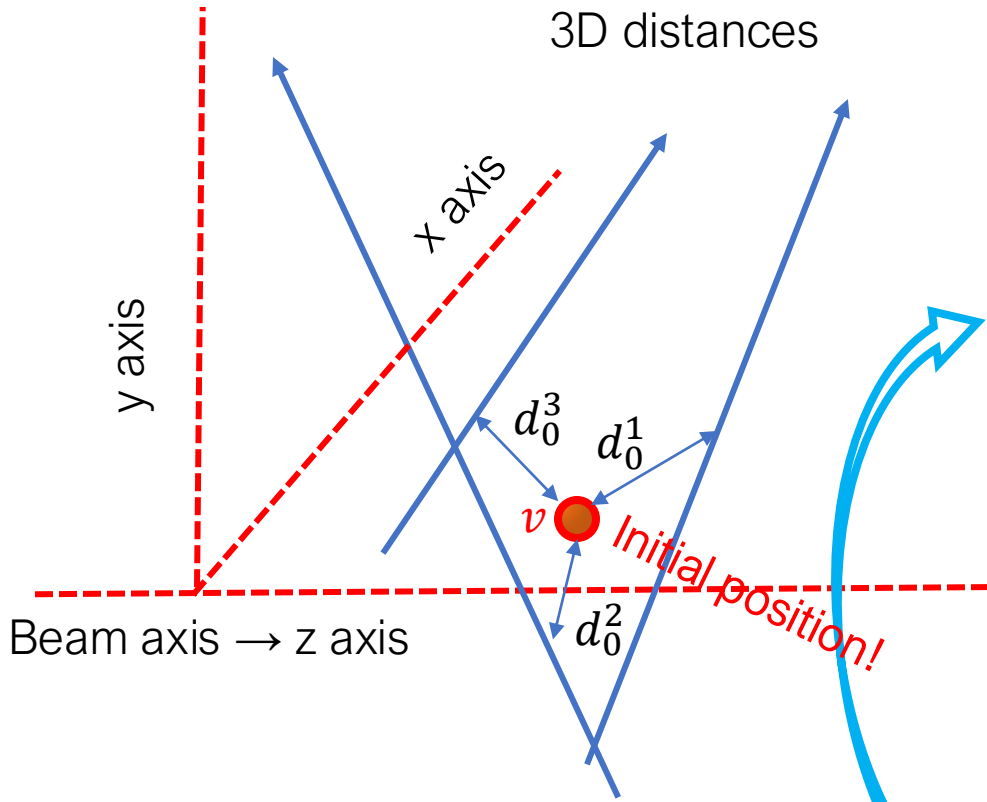




Vertex Finding and Fitting

$d_0^i = \text{distance of minimum approach of track } i \text{ to 3D vertex "v"}$

$\sigma_i = \text{error on } d_0^i$



Vertex fitting: identification of a vertex and computation of its 3D position. It is based on the use of **distance of minimum approach d_0^i between good quality tracks to the vertex (impact parameter).**

1. Start with a seed (beam spot of interaction region)
2. Compute distances of all tracks from vertex v and weight distances with a weight computed using formula

$$w_i(\chi_i^2) = \frac{\exp(-\chi_i^2/2T)}{\exp(-\chi_i^2/2T) + \exp(-\chi_c^2/2T)}$$

3. Minimize

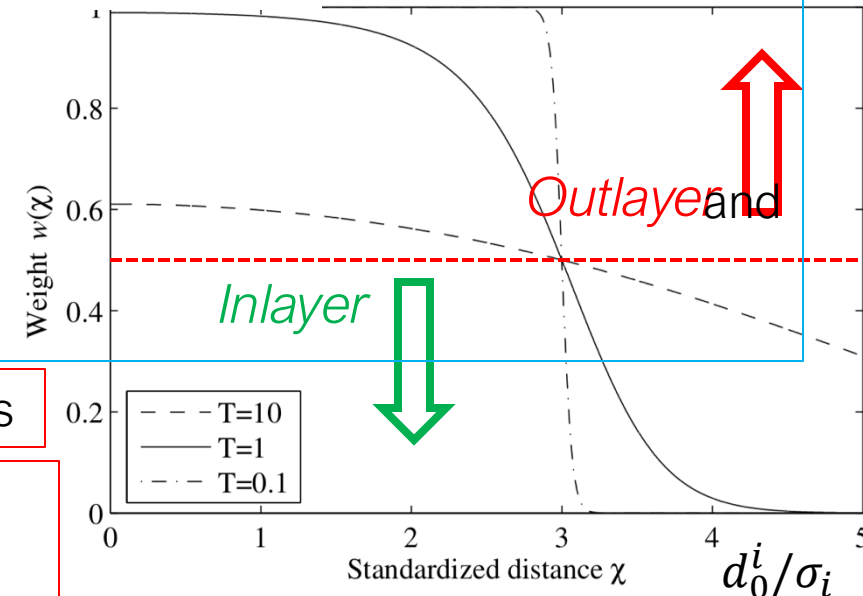
$$\frac{1}{2} \sum_{i=1}^n d_i^2(v) / \sigma_i^2$$

find new v

4. Vertex $v_n = v_{n-1}$?

No → Lower T

Yes



What counts is the ratio d_0^i / σ_i

No improvement during last step, vertex found. Remove tracks incompatible with vertex ($w_i < 0.5$) and use them for a secondary vertex



EM – Calorimetry: Calibration

Going from an electronic signal to an energy deposition: a long way...

Use test signals and

$Z \rightarrow e^+e^-$ and $J/\psi \rightarrow e^+e^-$ events

$$E_{\text{cell}} = F_{\mu\text{A} \rightarrow \text{MeV}} \times F_{\text{DAC} \rightarrow \mu\text{A}} \times \frac{1}{\frac{M_{\text{phys}}}{M_{\text{cali}}}} \times G \times \sum_{j=1}^{N_{\text{samples}}} a_j (s_j - p),$$

s_j : what you measure

← Direction of motion

current to deposited energy $F_{\mu\text{A} \rightarrow \text{MeV}}$ converts Signal (ADC) current in μA ;

$$E_{\text{cell}} = F_{\mu\text{A} \rightarrow \text{MeV}} \times F_{\text{DAC} \rightarrow \mu\text{A}}$$

Equalisation of physical and calibration pulses.

$$\frac{M_{\text{phys}}}{M_{\text{cali}}} \times \frac{1}{\frac{M_{\text{phys}}}{M_{\text{cali}}}} \times G \times \sum_{j=1}^{N_{\text{samples}}} a_j (s_j - p),$$

s_j digital signal (ADC)

p electronic pedestal

weights from shape of the ionisation a_j

The cell gain G equalises response



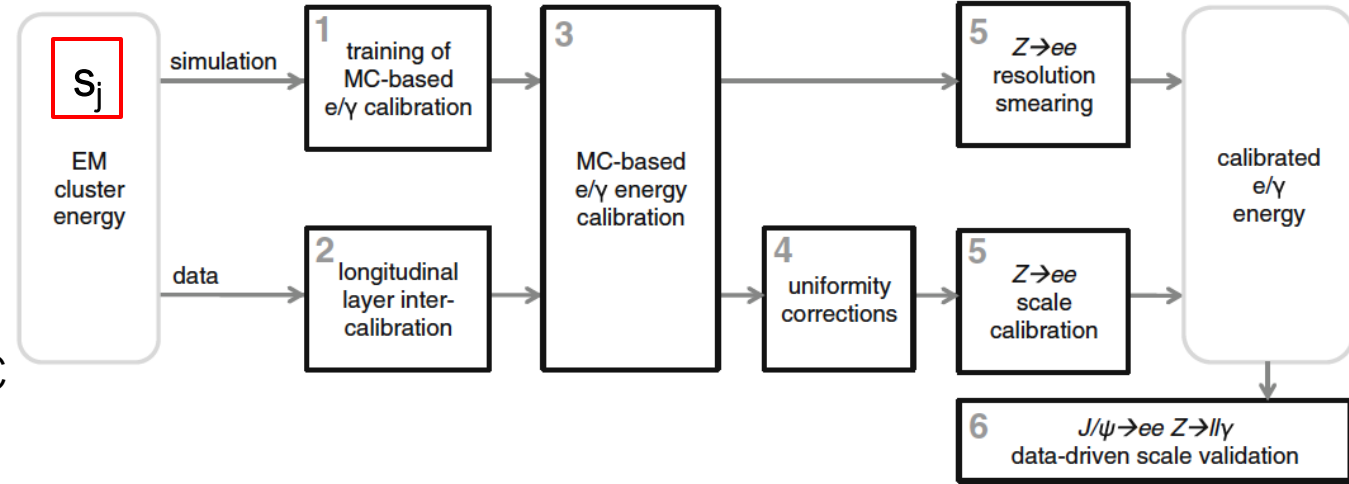
EM – Calorimetry: Calibration

From electronic signals to energy: a long way

$$E_{\text{cell}} = F_{\mu\text{A} \rightarrow \text{MeV}} \times F_{\text{DAC} \rightarrow \mu\text{A}} \times \frac{1}{\frac{M_{\text{phys}}}{M_{\text{cali}}}} \times G \times \sum_{j=1}^{N_{\text{samples}}} a_j (s_j - p),$$

- s_j are the digital signal digitised, measured in ADC counts
- p is the read-out electronic pedestal, measured in dedicated calibration runs;
- a_j weights are coefficients derived from the predicted shape of the ionisation
- The cell gain G is computed by injecting a known calibration signal and reconstructing the corresponding cell response. (**equalise response**)
- The factor $M_{\text{phys}}/M_{\text{cali}}$ quantifies the ratio of the maxima of the physical and calibration pulses

corresponding to the same input current, *corrects the gain factor G obtained with the calibration pulses to adapt it to physics-induced signals;*



- The factor $F_{\text{DAC} \rightarrow \mu\text{A}}$ converts digital-to-analog converter (DAC) counts set on the calibration board to a current in μA ;
- The factor $F_{\mu\text{A} \rightarrow \text{MeV}}$ converts the ionisation current to the total deposited energy at the EM scale and is determined from test-beam studies.

Calibration pulses and physical pulses are different



EM – Calorimetry: Absolute Calibration

Z and J/Ψ decays to a pair of e⁺e⁻ can be used to verify and adjust the calibration of EM calorimeters (but use also W → eν):

Well known! $m_{Z,J/\psi}^2 = (E_{e^+} + E_{e^-})^2 - (\vec{p}_{e^+} + \vec{p}_{e^-})^2 = f(E_{e^+}, E_{e^-}) \rightarrow$

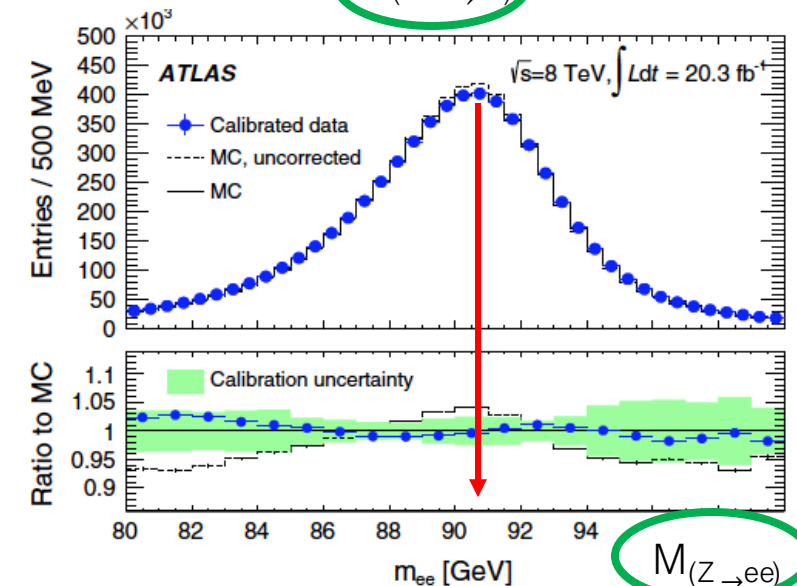
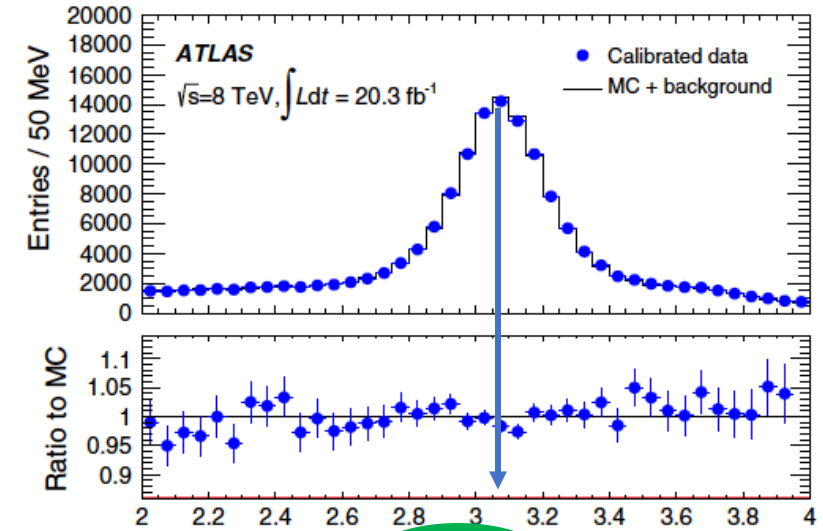
Find the transformation (simple example: $E^{corrected} = a \cdot E$), of the two energies that which gives the

- Correct mass of Z and J/Ψ
- Gives the narrowest invariant mass distribution

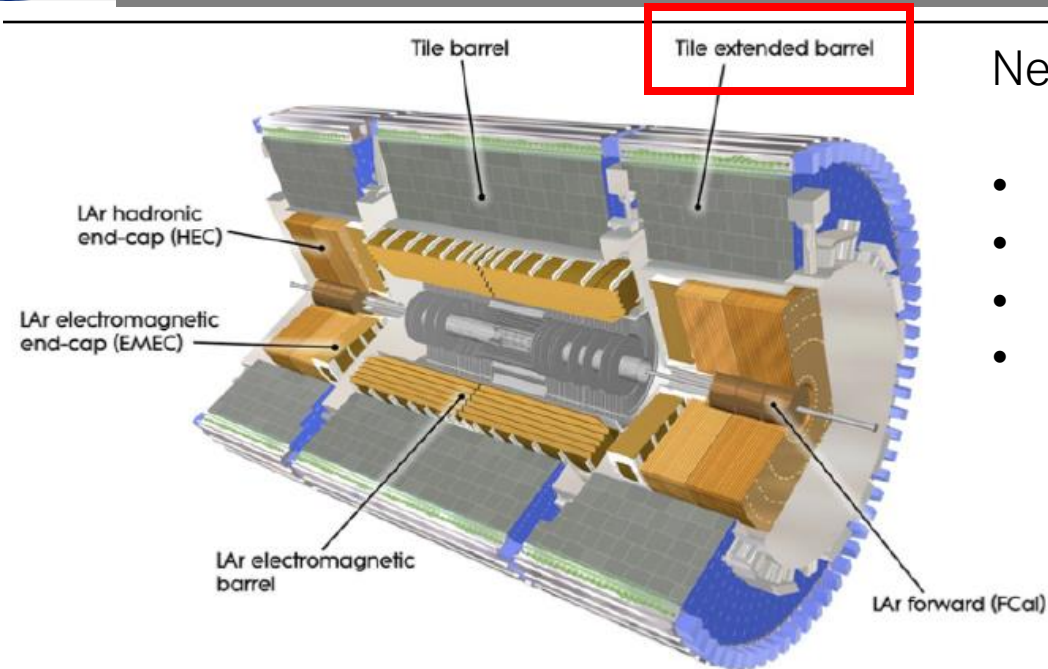
Use large samples of events → (and verify if the response is constant in different η, φ regions (*Also adjust MC!*)).

| Process | Selections | N_{data}^{events} |
|-------------------------|--|---------------------|
| $Z \rightarrow ee$ | $E_T^e > 27 \text{ GeV}, \eta^e < 2.47$ | 5.5 M |
| | $80 < m_{ee} < 100 \text{ GeV}$ | |
| $W \rightarrow e\nu$ | $E_T^e > 30 \text{ GeV}, \eta^e < 2.47$ | 34 M |
| | $E_T^{miss} > 30 \text{ GeV}, m_T > 60 \text{ GeV}$ | |
| $J/\psi \rightarrow ee$ | $E_T^e > 5 \text{ GeV}, \eta^e < 2.47$ $2 < m_{ee} < 4 \text{ GeV}$ | 0.2 M |

Different kinematic regions



Hadron Calorimetry (example: ATLAS)



Need: keep Hadron-Calorimeter cells calibrated at the % precision

- good jet and missing transverse energy performance
- jet energy scale (JES) is a measure of the uncertainty
- The JES is one of the main uncertainties in many physics results
- This uncertainty is illustrated in Fig. as a function of η for jets $p_T = 300\text{GeV}$. In the central η region the uncertainty is $\sim 1\%$.

Mostly used for jets reconstruction.

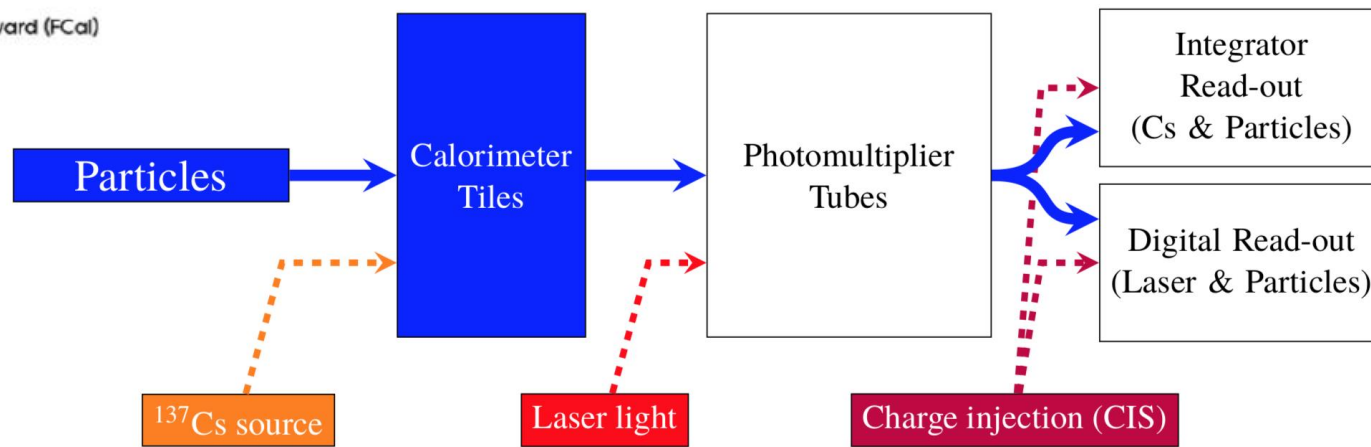
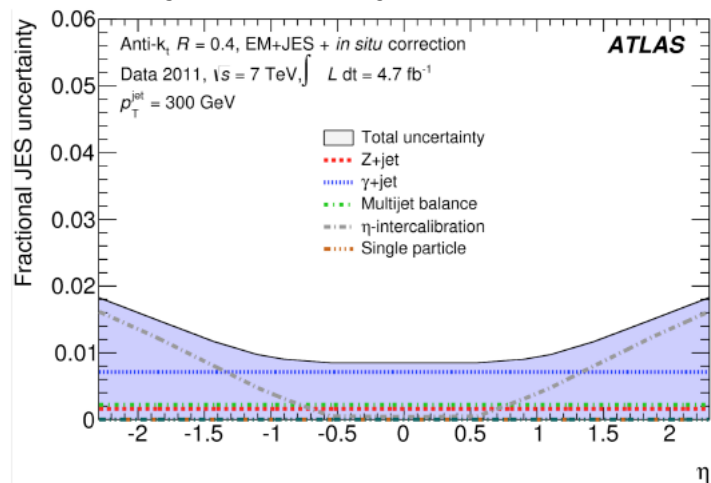


Figure 13: The signal paths for each of the three calibration systems used by the TileCal. The physics signal is denoted by the thick solid line and the path taken by each of the calibration systems is shown with dashed lines.



Hadron Calorimeters: Absolute Calibration

In EM calorimeters decays to Z and J/Ψ to e± to check reconstruction.

Hadron Calorimeters: two approaches are used.

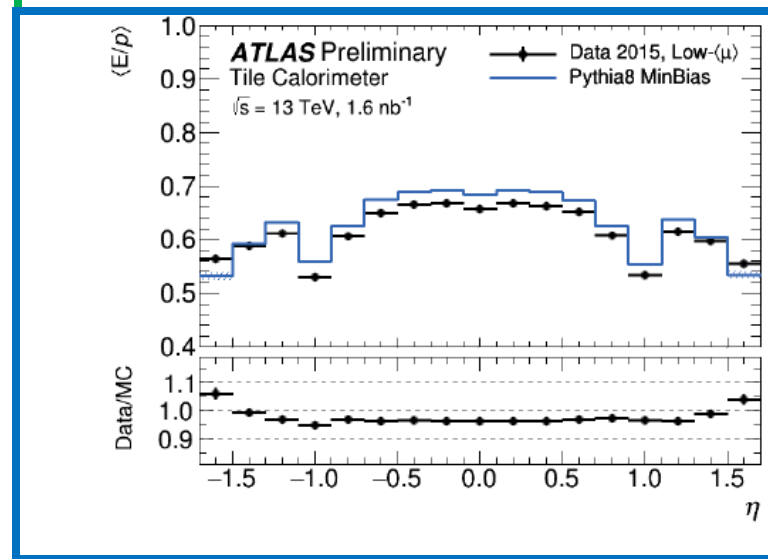
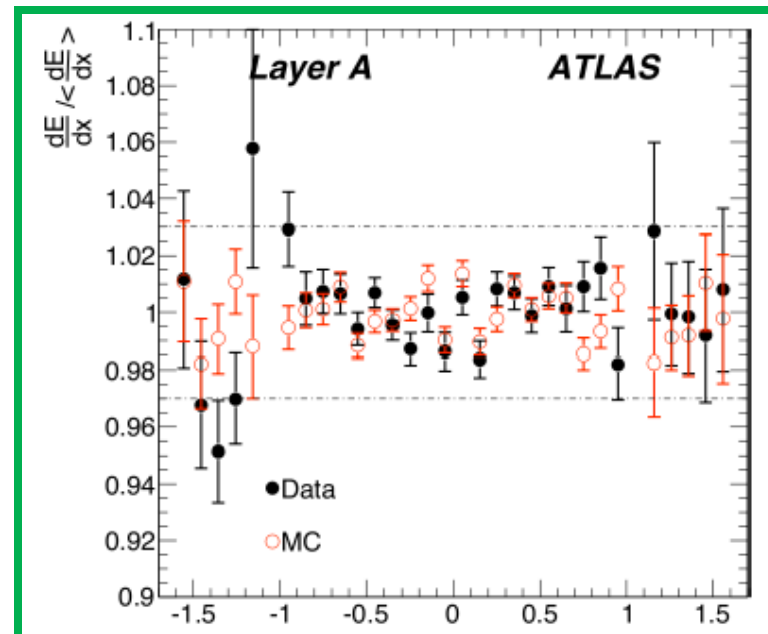
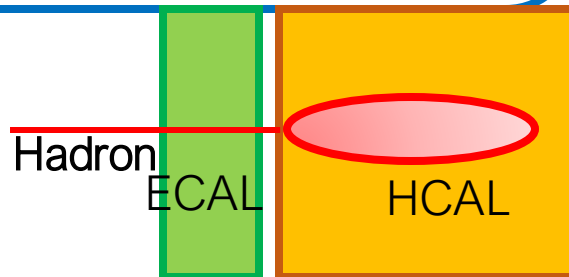
- Use cosmic muons: single isolated muons (from cosmic muons or Z/W decays), measure

energy deposited/path length (~very large extrapolation!!)

- Use single isolated charged hadrons, *require a signal compatible with a minimum ionizing particle in the electromagnetic calorimeter in front of the hadron calorimeter was required* (shower starts in Hadron Calorimeter) measure

energy measured/momentum of charged tracks

→ compare data & MC → good agreement



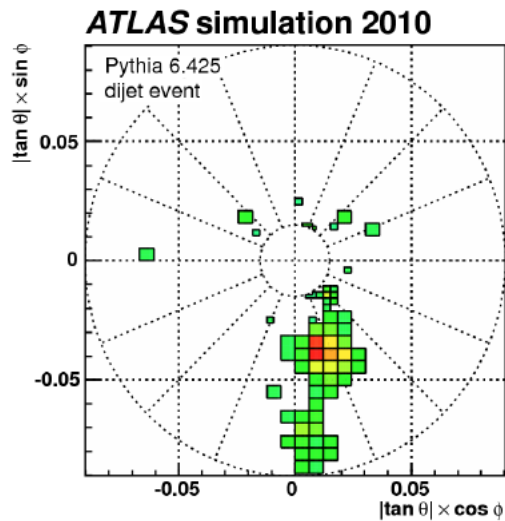


(Topological) Clusters in Calorimeters

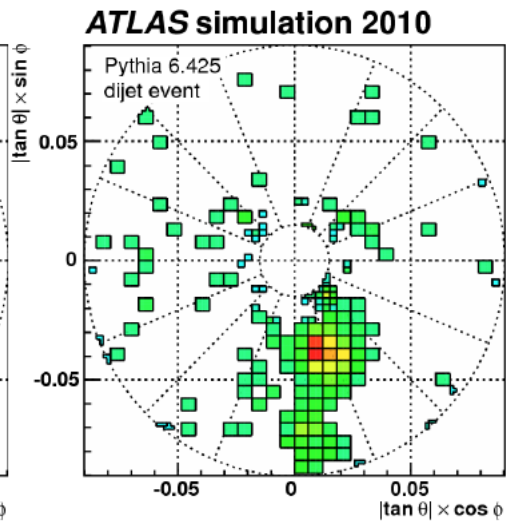
Cells in calorimeters → Clusters of energy deposition

- Identify 'starting' cells (seeds) with energy measurements $E_{deposition} > 4 \cdot \sigma_{noise}$
- Associate more cells laterally and longitudinally in two steps
 - ✓ add all adjacent cells with energy measurements $E_{deposition} > 2 \cdot \sigma_{noise}$
 - ✓ add all adjacent cells with energy measurements $E_{deposition} > \sigma_{noise}$
- Split two local energy maxima into separate clusters

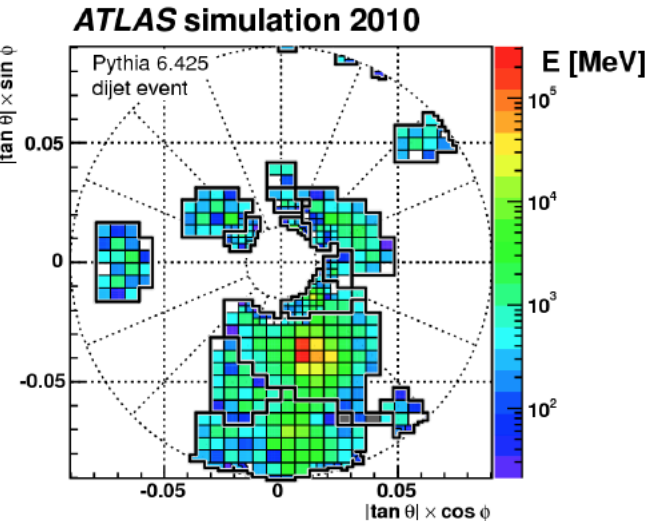
σ_{noise} is the threshold electronic signal that indicates a significant $E_{deposition}$



$$|E_{cell}^{EM}| > 4 \sigma_{noise,cell}^{EM}$$



$$|E_{cell}^{EM}| > 2 \sigma_{noise,cell}^{EM}$$



$$|E_{cell}^{EM}| > 0 \sigma_{noise,cell}^{EM}$$

Problems:

- Correctly account for hadronic showers starting in EM calorimeters
- low energy particles do not always satisfy the condition $E_{deposition} > 4 \cdot \sigma_{noise}$.



Comments to EM Topo-Clusters

The topological clustering algorithm employed in ATLAS is not designed to separate energy deposits from different particles, but rather to separate continuous energy showers of different nature, i.e. electromagnetic and hadronic, and also to suppress noise.

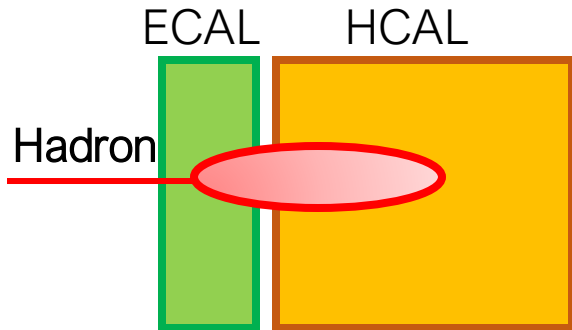
Few comments:

- A large fraction of low-energy particles are unable to seed their own clusters: In the central barrel 25% of 1 GeV charged pions do not seed their own cluster.
- They are *initially calibrated to the electromagnetic scale (EM scale)* to give the same response for electromagnetic showers from electrons or photons.
- Hadronic interactions produce responses that are lower than the EM scale, by amounts depending on where the showers develop.
- To account for this, the mean ratio of the energy deposited by a particle to the momentum of the particle is determined based on the position of the particle's shower in the detector. A local cluster (LC) weighting scheme is used to calibrate hadronic clusters to the correct scale.
- → Further development is needed to combine this with particle flow



Split Showers in ECAL and HCAL Calorimeters

Hadrons may deposit energy in both Electromagnetic calorimeters (ECAL) and Hadron calorimeters (HCAL).



Conversion factors $E_{deposition} \rightarrow True Energy$ are different for ECAL & HCAL and depend on particle type, position, true energy

$$\rightarrow E_{calibrated} = a + b(E)f(\eta)E_{ECAL} + c(E)g(\eta)E_{HCAL}$$

- $E_{calibrated}$ is the 'real particle energy'
- E_{ECAL} and E_{HCAL} are the energies measured in the ECAL and the HCAL
- a accounts for energy lost because of σ_{noise} threshold
- $b(E)$ and $c(E)$ are conversion factors
- $f(\eta)$ and $g(\eta)$ correct energy in different η regions

These parameters have to be determined from data: use

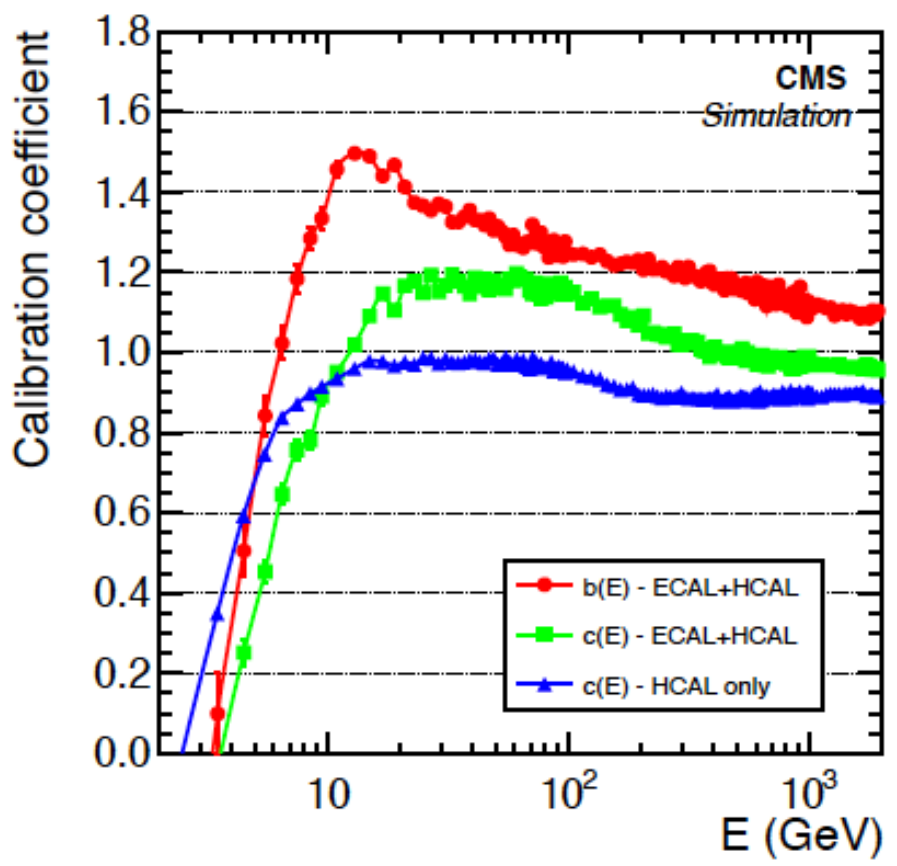
$$\chi^2 = \sum_{i=1}^N \frac{(E_i^{calib} - E_i)^2}{\sigma_i^2},$$

- Simulated data: true energy (MC!) is taken as $E_{calibrated}$
- Large samples of isolated charged showers: the momentum reconstruction is taken as $E_{calibrated}$

In a first pass, the functions $f(\eta)$ and $g(\eta)$ are fixed to unity.

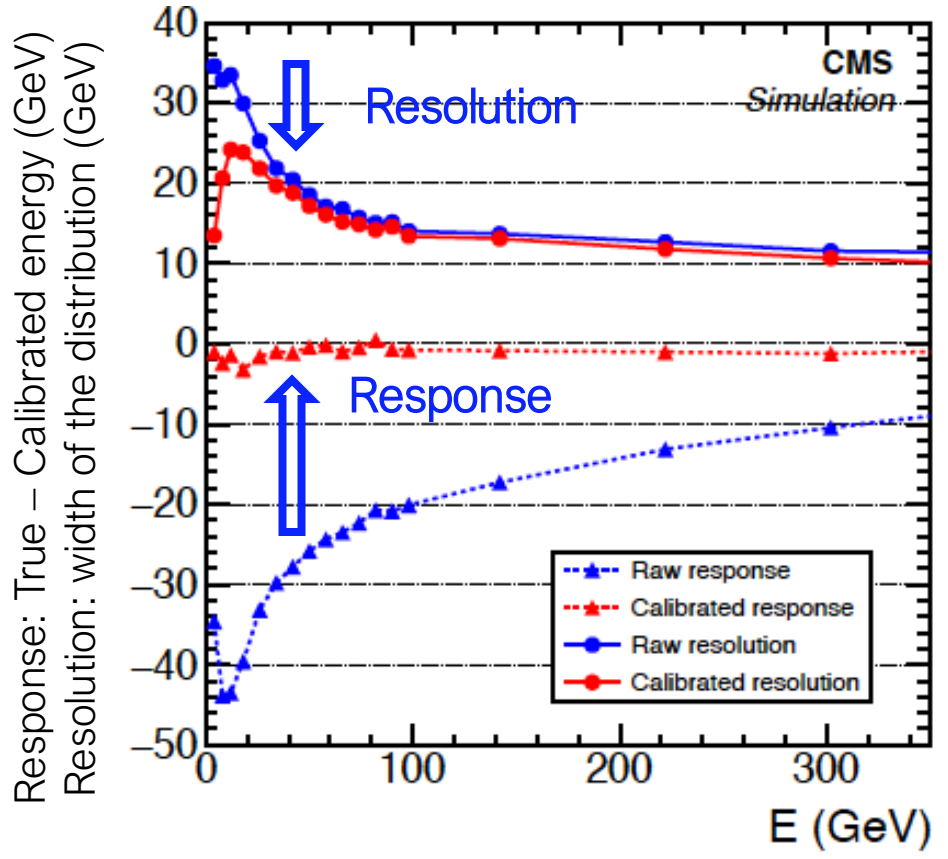


$$Results: (E_{calibrated} = a + b(E)f(\eta)E_{ECAL} + c(E)g(\eta)E_{HCAL})$$



Calibration coefficients vs energy E, for hadrons

- HCAL only (blue triangles),
- ECAL and HCAL, for
 - ✓ the ECAL (red circles) and
 - ✓ for the HCAL (green squares)



Single isolated hadrons:

- Relative raw (blue) and calibrated (red) energy response (dashed curves and triangles)
- resolution (full curves and circles)



Muon Reconstruction at LHC

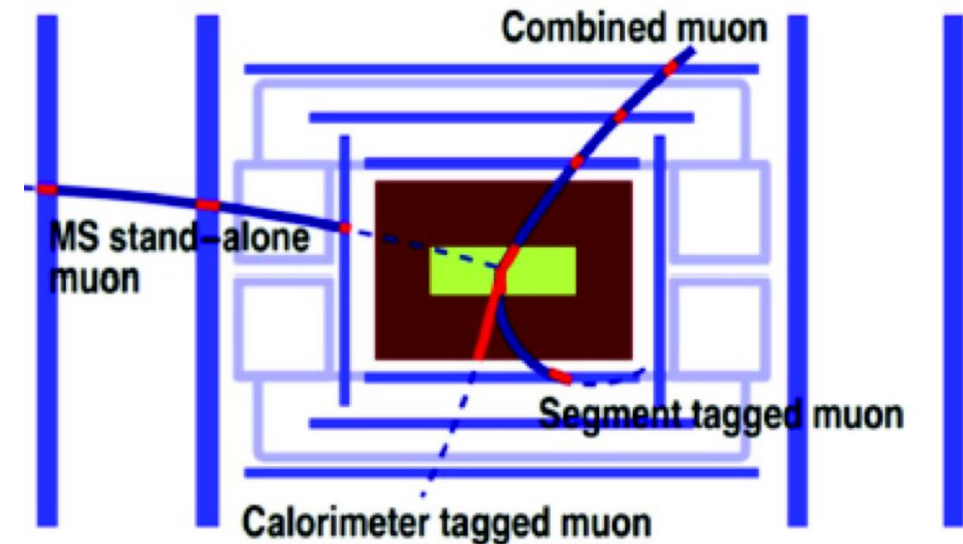
| Issue | ATLAS | CMS |
|------------------|---|--|
| Design | Air-core toroid magnets Standalone muon reconstruction | Flux return instrumented Tracks point back to collision point |
| Barrel Tracking | Drift tubes Precision: $\sim 80\text{-}120\ \mu\text{m}$ | Drift tubes Precision: $100\text{-}500\ \mu\text{m}$ |
| End-cap Tracking | Cathode strip chambers High rate capability | Cathode strip chambers High rate capability |
| Barrel Trigger | Resistive plate chambers Fast response [5 ns] | Resistive plate chambers Fast response [5 ns] |
| End-cap Trigger | Thin gap chambers Fast response, high rates | |



Muon Reconstruction in ATLAS

Muons

- are filtered by calorimeters
- Seen in the Inner detector and in the muon spectrometer.
 - These two tracks have to be associated @ reference plane
 - The momentum has to be computed by combining the two associated tracks + account the energy lost in calorimeters



Very high energy muons (close to 1 TeV) may shower like electrons, these cases are called “catastrophic energy losses”

Different types (== different reconstructions)

- **Combined**: ID + MS + full track refit. Main reconstruction type
- **Stand-alone (SA)**: MS-only track with identification and reconstruction. Recovers muons for $|\eta| > 2.5$
- **Segment-tagged**: one ID track is associated to one segment of track measured in the MS (incomplete MS track)
- **CaloTag**: charged track in the ID associated to an energy deposition of a minimum ionizing particle in the calorimeter. Low energy muons that do not penetrate up to the MS



Muon Reconstruction in CMS

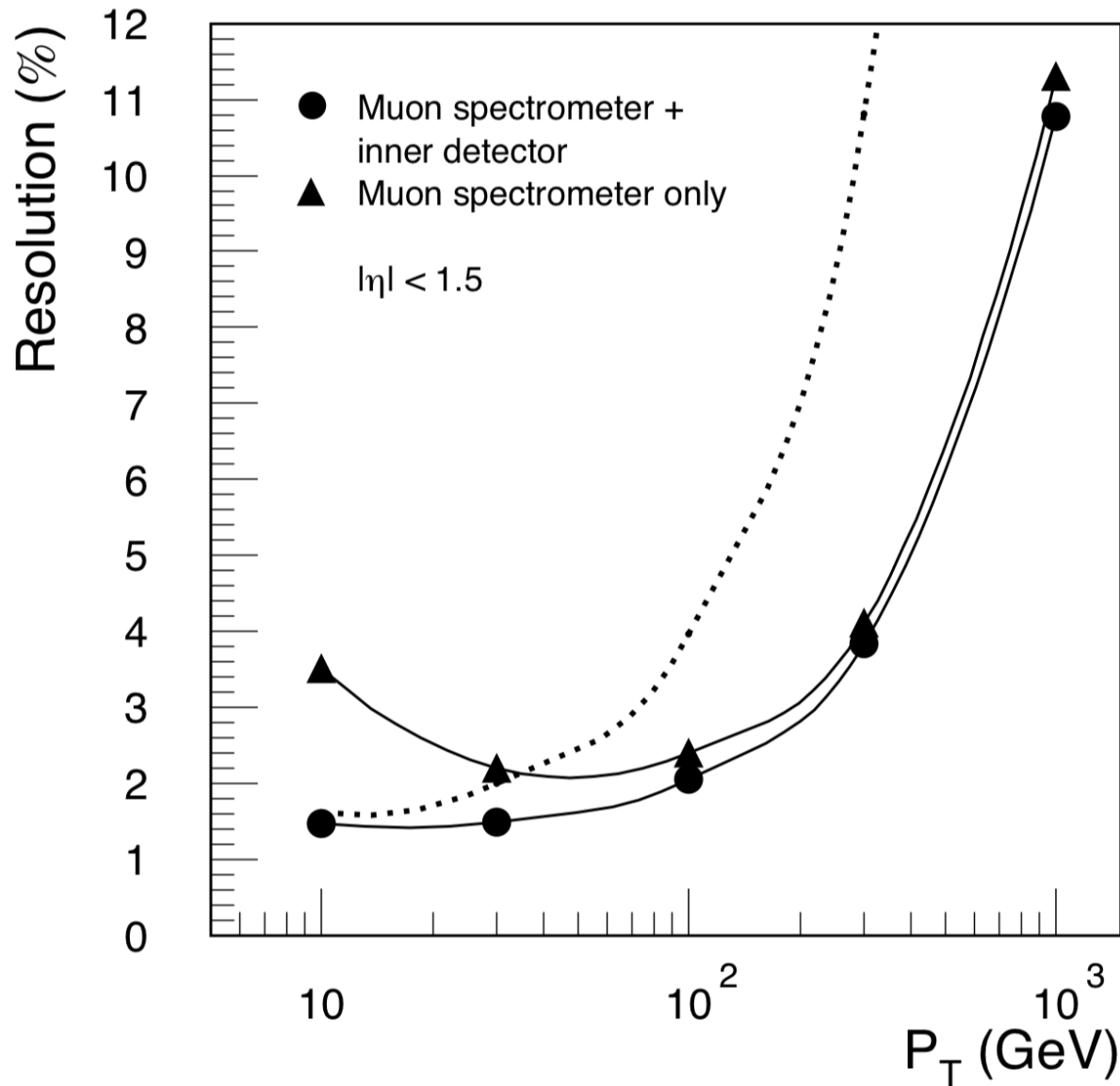
The momentum of muons is measured both in the inner tracker and in the muon spectrometer. There are three different muon types:

- *standalone muon*. Hits in the muon spectrometer only are used to form muon segments that are combined in a track describing the muon trajectory. The result of the final fitting is called a standalone-muon track.
- *global muon*. Each standalone-muon track is matched (if possible!) to a track in the inner tracker if the parameters of the two tracks propagated onto a common surface are compatible. The hits from the inner track and from the standalone-muon track are combined and fit to form a global-muon track. At large transverse momenta, $p_T > 200$ GeV, the global-muon fit improves the momentum resolution with respect to the tracker-only fit.
- *tracker muon*. Each inner track with p_T larger than 0.5 GeV and a total momentum p in excess of 2.5 GeV is extrapolated to the muon system. If at least one muon segment matches the extrapolated track, the inner track is defined as a tracker muon track.

About 99% of the muons produced within the geometrical acceptance of the muon system are reconstructed either as a global muon or a tracker muon and very often as both. Global muons and tracker muons that share the same inner track are merged into a single candidate. Muons reconstructed only as standalone-muon tracks have worse momentum resolution and are contaminated by cosmic. Charged hadrons may be mis-reconstructed as muons if some part of the hadron shower reach the muon system (punch-through).



Muon p_T Resolution in ATLAS



Combining ID + MS improves resolution always.

Effect is mostly visible at low p_T values ~ 10 GeV where a factor of two is gained in resolution

At high p_T (~ 1 TeV) the resolution mostly comes from the MS

Tag & Probe Method

How to check the reconstruction efficiency of muons?

Total reconstruction efficiency

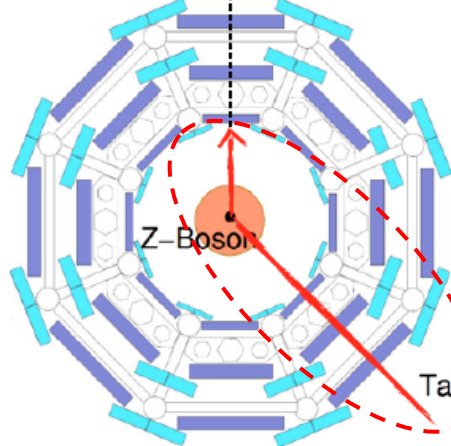
$$\epsilon = \epsilon(ID) \times \epsilon(MS) \times \epsilon(comb)$$

Inner tracker reconstruction efficiency

Muon Spectrometer reconstruction efficiency

Combination efficiency

How many times is a 'Probe' muon found?

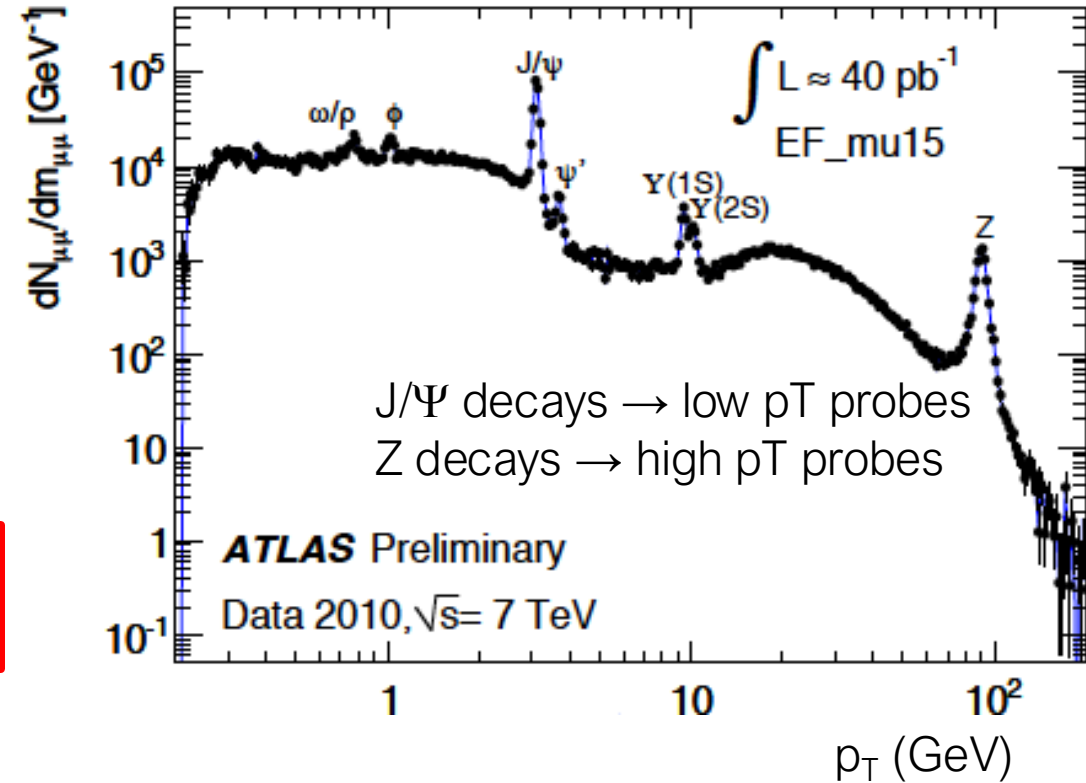


The muon reconstruction efficiency is measured with respect to Inner Detector tracks

$$Z \rightarrow \mu^- \mu^+ \rightarrow m_Z$$

= real muon

$$SF = \frac{\epsilon^{Data}(Type)}{\epsilon^{MC}(Type)}$$

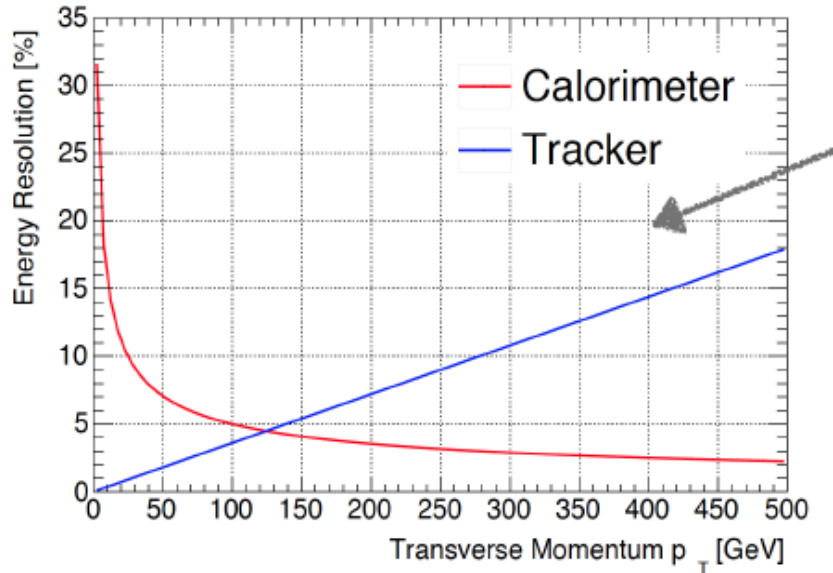


The measurement of the muon reconstruction efficiency is done using well known resonances:

1. A combined muon **"Tag"**
2. the tag is paired with an ID track giving an invariant mass close to the considered resonance mass
3. the fraction of reconstructed signal **"Probes"** measures the muon identification efficiency



Modern Experiments: Particle Flow, Basic Idea



Parametrisation of the relative resolution of

- calorimeters and
- p_T measured in the Inner Detector

$$\frac{\sigma(E)}{E} = \frac{50\%}{\sqrt{E}} \oplus 3.4\% \oplus \frac{1\%}{E}, \text{ Calorimeters}$$

$$\sigma\left(\frac{1}{p_T}\right) \cdot p_T = 0.036\% \cdot p_T \oplus 1.3\%, \text{ Inner Detector}$$

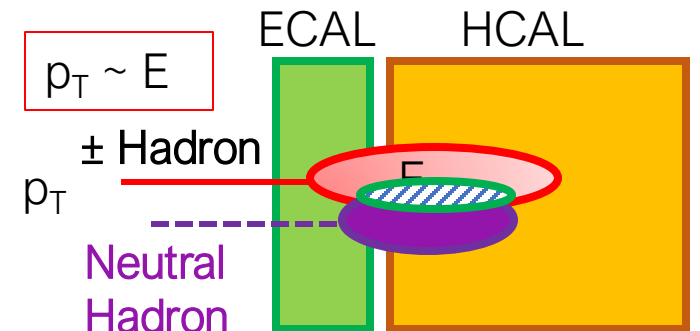
→ For low-energy charged particles, the momentum resolution of the tracker is significantly better than the energy resolution of the calorimeter.

Problem #1

A charged particle is measured in trackers (p_T) and in calorimeters (ECAL & HCAL) → **avoid double-counting its energy** → associate tracks and showers → choose only one!

Problem #2

Showers are often superimposed → subtract a part of the energy deposition



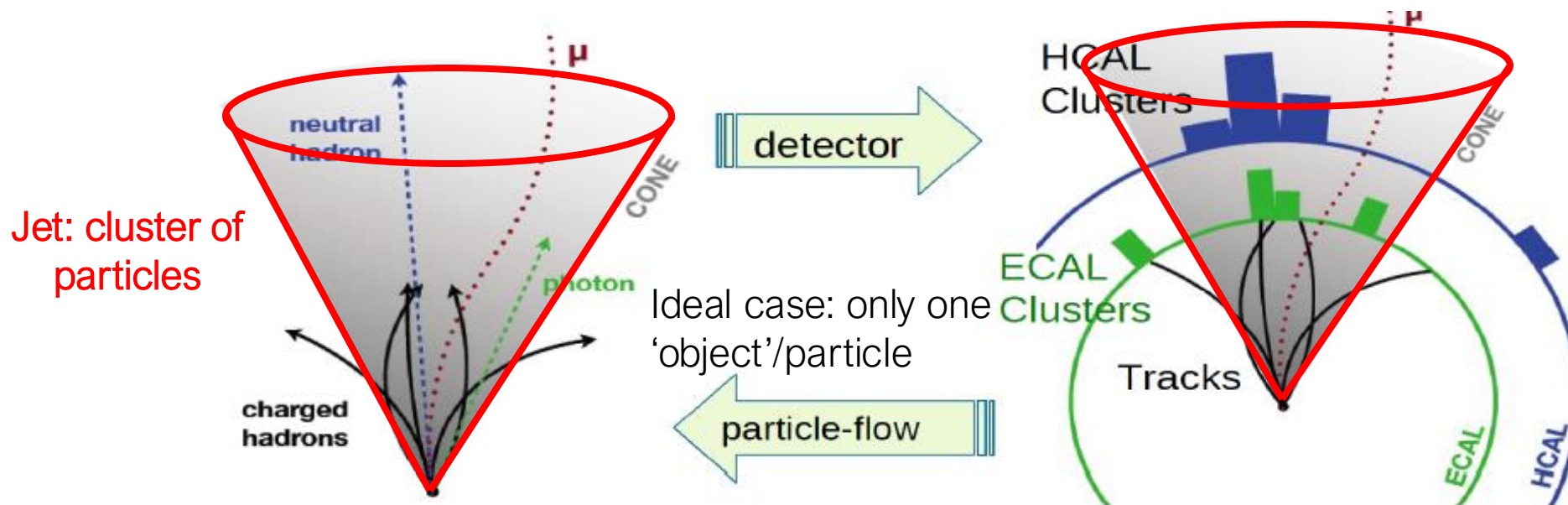


Particle Flow (~Jets): basic idea

Why Particle Flow (PF)?

Two possibilities to reconstruct the topology (*) of one event

- **Use calorimeters:** they are sensitive to ALL particles, charged, neutral, photons hadrons, (partly) muons. BUT the energy resolution ~not very good at ~low/medium energies
- **use PF:** it gives an optimal use of measurements: when you have two independent measurements of the same particle → take the best!



(*) Topology = general characteristics of the event, like # of jets



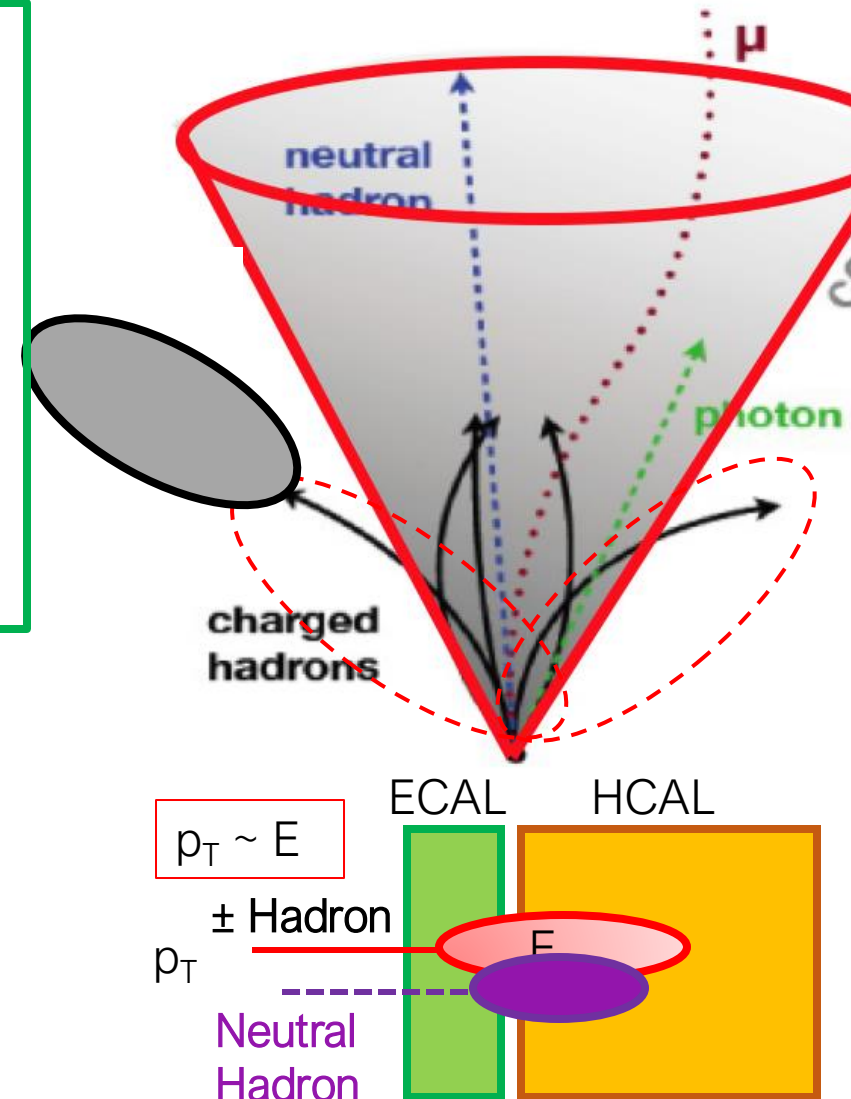
Particle Flow: Advantages & Disadvantages

- Particles below detection threshold;
- $\sigma_{direction}^{Tracker} \ll \sigma_{direction}^{Calorimeter}$
- Low- p_T tracks in a jet are swept out of the jet cone by the magnetic
- \rightarrow use track's coordinates at the IP \rightarrow these particles are recovered into the jet.
- pile-up interactions: distinguish primary vertex from pile-up vertices

For each charged particle

- Avoid double-counting energy (Calorimeters) & Momentum (trackers)
- Cancel E_{dep} calorimeters of charged tracks \rightarrow only neutrals

➤ H Do not remove any energy deposited by neutral particles.





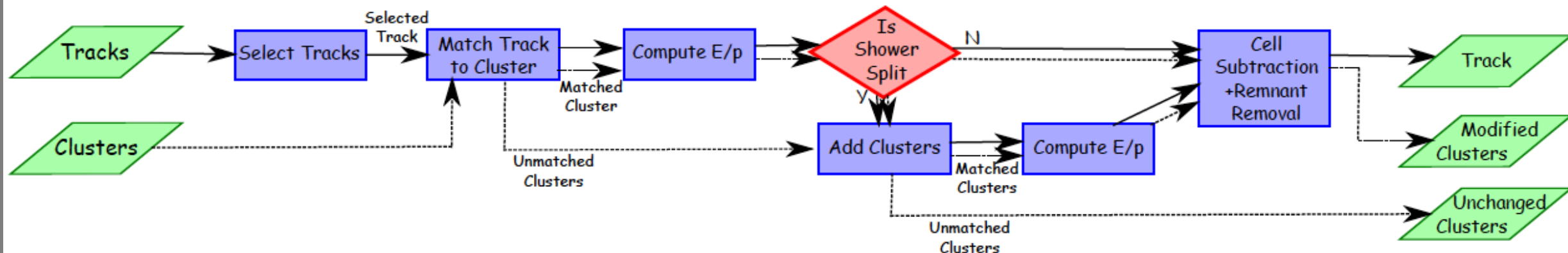
The Particle Flow Algorithm

Before applying PF Algorithm it is necessary to know how much energy $\langle E_{dep} \rangle$ a particle with measured momentum p_{trk} deposits on average in calorimeters. This is needed to correctly subtract the energy from the calorimeter for a particle whose track has been reconstructed. This is done using the expression

$$\langle E_{dep} \rangle = p^{trk} \cdot \langle E_{ref}^{clus} / p_{ref}^{trk} \rangle$$

The value $\langle E_{ref}^{clus} / p_{ref}^{trk} \rangle$ (which is also a measure of the mean response) is determined using single-particle samples without pile-up by summing the energies of topo-clusters in a R cone of size 0.4 around the track position, extrapolated to the EM calorimeter. This cone size is large enough to entirely capture the energy of the majority of particle showers. The subscript 'ref' indicates values $\langle E_{ref}^{clus} / p_{ref}^{trk} \rangle$ determined from single-pion samples.

The PF algorithm is skematically shown below





Particle Flow in One Cartoon

Match Tracks to Clusters

A cluster can contain a single, many or part of the shower

Does the cluster energy match the track (E/p)?

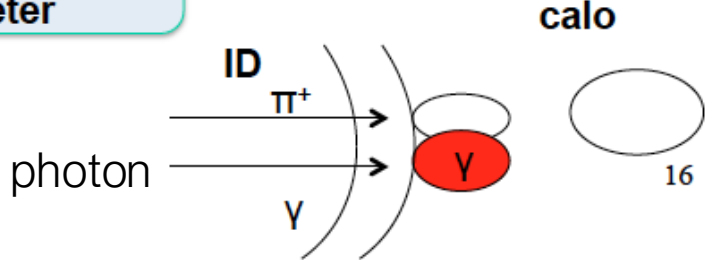
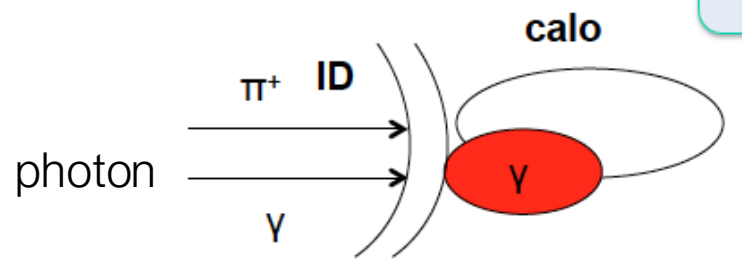
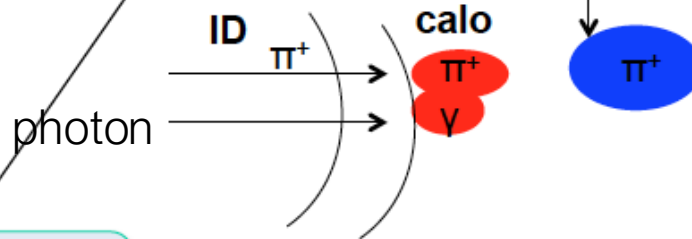
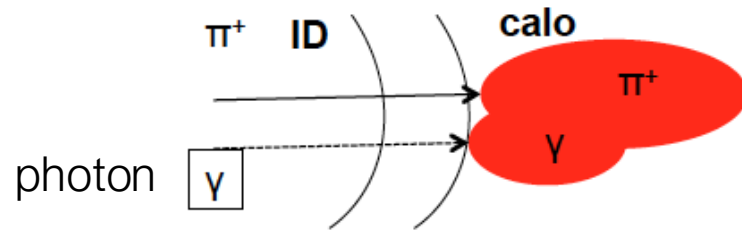
YES

NO

Match all clusters in $\Delta R < 0.2$ to recover split showers

isolated shower

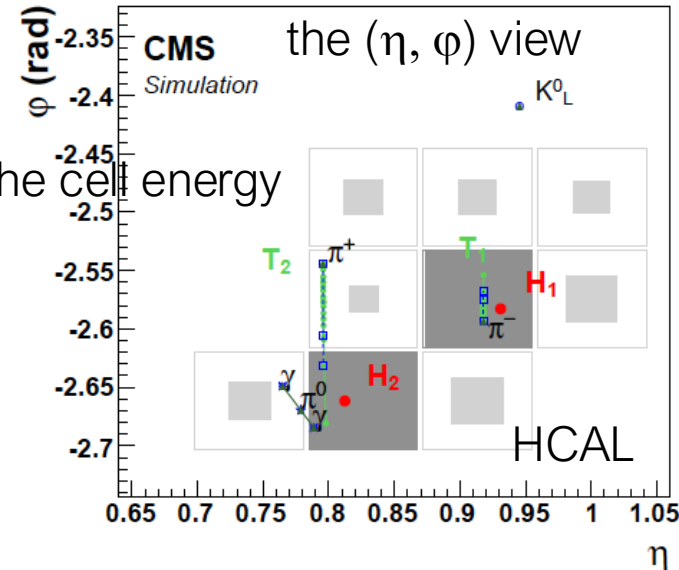
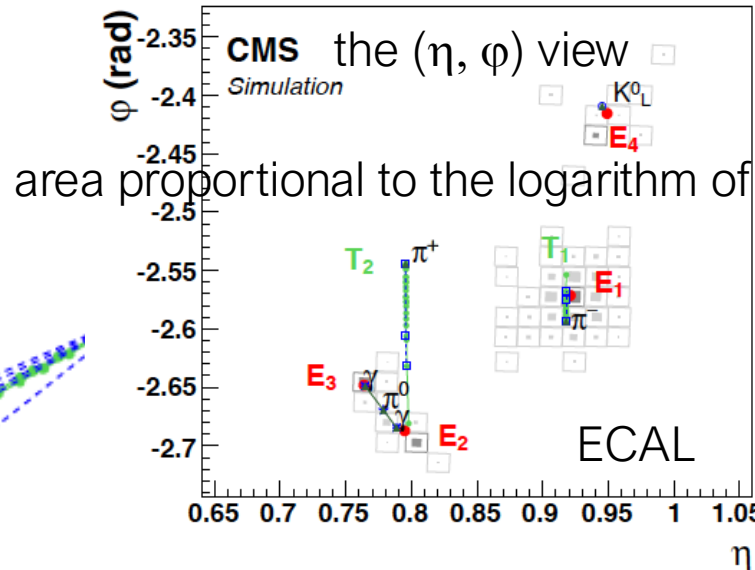
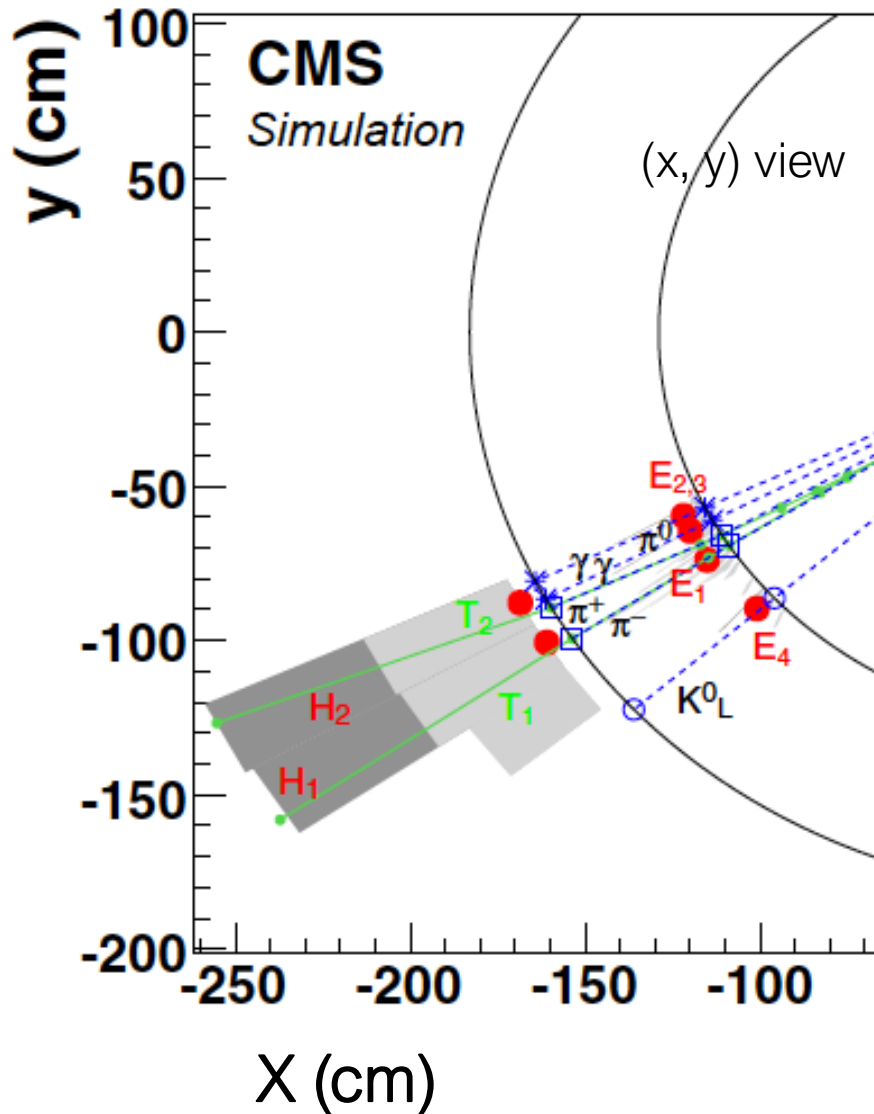
Subtract matched energy deposit cell-by-cell from the calorimeter



PF in CMS, one Event

jet made of five particles only

ECAL is EM calorimeter HCAL is the hadronic calorimeter



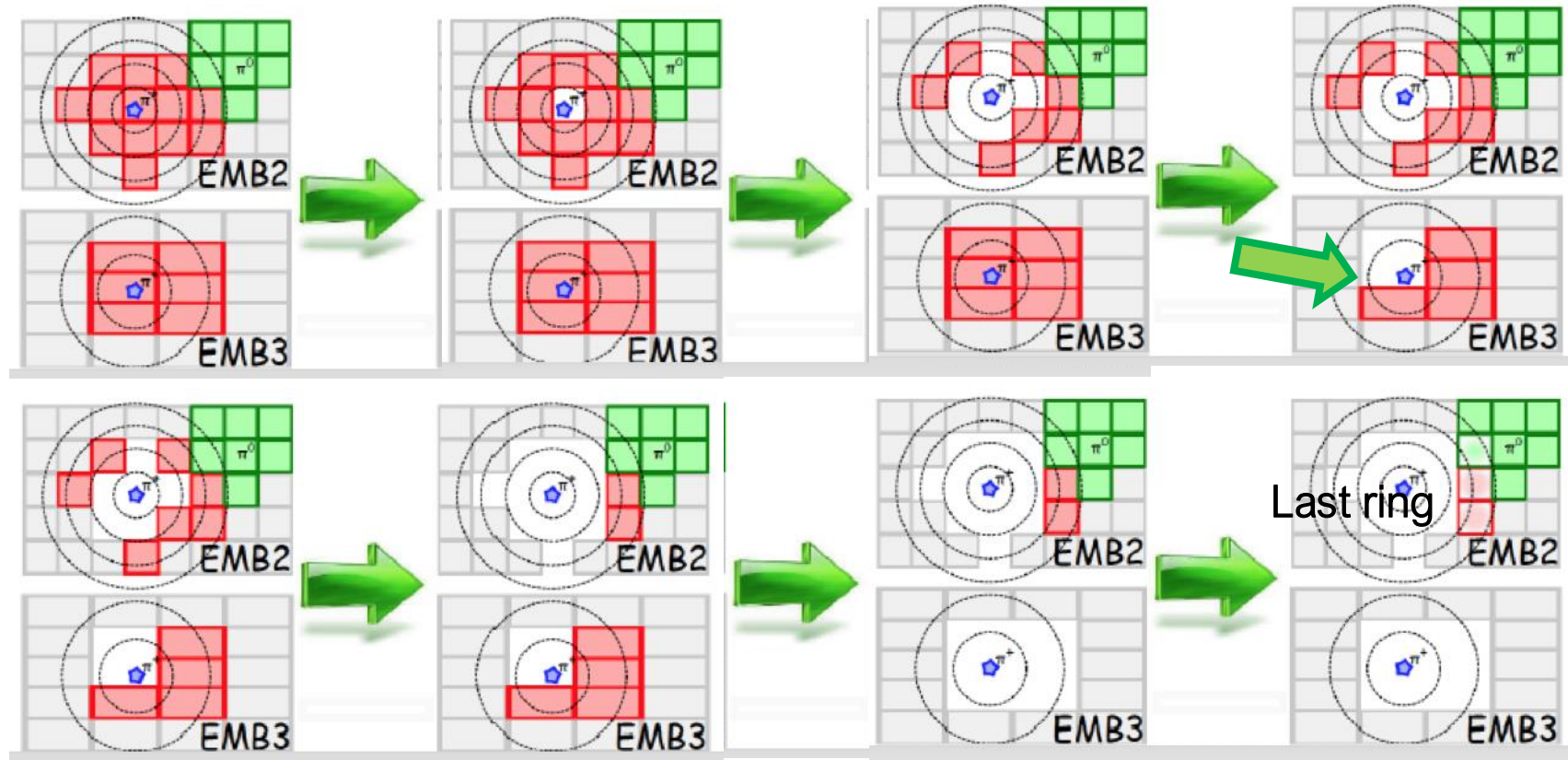
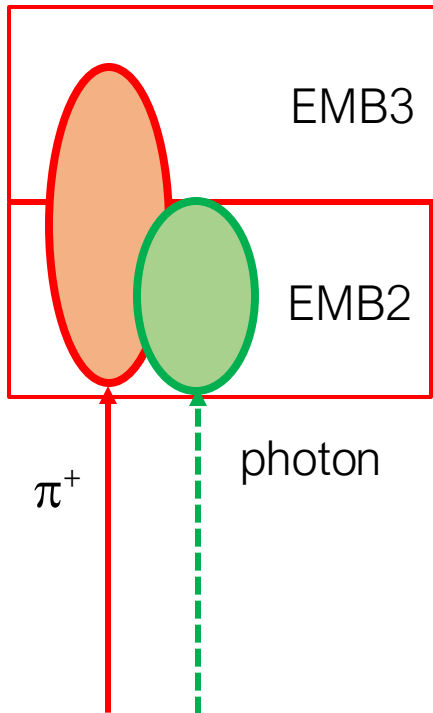
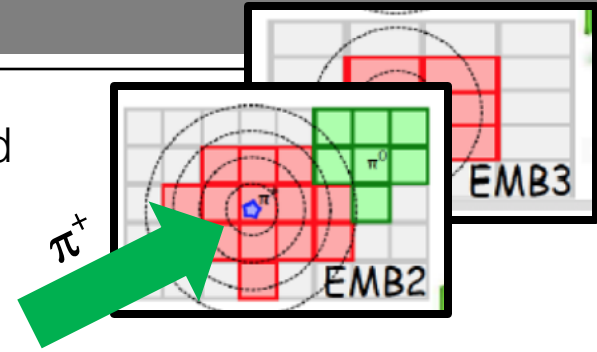
area proportional to the logarithm of the cell energy

The K_0^L , the π^- , and the two photons from the π^0 decay are detected as four well-separated ECAL clusters denoted E1,2,3,4. The π^+ does not create a cluster in the ECAL. The two charged pions are reconstructed as charged-particle tracks T1,2, appearing as vertical solid lines in the (η, ϕ) views and circular arcs in the (x, y) view. These tracks point towards two HCAL clusters H1,2 cluster positions are represented by dots, the simulated particles by dashed lines, and the positions of their impacts on the calorimeter surfaces by various open markers.

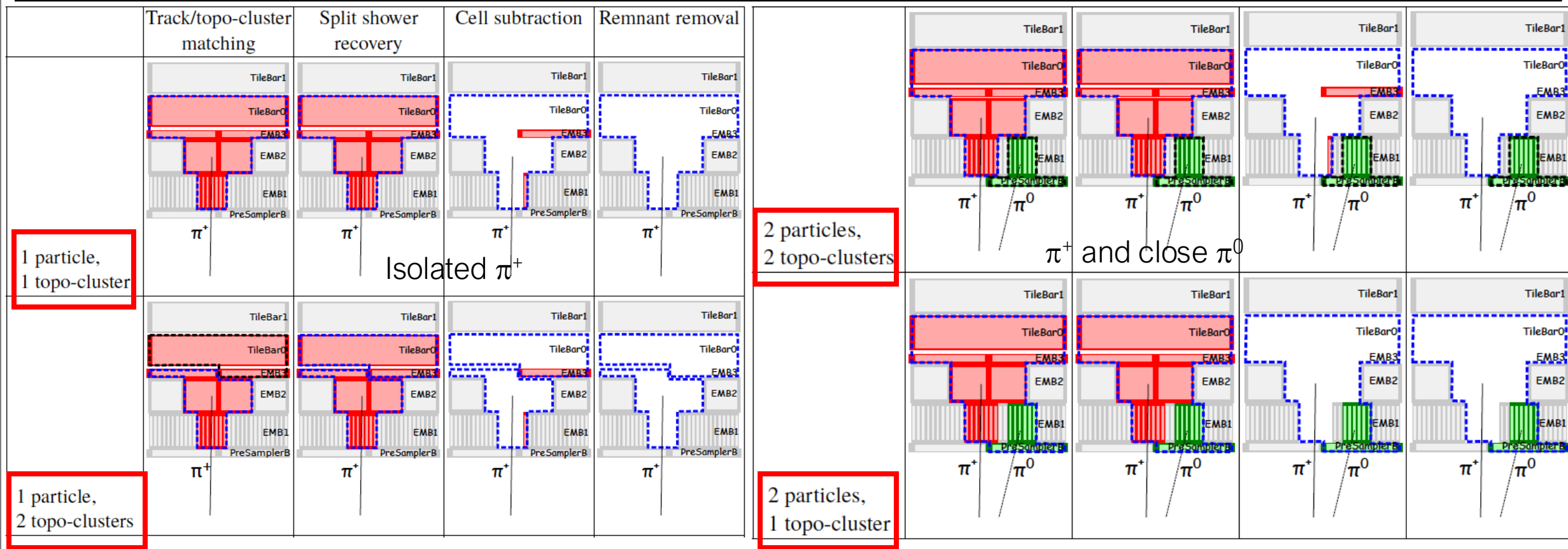
Subtracting Calorimeter Cells

- Important parameter: the ratio $E_{calorimeter}/p^{trk} \rightarrow$ rings around the extrapolated track
- Remove rings if $E_{cl} > p^{trk}$

EMB2 & EMB3 two calorimeter layers



Particle Flow in Action: Example



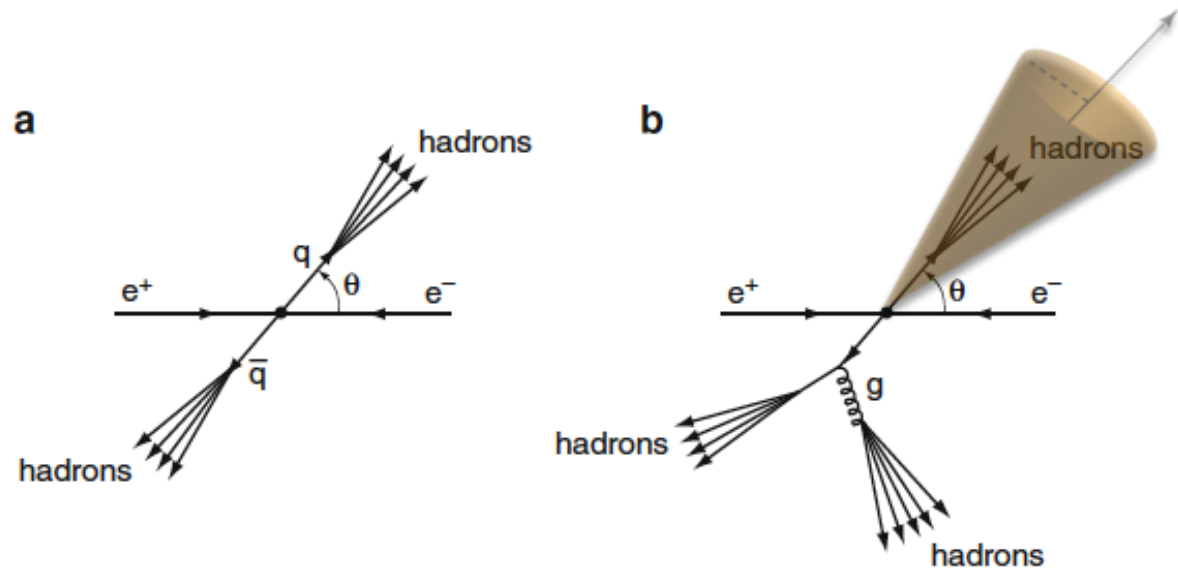
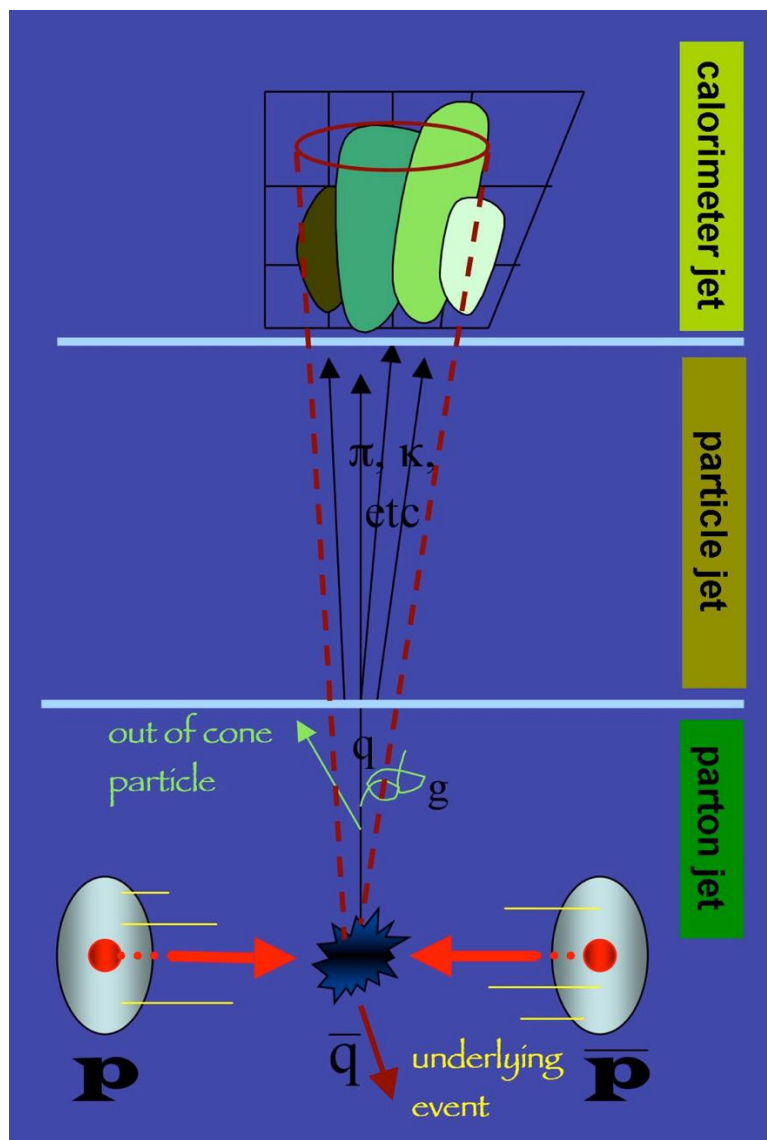
- The red cells are from the π^+ ,
- the green cells energy from the photons from the π^0 decay
- the dotted lines represent the borders of the calorimeter-cluster

Jets: Introduction

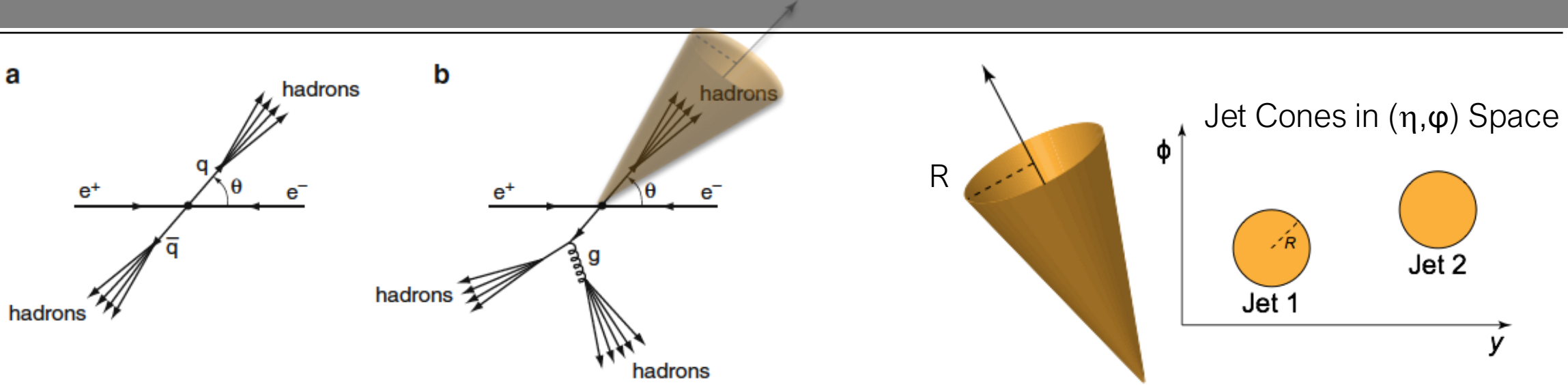
Jets are a collection of 'close by' objects that reflect the initial parton
 → try to reconstruct the momentum of the initial parton

Construction of jets:

- Before Particle Flow → calorimeters
- After Particle Flow → the best defined object between with track or calorimeter cluster



Jets (What & How?)

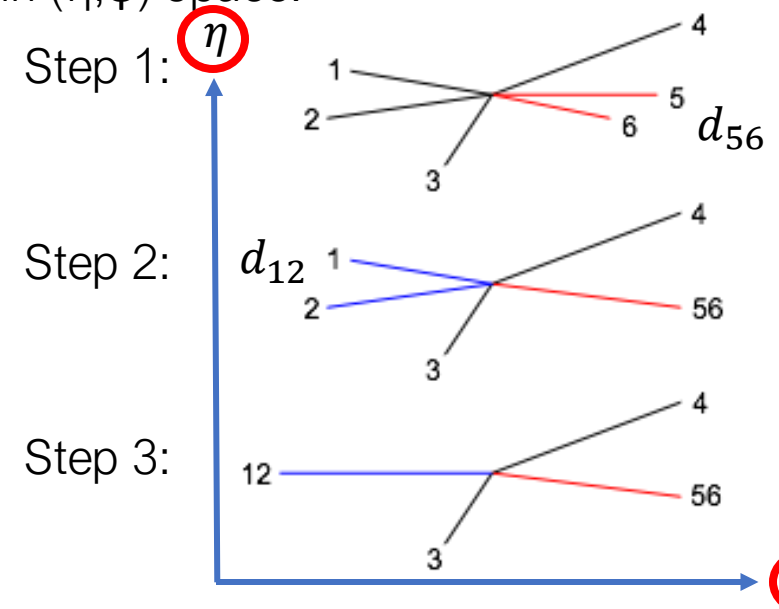


Iterative cone algorithms: Jet defined as energy flow within a cone of radius R in (η, ϕ) space:

$$R = \sqrt{(\eta - \eta_0)^2 + (\Phi - \Phi_0)^2}$$

- Start with most energetic energy deposition
- Define distance measure d_{ij}
- Calculate d_{ij} for all pairs of objects ...
- Combine particles with minimum d_{ij} below cut ..
- Stop if minimum d_{ij} above cut ..

Limit: all 'distances' count the same! → weight using momentum or energy





Jets, Different Algorithms, see reference(*)

The definition of distance is very important: the formula below is most used today. NOTE the parameter ' p ' in $k_{t,i}^{2p}$.

- $k_{t,i}$ is the transverse momentum of particle i
- $\Delta_{ij}^2 = (\eta_i - \eta_j)^2 + (\phi_i - \phi_j)^2$

$$d'_{ij} = \text{distance}' = \min(k_{t,i}^{2p}, k_{t,j}^{2p}) \frac{\Delta_{ij}^2}{R^2},$$

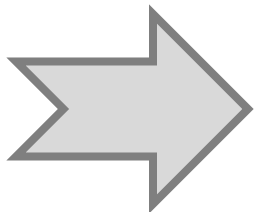
R^2 is a parameter of the algorithm
→ opening of the cone

If $p=0$ you have the so-called *Cambridge/Aachen* algorithm

$$d_{ij} = \min(k_{t,i}^{2p}, k_{t,j}^{2p}) \frac{\Delta_{ij}^2}{R^2} \rightarrow d_{ij} = \frac{\Delta_{ij}^2}{R^2}$$

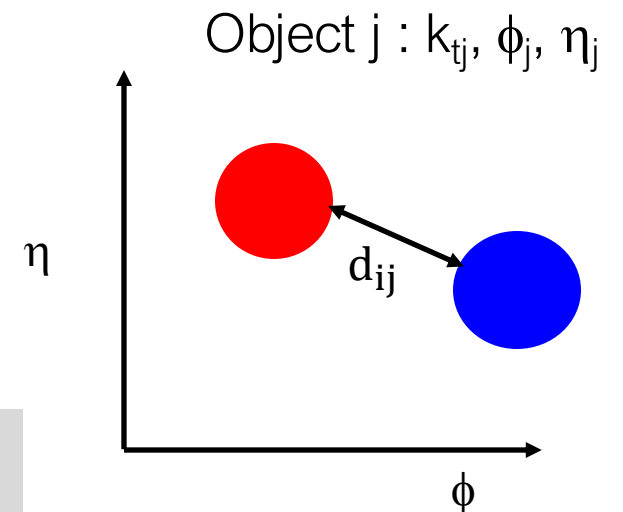
If $p=1$ you have the so-called K_T algorithm

$$d_{ij} = \min(k_{t,i}^2, k_{t,j}^2) \frac{\Delta_{ij}^2}{R^2}$$



If $p=-1$ you have the so-called *anti K_T* algorithm

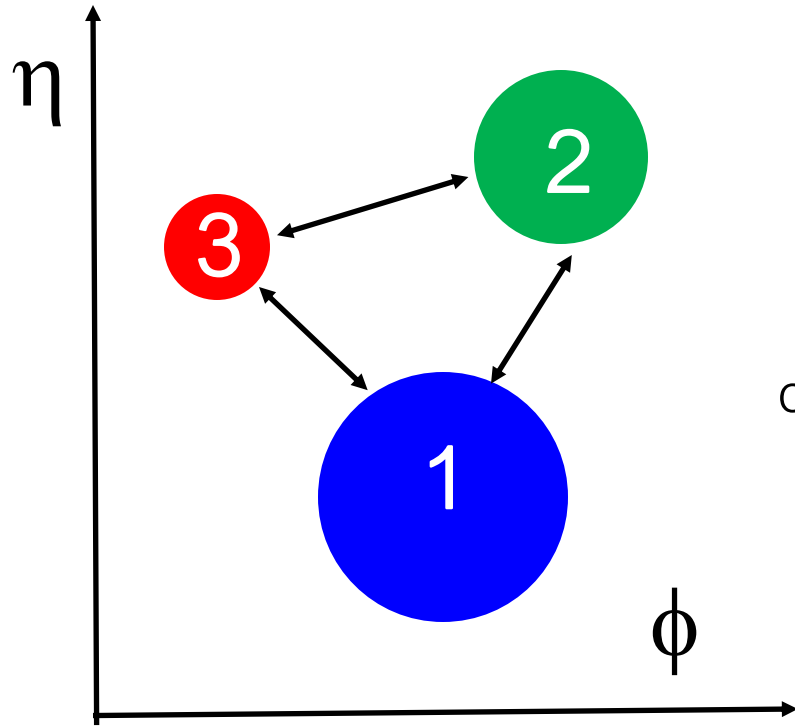
$$d_{ij} = \min\left(\frac{1}{k_{t,i}^2}, \frac{1}{k_{t,j}^2}\right) \frac{\Delta_{ij}^2}{R^2}$$



(*) Cacciari et al. <https://arxiv.org/pdf/0802.1189>



k_T and anti- k_T Jet Algorithms



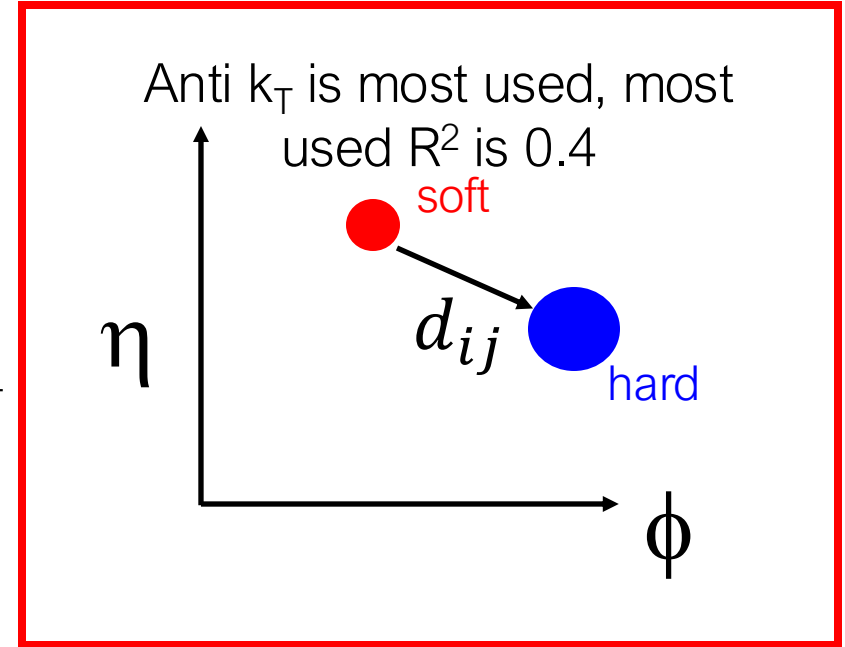
$$d_{ij} = \min(k_{t,i}^{2p}, k_{t,j}^{2p}) \frac{\Delta_{ij}^2}{R^2}$$

neglect case with $p=0$, only of historical interest, does not contain any dependence on $E/p/p_T$

$$\Delta_{ij}^2 = (\eta_i - \eta_j)^2 + (\phi_i - \phi_j)^2$$

Δ_{ij}^2 are \sim similar

$p_T: 1 > 2 > 3$



k_T $d_{ij} = \min(k_{t,i}^2, k_{t,j}^2) \frac{\Delta_{ij}^2}{R^2}$

$$d_{13} < d_{23} < d_{12}$$

Distance $\sim (p_T)^2 \rightarrow$ cluster around the particle with smallest $p_T \rightarrow$ **particle 3**

Anti k_T $d_{ij} = \min\left(\frac{1}{k_{t,i}^2}, \frac{1}{k_{t,j}^2}\right) \frac{\Delta_{ij}^2}{R^2}$

$$d_{13} < d_{23} < d_{32}$$

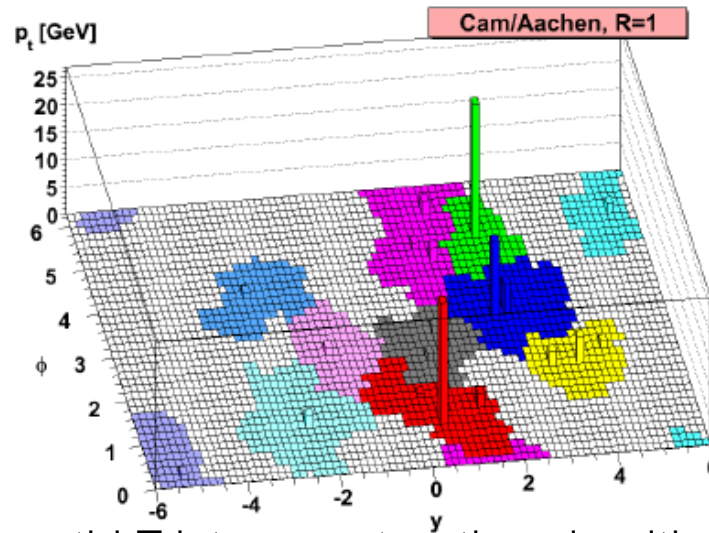
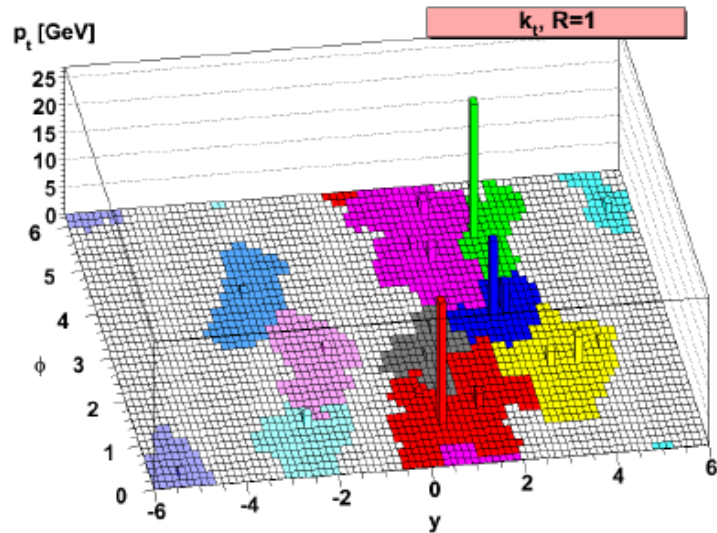
Distance $\sim (1/p_T)^2 \rightarrow$ cluster around the particle with highest $p_T \rightarrow$ **particle 1**

Natural choice: the particle with highest energy in a jet keeps the best memory of the initial parton



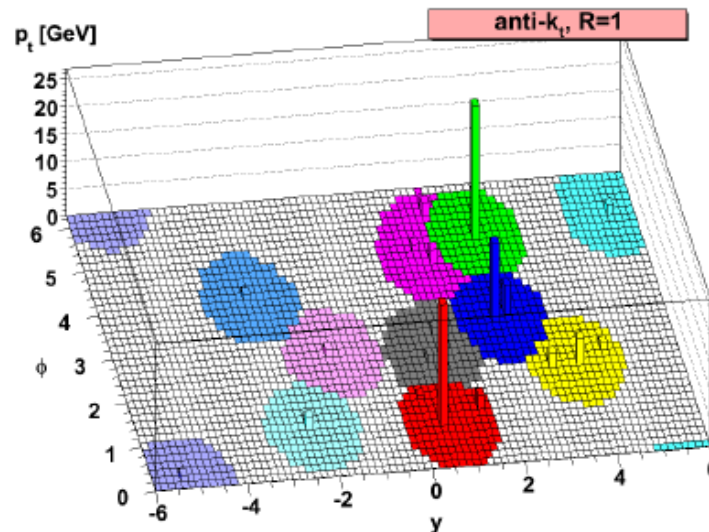
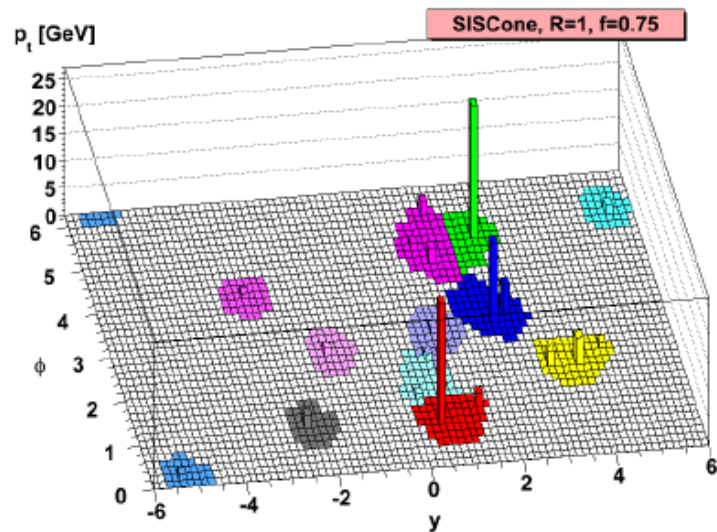
Jet Shapes in Different Algorithms

kT jet reconstruction algorithm



Simulated events: 3 partons + large number of ghosts

anti-kT jet reconstruction algorithm

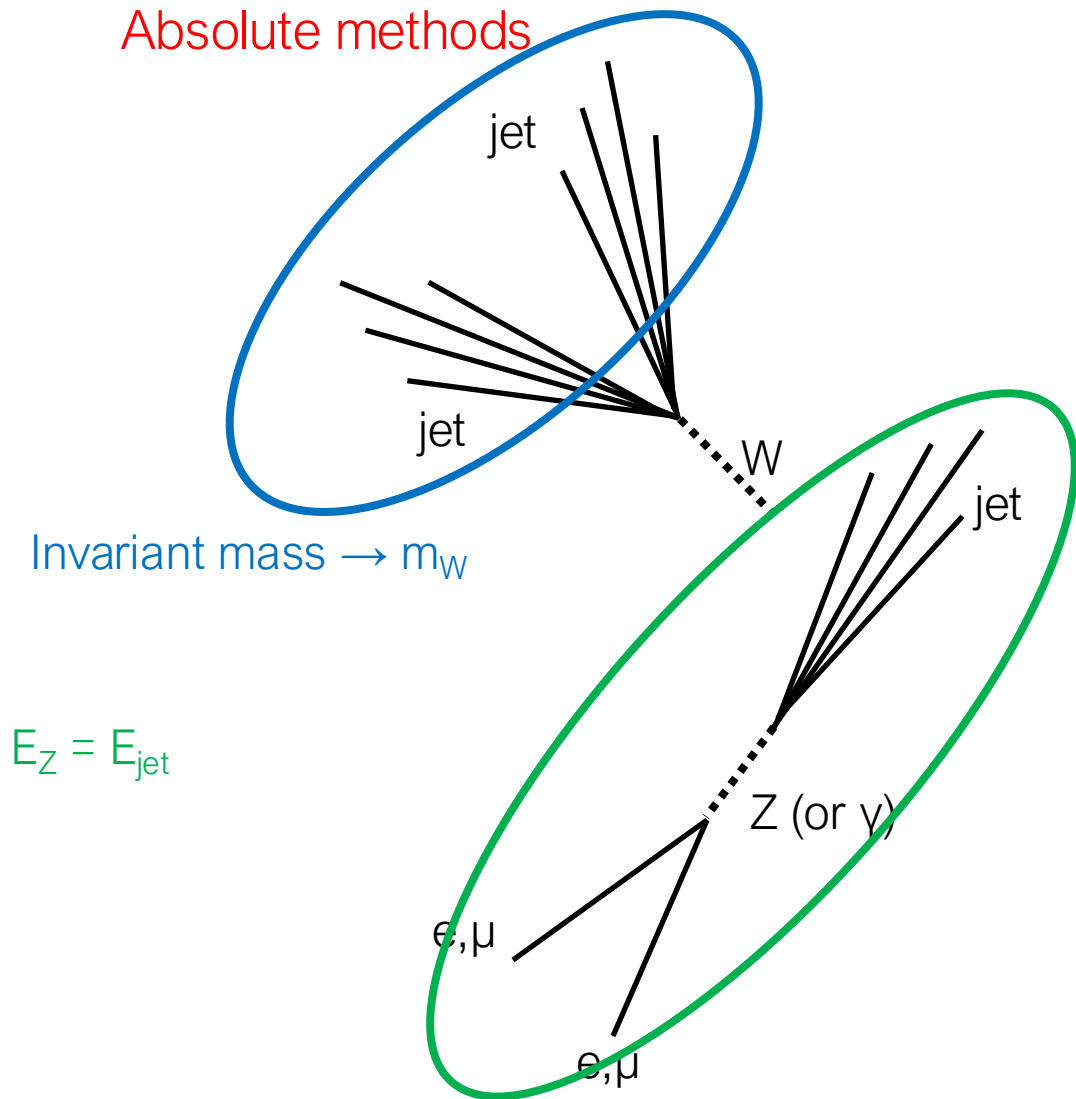


In the anti-kT jet reconstruction algorithm, are all circular

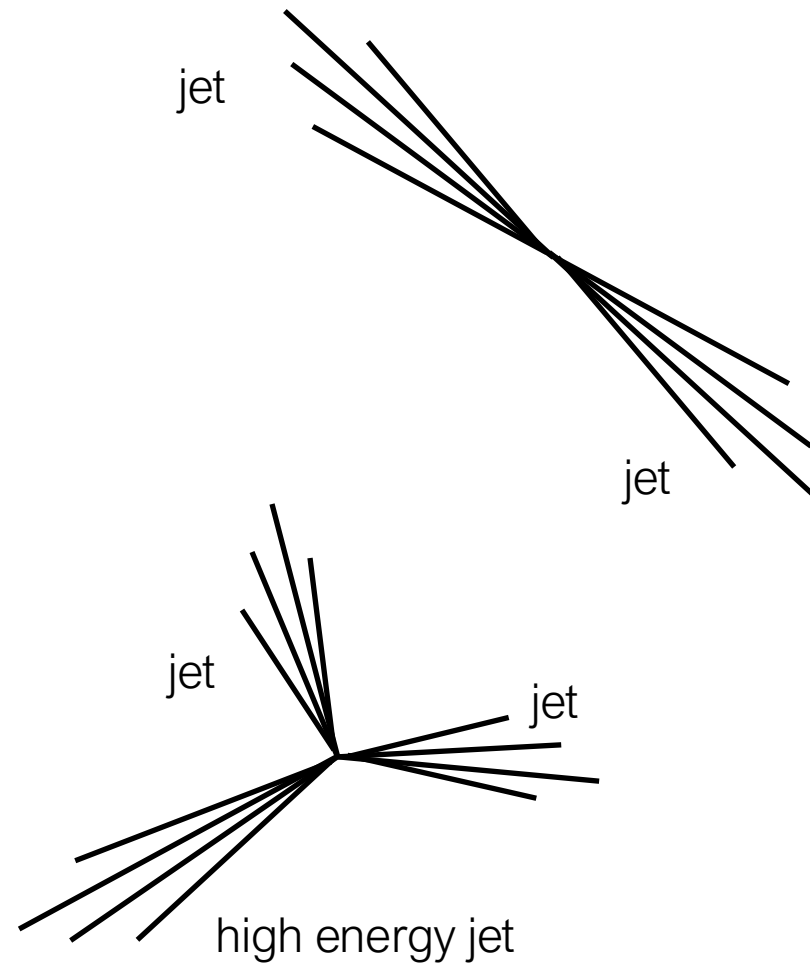


How to Calibrate a Jet?

Absolute methods



Relative methods [Inter-calibration]

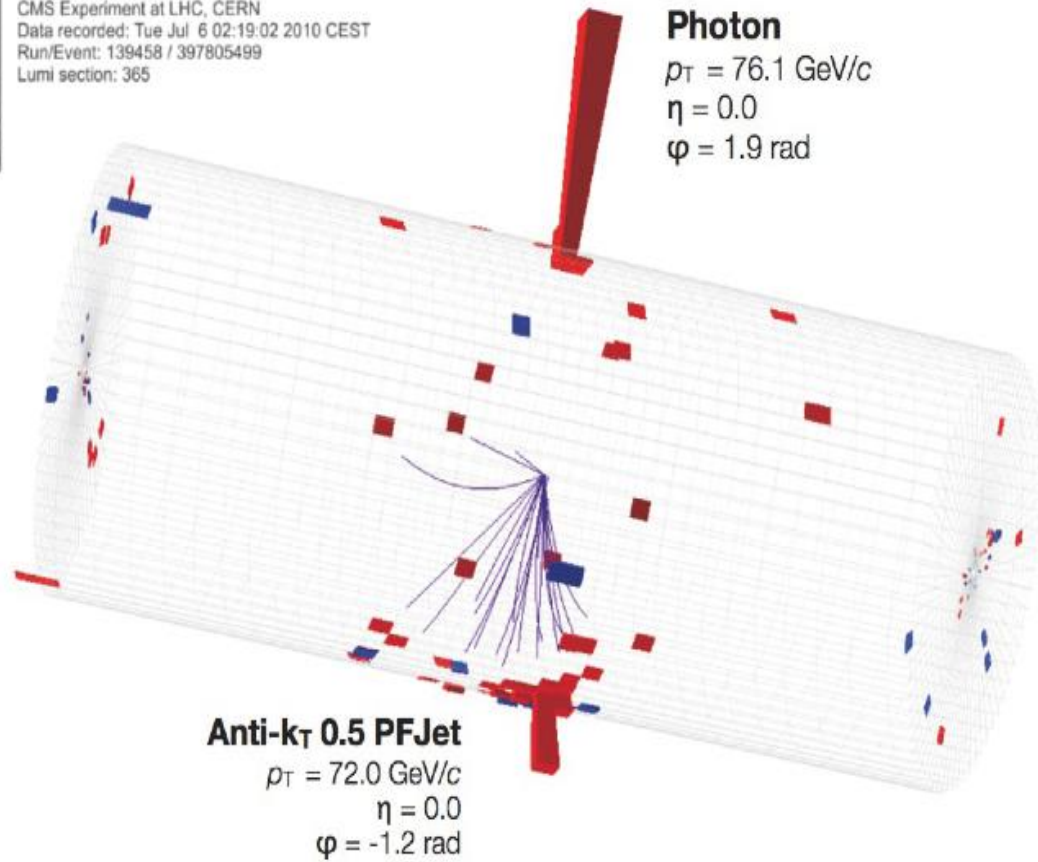




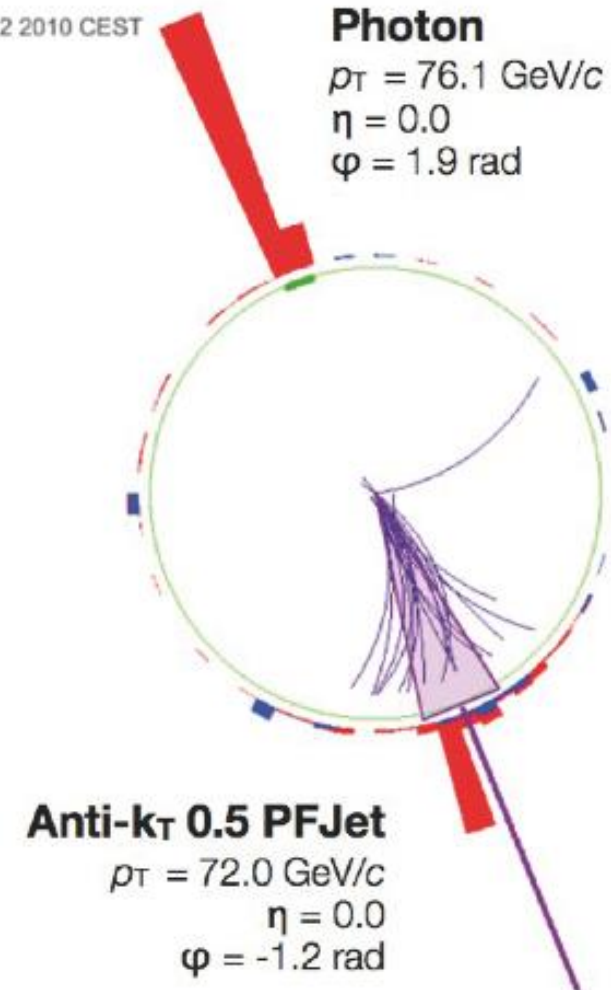
One CMS Example



CMS Experiment at LHC, CERN
Data recorded: Tue Jul 6 02:19:02 2010 CEST
Run/Event: 139458 / 397805499
Lumi section: 365



2 2010 CEST



Absolute Method Uses p_t balance in back-to-back photon+jet events



Missing Transverse Energy E_T

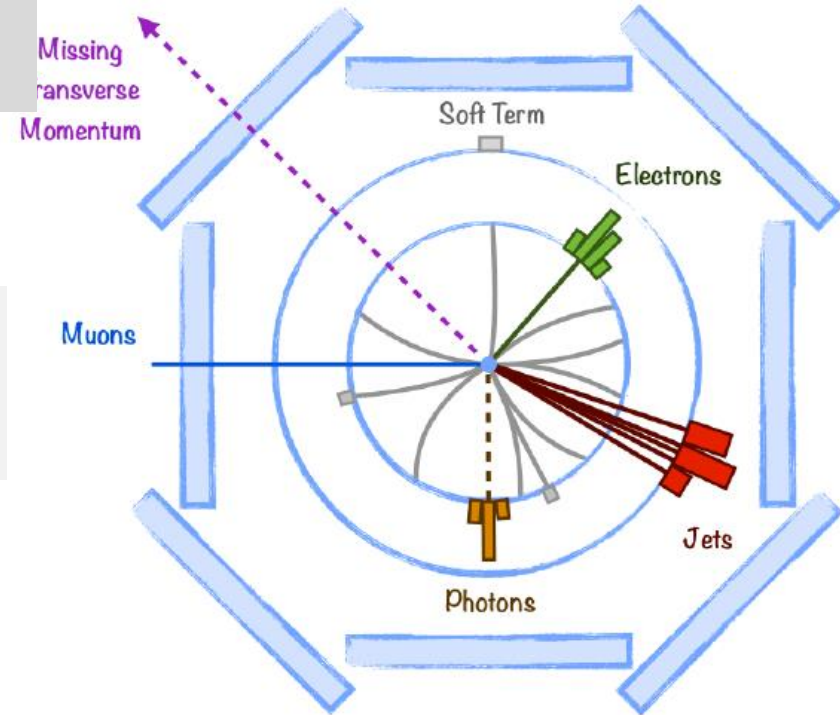
It is ONLY in the transverse plane that p_T is conserved (at hadron colliders)

$$\sum_{\text{All particles}} p_T = 0. \quad \sum_{\text{All particles}} p_l = ? \quad (x_1, x_2 \text{ unknown!})$$

$$\vec{E}_T^{\text{miss}} = -\sum_i \vec{E}_T^i$$

missing transverse energy = **minus** the vector sum of the transverse energy deposits. It is a proxy of the energy carried away by undetected particles.

→ *W bosons, top quark events and supersymmetric particle searches (with neutrinos or neutrinos-like particles in the decay channels).*



Another important quantity that is often referred to is the total transverse energy, which is the scalar sum of the transverse energy deposits:

$$\sum E_T = \sum_i E_T^i$$

Total Transverse Energy (MET)

The missing transverse energy and the total energy measurements are calculated using objects from Particle Flow



ATLAS & CMS in 2 Words

ATLAS: To reconstruct E_T^{miss} , fully calibrated electrons, muons, photons, hadronically decaying τ -leptons, and jets, reconstructed from calorimeter energy deposits, and charged-particle tracks are used. These are combined with the soft hadronic activity measured by reconstructed charged-particle tracks not associated with the hard objects. Possible double counting of contributions from reconstructed charged-particle tracks from the inner detector, energy deposits in the calorimeter, and reconstructed muons from the muon spectrometer is avoided by applying a signal ambiguity resolution procedure which rejects already used signals when combining the various E_T^{miss} contributions

CMS: The optimal response and resolution of E_T^{miss} can be obtained using a global particle-flow reconstruction. The particle-flow technique reconstructs a complete, unique list of particles (PF particles) in each event using an optimized combination of information from all CMS subdetector systems. Reconstructed and identified particles include muons, electrons (with associated bremsstrahlung photons), photons (including conversions in the tracker volume), and charged and neutral hadrons. Particle-flow jets (PF Jets) are constructed from PF particles.



Computing MET

Use:

- electrons,
- muons,

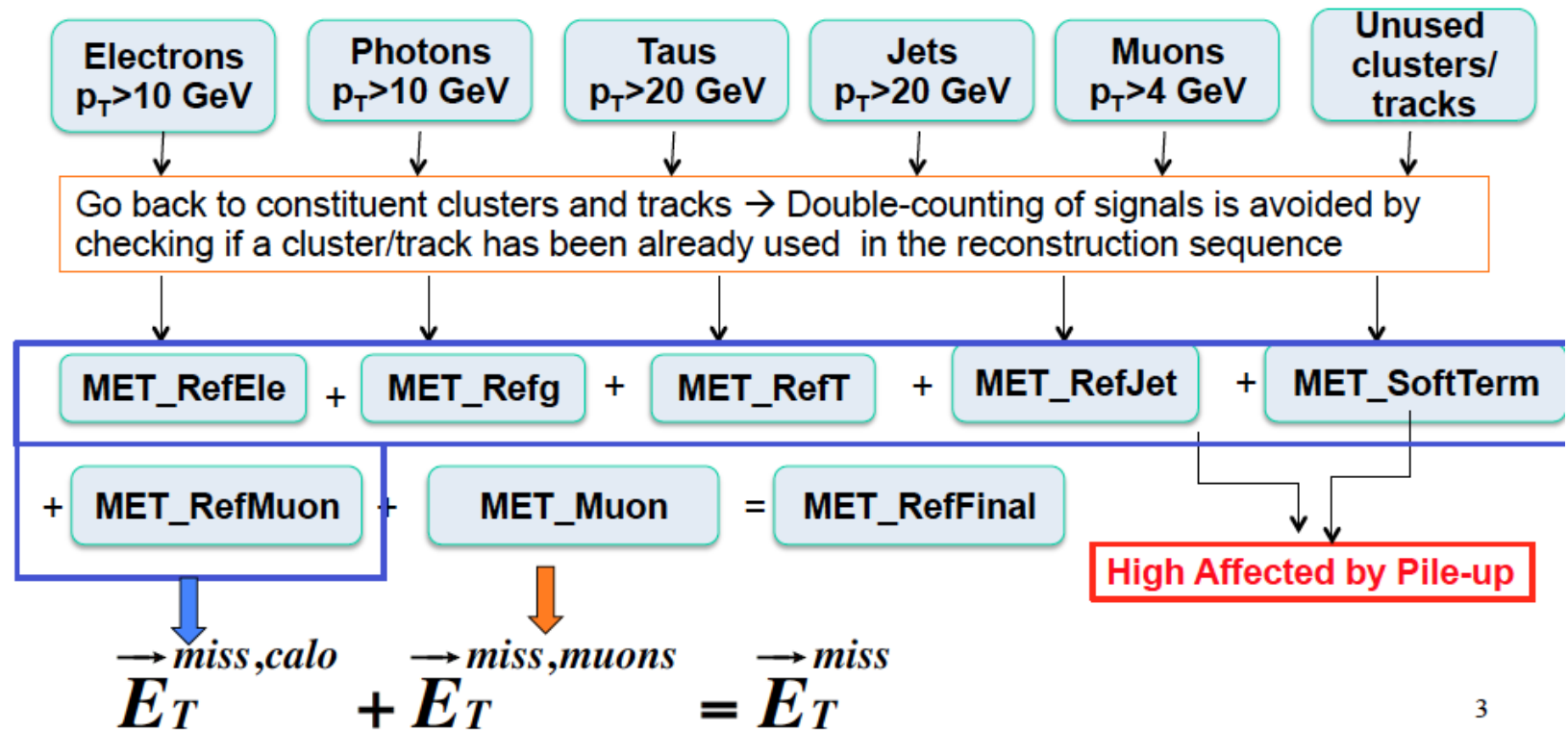
- photons,
- hadronically decaying τ -leptons,
- jets, from calorimeters & charged-particles
- soft hadronic activity

Avoid

Double counting!

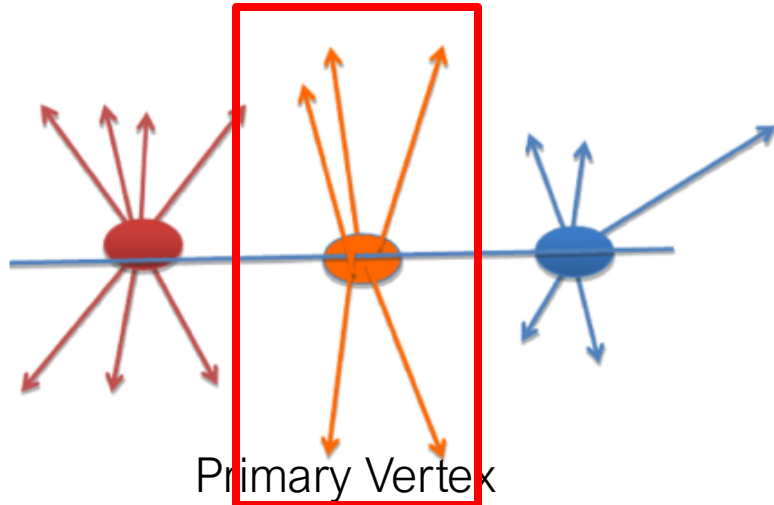
MET implies

- Different objects are used \rightarrow many different corrections
- Avoid double counting (\rightarrow PF algorithm)



MET & Pile-Up & Soft Terms

MET is affected by pile-up



- Tracks **can** be associated to vertices
- Energy depositions in calorimeters **cannot** be associated to vertices

Compute the ratio Jet Vertex Fraction for each jet:

$$JVF = \frac{\sum_{tracks, PV} p_T}{\sum_{tracks} p_T}$$

How much total momentum of a jet does not come from the PV?

Remove Jets with $JVF < \text{cut}$

Soft Term = un-associated E_{dep} s in calorimeters

Methods developed to remove *Soft term*



E_T^{miss} Resolution in ATLAS & CMS

Study the $(E_{miss})_{x,y}$ distribution for a sample of “minimum bias events” (expected to have no real E_T^{miss}).

Use events with one Z boson or an isolated γ (converting!) is present. These events are produced in collisions

- $q\bar{q} \rightarrow q\gamma$,
- $q\bar{q} \rightarrow Z$,
- $q\bar{q} \rightarrow qZ$, and
- $q\bar{q} \rightarrow \gamma$.

$E_T^{miss} \sim 0$. is in these events

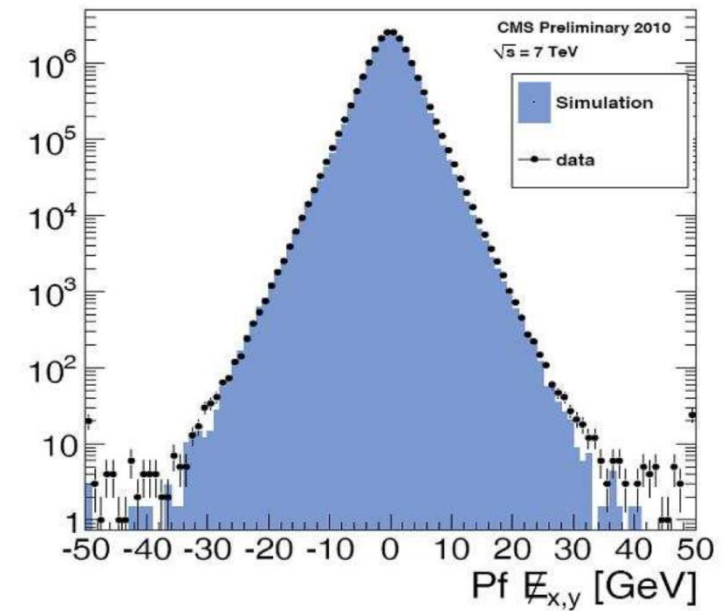
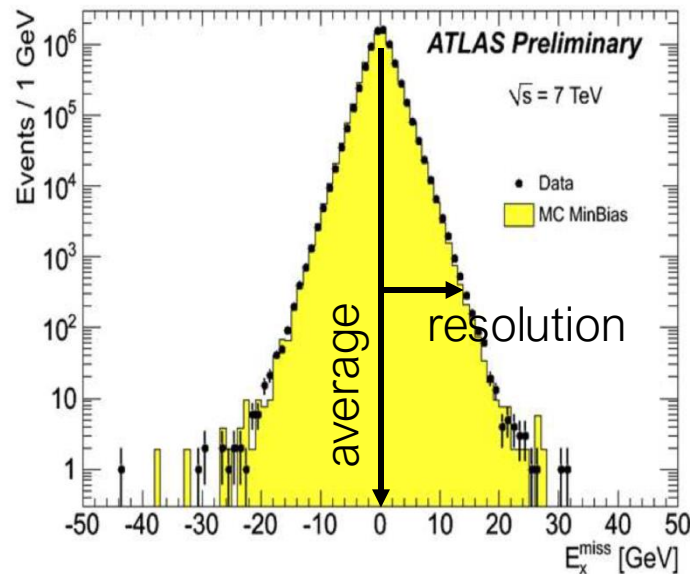
- remove objects from the Z, γ decay/conversion
- $E_T^{miss} \sim E_T^{Z,\gamma}$
- Compare the momenta of the well-measured boson to the E_T^{miss}

A study of the performance gives:

$$\sigma(E_{miss}) = 37\% / \sqrt{\sum E}$$

$$\sigma(E_{miss}) = 45\% / \sqrt{\sum E} \text{ for CMS.}$$

The two results are ~similar, some of the PFs approaches used in CMS also used in clustering algorithms in ATLAS





Use of Simulation in Data Analysis

Use of Simulation in Data Analysis



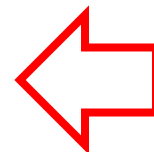
The Reason Why we Need Monte Carlo Events

The way to a cross section measurement (real life)

- Identify a measurement you are interested in (call it “signal”), understand its topology and kinematics
- Identify possible “background” processes with similar topology and kinematics (in general $N_b \gg N_s$)
- Identify a possible **selection** that produces a sample of events rich in signal and poor in background events → **Magnify ratio your signal over background**
- Apply the selection and count events

| | |
|---|---------------------------|
| $\sigma = \frac{N_{Signal\ Events}}{\mathcal{L}}$ | Ideal expression |
| $\sigma = \frac{N_{selected} - N_{background}}{\mathcal{L} \cdot efficiency}$ | More realistic expression |
| $\sigma = \frac{N_{selected} - N_{background}}{\mathcal{L} \cdot \epsilon_{trigger} \cdot \epsilon_{selection} \cdot Acceptance}$ | Realistic expression |

$$\sigma = \frac{N_{selected} - N_{background}}{\mathcal{L} \cdot \epsilon_{trigger} \cdot \epsilon_{selection} \cdot Acceptance}$$



All parameters differ between
Signal and Background



Of Monte Carlo Events in Analysis

This is the ideal case:

$$\sigma^{signal} = \frac{N_{total}^{signal}}{\mathcal{L}}$$

your detector sees everything
with perfect resolution, no loss no
imperfection

\Rightarrow

$$\frac{N_{selected} - N_{background}}{\mathcal{L} \cdot \epsilon_{trigger} \cdot \epsilon_{selection} \cdot Acceptance}$$

This is the real life:

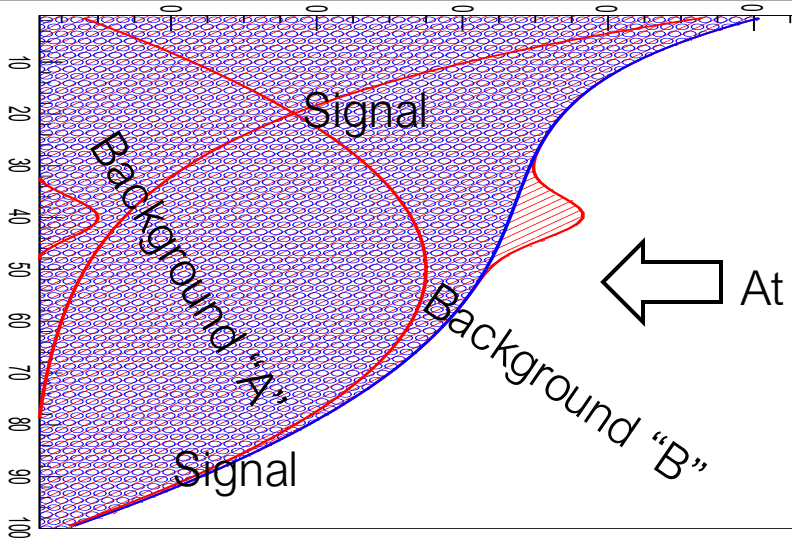
your detector does NOT see everything
has a resolution, has losses, imperfections

- σ^{signal} is the cross section of the interaction you want to study
- \mathcal{L} is the total luminosity you have collected
- N_{total}^{signal} is the number of signal events with cross section σ
- $N_{selected}$ is the number of events at the end of you analysis (signal + background!)
- $N_{background}$ is the number of background events at the end of you analysis. How to evaluate them? **Later**
- Data have been collected using a trigger. All triggers have inefficiencies \rightarrow trigger efficiency $\epsilon_{trigger}$
- To improve the visibility of your signal over background you apply selection cuts \rightarrow only a fraction of events survive $\epsilon_{selection}$
- Your detector is NOT really hermetic, there are holes, cracks, non-instrumented zones \rightarrow only a fraction of events are in the sensitive region of your experiment \rightarrow *Acceptance*



Of Monte Carlo Events in Analysis

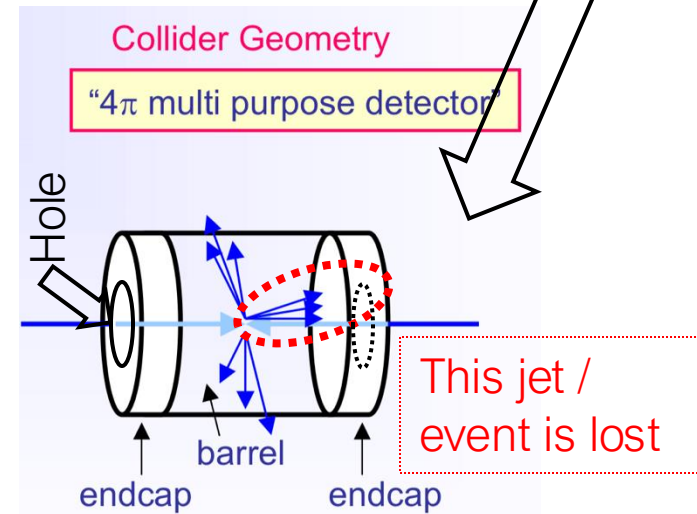
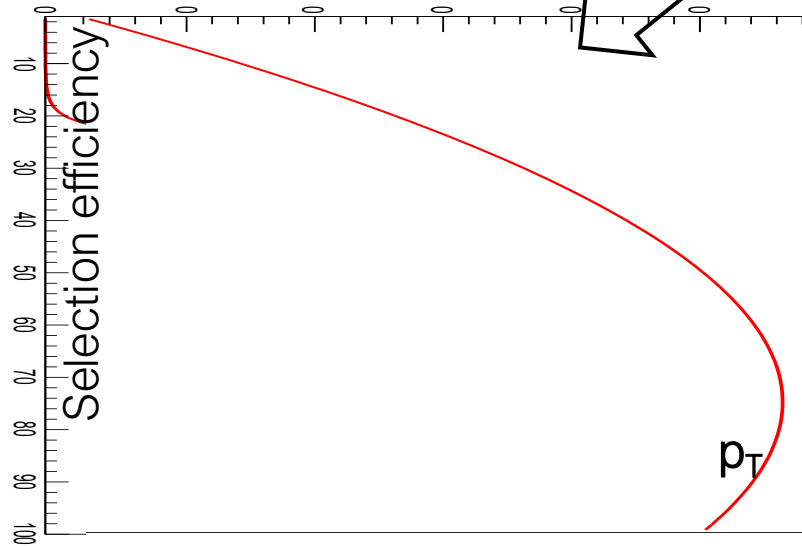
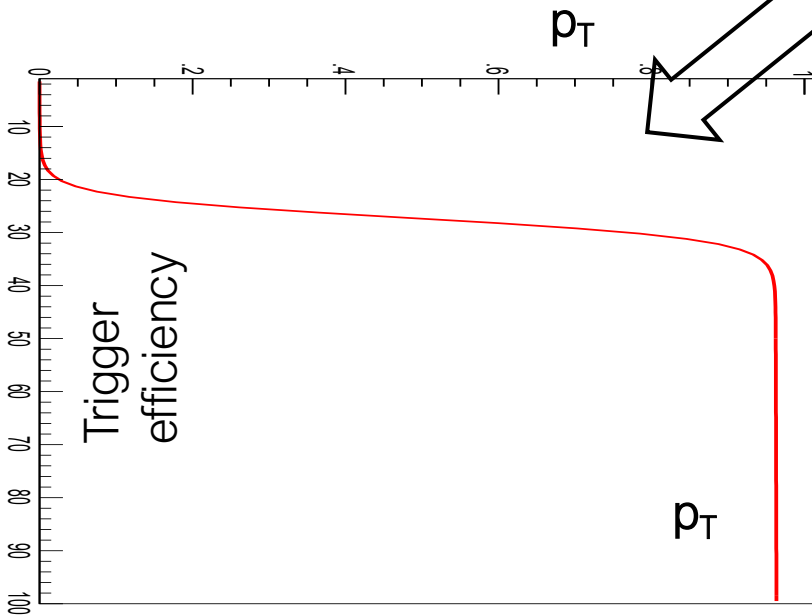
$$\sigma^{signal} = \frac{N_{total}^{signal}}{\mathcal{L}} = \frac{N_{selected} - N_{background}}{\mathcal{L} \cdot \epsilon_{trigger} \cdot \epsilon_{selection} \cdot Acceptance}$$



At the start, you have signal events and two types of background events A and B

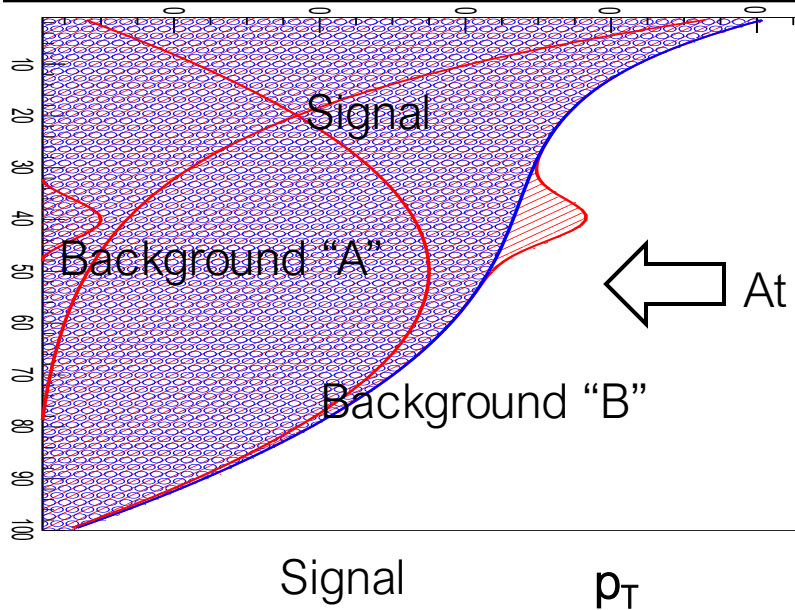
You collect events using a trigger

you select them to improve S/B





Of Monte Carlo Events in Analysis



$$\sigma^{signal} = \frac{N_{total}^{signal}}{\mathcal{L}} = \frac{N_{selected} - N_{background}}{\mathcal{L} \cdot \epsilon_{trigger} \cdot \epsilon_{selection} \cdot Acceptance}$$

At the start, you have signal events and two types of background events A and B

- $N_{selected}$ is counted
- \mathcal{L} is measured
- $\epsilon_{trigger}$ is \sim measured

Correct 'too good' simulations:

- Use 'standard candles'
- Use Control Regions (next slide) and Validation Regions to check/calibrate/modify your simulation

- $\epsilon_{selection}$, $Acceptance$, $N_{background}$ are estimated using simulated events (+ verified using data)

NB: the Monte Carlo is

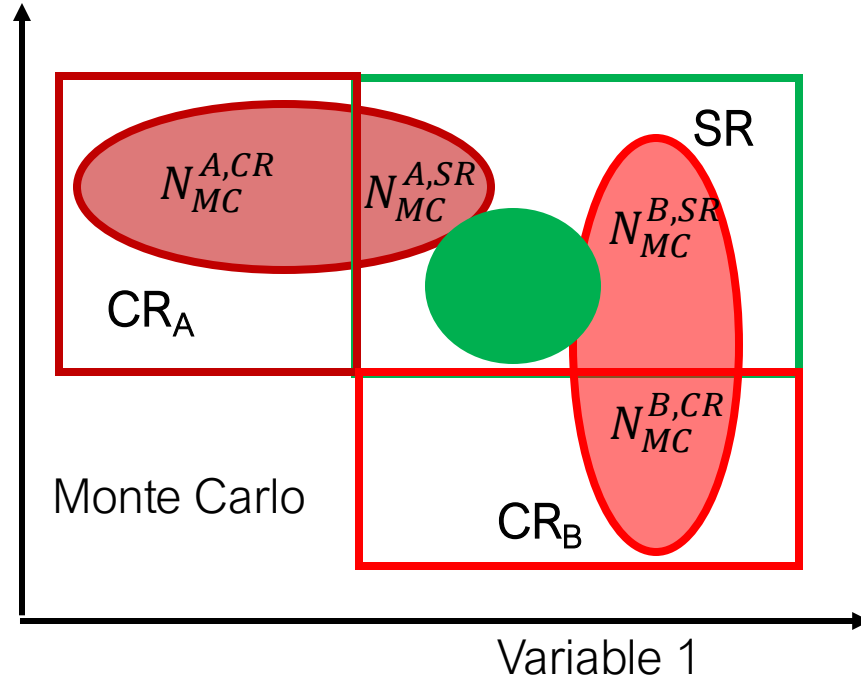
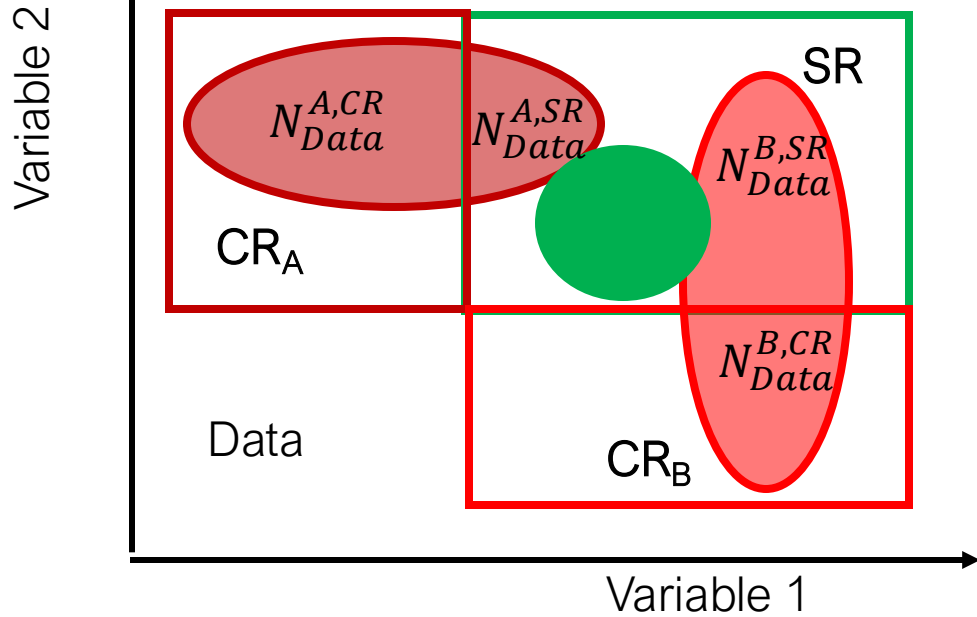
- almost always 'optimistic' \rightarrow material, resolution, efficiency
- Mitigate 'optimism': add additional smearing: if the resolution is too good add a gaussian random number with appropriate characteristics every measurement

$$p_T^{add.smearing} = p_T + rndm \cdot \sigma_{add.smearing} \rightarrow \text{worsen resolution}$$

The p_T of a track in your simulated event



Control Regions



Use Simulation and Control Region(s)

ASSUME that

$$N_{Data}^{A,SR} / N_{Data}^{A,CR} = N_{MC}^{A,SR} / N_{MC}^{A,CR}$$

$$N_{Data}^{B,SR} / N_{Data}^{B,CR} = N_{MC}^{B,SR} / N_{MC}^{B,CR}$$

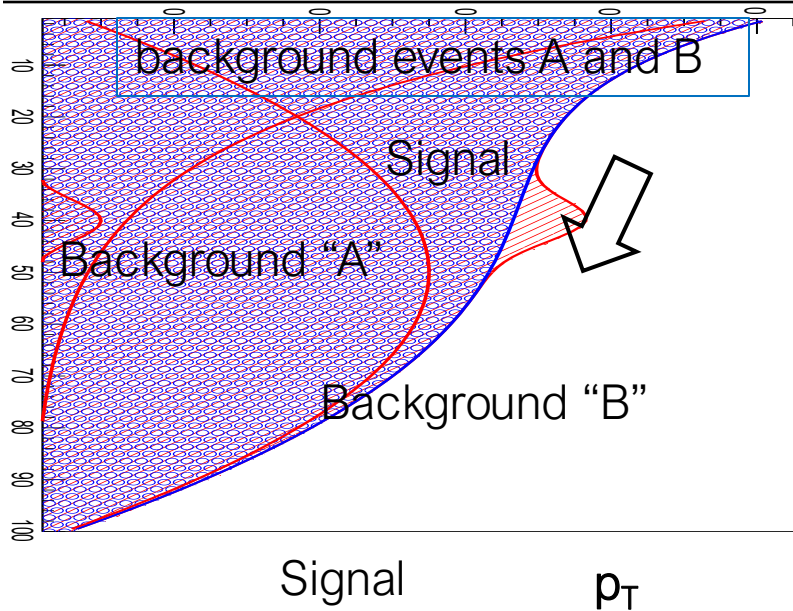
Normalise MC prediction to Data Shape from MC

$$N_{Data}^{B,SR} = N_{MC}^{B,SR} * N_{Data}^{B,CR} / N_{MC}^{B,CR}$$

(Integral of distribution)



Data-driven Background Estimation



Use Simulation and Control Region(s)

ASSUME that

$$N_{Data}^{A,SR} / N_{Data}^{A,CR} = N_{MC}^{A,SR} / N_{MC}^{A,CR}$$

$$N_{Data}^{B,SR} / N_{Data}^{B,CR} = N_{MC}^{B,SR} / N_{MC}^{B,CR}$$

Define Control Regions!

Signal Region: 'optimised' kinematical region that contains your **signal** (selection cuts)

- Count background events in SRs as predicted by Monte Carlo: $N_{MC}^{A,SR}$, $N_{MC}^{B,SR}$

Control Region (CRs): kinematical region ORTOGONAL to the signal region that

- Contains the **background** you want to measure
- Doesn't contain signal events
- Count events in CRs: both Monte Carlo and Data

- MC simulated events: $N_{MC}^{A,CR}$, $N_{MC}^{B,CR}$

- Data: $N_{Data}^{A,CR}$, $N_{Data}^{B,CR}$

$$N_{Data}^{B,SR} = N_{MC}^{B,SR} * N_{Data}^{B,CR} / N_{MC}^{B,CR}$$

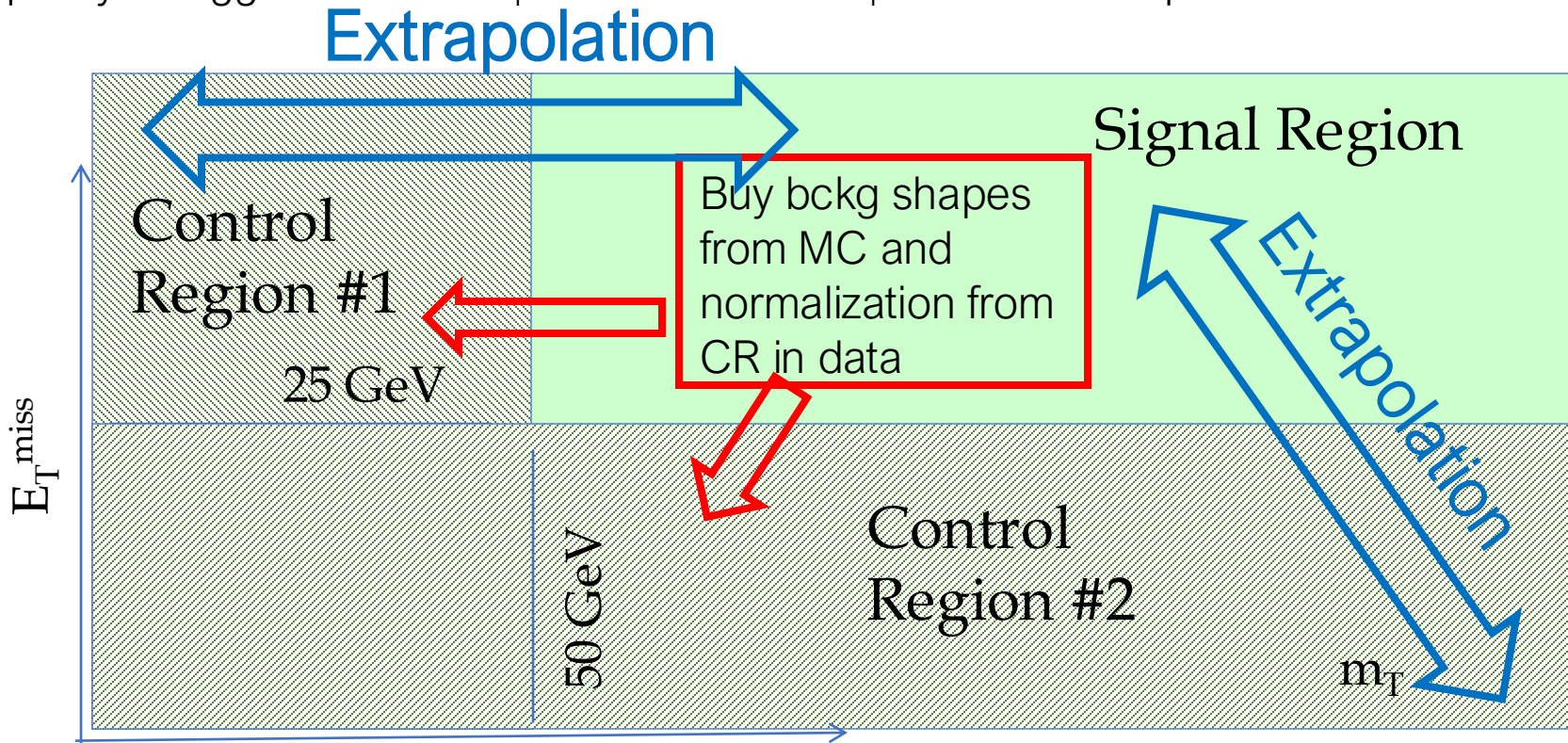
(Integral of distribution)

Normalise MC prediction to Data



Control Regions (2D cartoon)

- Signal Region (SR) contains events we want to select, Control Regions are close to SR but **ortogonal**. Need to have no correlation between **SR&CR**. You choose them to be mostly populated by the background you want to control
- SR: Lepton quality & trigger match & $E_T^{\text{miss}} > 25 \text{ GeV}$ & $m_T > 50 \text{ GeV}$ & lepton isolation & Overlap Removal (OR)



Background from heavy flavours decays and (for electrons) photon conversions determined using a “data-driven” technique.



Material

[CERN School 2017: Rende Steerenberg: Hadron Accelerators-1](#)

[CERN School 2017: Rende Steerenberg: Hadron Accelerators-2](#)

[The Physics of Particle Detectors](#)

[M. Tanabashi et al. \(Particle Data Group\), Phys. Rev. D 98, 030001 \(2018\)](#)

Passage of particles through matter, pages 446-460

Particle detectors at accelerators, pages 461-495



Books

1. Sylvie Braibant, Paolo Giacomelli, Maurizio Spurio: Particles and Fundamental Interactions, An Introduction to Particle Physics. Springer
2. DetectorsTokyo.pdf
3. Particle-detectors.pdf
4. Detectors-Full.pdf



End of Detectors

Particle Physics
Toni Baroncelli
Haiping Peng
USTC